STUDY OF NONLINEAR OSCILLATIONS AND WAVES IN PLASMA

By

Prabal Singh Verma

INSTITUTE FOR PLASMA RESEARCH, GANDHINAGAR

A thesis submitted to the
Board of Studies in Physical Sciences

In partial fulfillment of the requirements
For the Degree of

DOCTOR OF PHILOSOPHY

of

HOMI BHABHA NATIONAL INSTITUTE

August 2012

Homi Bhabha National Institute

Programme: Ph.D.

Board of Studies in Physical **Sciences**

1. **Name of the Constituent Institution:** Institute for Plasma Research

2. **Name of the Student:** Prabal Singh Verma
3. **Enrolment Number:** PHYS06200704011
4. **Date of Enrolment in HBNI:** September 3, 2007
5. **Date of Submission of Thesis:** May 9, 2012
6. **Title of the Thesis:** Study of Nonlinear Oscillations and Waves in Plasma

7. **Composition of the Doctoral Committee:**

Sr No	Composition	Designation in HBNI	Name
a.	**Chairman** A. Sen	Sr. Prof.	Abhijit
b.	**Convener** (Guide) P. K. Kaw	Sr. Prof.	Pkaw (P.K.Kaw)
c.	**Co-Guide**, if any		
d.	**Member** Amita Das	Asso. Prof.	Amita Das
e.	**Member** S. Sengupta	Asst. Prof.	(S. SENGUPTA)
f.	**The Technology Adviser**, if any	**Invitee**	

8. **Number of Doctoral Committee Meetings held with respective dates:** Five
(1) 08/10/2008, (2) 25/12/2009, (3) 11/03/2011, (4) 09/11/2011
(5) 07/02/2012

9. **Name and Organization of the Examiner 1:** Prof. Vinod Krishan,
Indian Institute of Astrophysics, Bangalore
Recommendations of the Examiner 1 (Thesis Evaluation) (i) [✓ accepted], (ii) accepted after revisions, or (iii) rejected:

10. **Name and Organization of the Examiner 2:** Dr. Surjalal Sharma,
University of Maryland, MD, USA
Recommendations of the Examiner 2 (Thesis Evaluation) (i) [✓ accepted], (ii) accepted after revisions, or (iii) rejected:

Name & Signature of Dean-Academic, CI:

Smukherjee
Dr. S. Mukherjee

Recommendations of the Viva Voce Board

1. **Date of Viva Voce Examination:** 22/08/2012

2. **Recommendations for the award of the Ph.D. degree: [✓ Recommended] / Not Recommended**
(If Recommended, give summary of main findings and overall quality of thesis)
(If Not Recommended, give reasons for not recommending and guidelines to be communicated by Convener of the Doctoral committee to the student for further work)

The Candidate, in this thesis has investigated the nature of the breaking of the waves and explored the validity of the theoretical results by carrying out the simulations over a wide range of physical parameters. The thesis includes several new results. The Candidate presented his work and answered all the questions and comments mentioned in the report. Minor suggestions for the sake of clarity were made by the examiner. The Candidate has taken care of all these matters. The thesis has been written very well. The research findings are of high quality. Strongly recommended for the award of the Ph.D. degree.

In case Not Recommended, another date will be fixed by the Dean-Academic, CI, which shall not be earlier than a month after and not later than six months from the date of first viva.

Date: 22/08/2012

Name and Signature of the Viva Voce Board (Doctoral Committee and External Examiner):

VINOD KRISHAN Vinod Krishan
Aug. 22, 2012

P. K. KAW Pkaw

A. SEN

AMITA DAS Amita Das.

SUDIP SENGUPTA

Homi Bhabha National Institute

Ph.D. Thesis Evaluation Report

1. **Name of the Constituent Institution:** Institute for Plasma Research
2. **Name of the Student:** Prabal Singh Verma
3. **Enrolment No. :** PHYS06200704011
4. **Title of the Thesis:** STUDY OF NONLINEAR OSCILLATIONS AND WAVES IN PLASMA
5. **Board of Studies:** Physical Sciences

Recommendations

Tick one of the following:

1. The thesis in its present form is commended for the award of the Ph.D. Degree. ☐
2. The thesis is commended for the award of the Ph.D. degree. However, my suggestions for improving the thesis may be considered at the time of the viva voce examination and if the viva voce board deems it appropriate, the same may be incorporated in the thesis based on the discussions during the viva voce examination. The revised thesis need not be sent to me. ☒
3. The thesis should be revised as per the suggestions enclosed. I would like to see the revised thesis incorporating my suggestions before I give further recommendations. ☐
4. The thesis is not acceptable for the award of the Ph.D. degree. ☐

VINOD
KRISHAN

VINOD KRISHAN
Raman Research Institute
Bangalore
2012-05-31 13:36+05:30

(Signature): Vinod Krishan

Name of Examiner: VINOD KRISHAN

Date: Aug. 22, 2012

Please give your detailed report in the attached sheet. You may use additional sheets, if required.

1. **Name of the Student** Prabal Singh Verma
2. **Enrolment No.** PHYS06200704011
3. **Title of the Thesi** STUDY OF NONLINEAR OSCILLATIONS AND WAVES IN PLASMA
4. **Board of Studies:** Physical Sciences

DETAILED REPORT

The candidate, in this thesis, has investigated the nature of the breaking of the nonlinear waves. The nonlinear waves could be initiated by any arbitrary density perturbation. The space and time evolution of the thus produced nonlinear oscillations is studied analytically as well as numerically. The author has carried out the study of the more general case of an arbitrary density profile in contrast to the similar earlier work on the special case of the sinusoidal density profile. The generality may particularly be useful for explaining the observed characteristics of nonlinear waves in systems such as the Laser-Plasmas.

The wave-breaking limits have been explored specifically for triangular and square wave forms. That the wave, in the presence of its second harmonic, does not break even when its amplitude exceeds the threshold is an interesting result of this study which is further confirmed by carrying out the 1D particle in cell simulations. This study is extended to include non harmonic waves along with the primary wave.

The author goes on to include the effects of viscous/ hyperviscous and resistive forces. The dependence of viscosity on the electron density is an important point of discussion in the thesis. As expected the dissipative effects enhance the threshold for the wave breaking. The relativistic effects for the breaking of the large amplitude waves such as exist in Laser-plasma systems in reference to their large phase velocity have also been studied. This study is of the paramount importance for wake-field type of electron acceleration processes. The analytical study has been complemented by the numerical study.

The inclusion of the ion dynamics becomes essential at long time behaviour of the high frequency nonlinear electron plasma waves. The present understanding is that the phase mixing and breaking of waves occurs at arbitrary small amplitudes and this is entirely attributed to the action of the nonlinear ponderomotive force exerted by the waves. The author, has, however, pointed out, additionally, the important role of the zero frequency modes, the ion-acoustic modes, in the breaking phenomena.

The author completes his investigation by exploring the regime beyond the wave breaking. This is the regime of plasma heating. The earlier some what erroneous conclusion that the entire electrostatic energy of the waves is randomized in the form of plasma heating is corrected and it is shown that the waves do not lose all but remain at a level below their wave breaking limit.

The last chapter includes the study of formation and collapse of the double layers for different initial conditions. Most of the work presented in the thesis has been published in internationally acclaimed journals. The thesis is well written. I have made a few comments on the thesis itself. These require an insertion of comments of the clarifying nature. The author may respond to the comments appropriately. I do not need to see the revisions.

In conclusion, I have absolutely no hesitation in recommending the acceptance of this thesis by Prabal Singh Verma.

Name of Examiner: Vinod Krishan

Signature and Date: VINOD KRISHAN
Aug. 22, 2012

VINOD
KRISHAN

VINOD KRISHAN
Raman Research Institute
Bangalore
2012-05-31 13:35+05:30

Homi Bhabha National Institute

Ph.D. Thesis Evaluation Report

1. **Name of the Constituent Institution:** Institute for Plasma Research
2. **Name of the Student:** Prabal Singh Verma
3. **Enrolment No. :** PHYS06200704011
4. **Title of the Thesis:** STUDY OF NONLINEAR OSCILLATIONS AND WAVES IN PLASMA
5. **Board of Studies:** Physical Sciences

Recommendations

Tick one of the following:

1. The thesis in its present form is commended for the award of the Ph.D. Degree. ☒
2. The thesis is commended for the award of the Ph.D. degree. However, my suggestions for improving the thesis may be considered at the time of the viva voce examination and if the viva voce board deems it appropriate, the same may be incorporated in the thesis based on the discussions during the viva voce examination. The revised thesis need not be sent to me. ☐
3. The thesis should be revised as per the suggestions enclosed. I would like to see the revised thesis incorporating my suggestions before I give further recommendations. ☐
4. The thesis is not acceptable for the award of the Ph.D. degree. ☐

(Signature):

Name of Examiner: A. SURJALAL SHARMA.

Date: 27 July 2012

Please give your detailed report in the attached sheet. You may use additional sheets, if required.

1. **Name of the Student:** Prabal Singh Verma
2. **Enrolment No.:** PHYS06200704011
3. **Title of the Thesis:** STUDY OF NONLINEAR OSCILLATIONS AND WAVES IN PLASMA
4. **Board of Studies:** Physical Sciences

DETAILED REPORT

Write your comments, if any.

The thesis presents many new and interesting results on nonlinear effects of plasma waves from studies using analytical and computational methods. These studies centered around wave-breaking phenomenon contribute to an improved understanding, and important implications for their applications.

Most of the results, already published, including one in Physical Review Letters, form a comprehensive set with a focus on nonlinear waves and oscillations in unmagnetized plasmas. The use of different methods, such as numerical integration of nonlinear evolution equations and particle-in-cell simulation enable detailed studies of the role of phase-mixing in nonlinear processes. The understanding of phase-mixing developed by the thesis, viz. the roles of zero-frequency mode and ponderomotive force, is a significant contribution.

The discussion on the potential topics for further studies presents not only ways to improve on the results by including more physics, e.g., ion dynamics in the case of relativistic travelling waves, but also the identification of new processes, such as acceleration of particles in nonlinear wave structures. This discussion reflects maturity of the thesis research.

The research presented in thesis clearly fulfills the requirements for the Ph. D. degree.

Name of Examiner: A. SURJALAL SHARMA

A. Surjalal Sharma

Signature and Date: 27 July 2012

CERTIFICATION FROM GUIDE

This is to certify that the corrections as suggested by the Referees in the thesis evaluation report have been incorporated in the copy of the thesis submitted to HBNI.

PKaw

Dated: 27 August 2012

Prof. P.K. Kaw
Research Guide

DECLARATION

I, Prabal Singh Verma, hereby declare that the investigation presented in the thesis has been carried out by me. The work is original and the work has not been submitted earlier as a whole or in part for a degree/diploma at this or any other Institution or University.

P.S. Verma

Prabal Singh Verma

STATEMENT BY AUTHOR

The dissertation has been submitted in partial fulfilment of requirements for the Ph.D. degree at Homi Bhabha National Institute (HBNI) and is deposited in the library to be made available to the borrowers under rules of HBNI.

Brief quotations from this dissertation are allowable without special permission, provided that proper acknowledgement of source is made. Requests for permission for extended quotation from or reproduction of this manuscript in whole or in part may be granted by the competent authority of HBNI when his/her judgement the proposed use of the material is in the interest of scholarship. In all other instances, however, permission must be obtained from the author.

P.S. Verma

Prabal Singh Verma

To my parents

ACKNOWLEDGEMENTS

First and foremost, I would like to express my sincere gratitude to my advisor Prof. P. K. Kaw for the continuous support of my Ph.D study and research, for his patience, motivation, enthusiasm, and immense knowledge. His guidance helped me in all the time of research and writing of this thesis. I could not have imagined having a better advisor and mentor for my Ph.D study. I really feel blessed and honoured to work with such a great personality of world fame like him. I also intend to thank my co-supervisor Dr. Sudip Sengupta with whom I started this work and many rounds of discussions on my Ph.D. with him helped me a lot. I would say he is the first person who inspired me to pursue research as a career and introduced me to basic tools and concepts of plasma physics which have been very useful through out. For me he is a great teacher and I am extremely indebted to him.

I would also like to thank my doctoral committee members Professor Abhijit Sen (Chairman), Dr. Sudip Sengupta, Prof. A. Das for their timely comments on the progress of my thesis. Special thanks to Prof. Amita Das, Dr. Srinivasan and Prof. Abhijit Sen for critically reading my manuscripts and providing valuable inputs on them. I also wish to express my gratitude for the earlier academic committee members namely Dr. R. Ganesh, Dr. S. Sengupta, Dr. P. Chattopadhyay and Dr. J. Ghosh for their useful feedback on my first year review. I extend my sincere gratitude for the chairman academic committee Dr. S. Mukherjee for accelerating the process of my thesis submission. I would also like to acknowledge all the staffs of library and computer center for their excellent facility and help throughout my Ph.D. Thanks are also due to people from administration, accounts, stores, purchase and canteen for their co-operation throughout my Ph.D., without which it would have been a rather difficult task.

When I started this work I knew a very little about numerical programming and particle in cell (pic) simulation. It was Gurusharan Singh who brought my pic code in working condition. I am extremely grateful to him.

I extend my thank to Deepak (one of my close friends at IPR) who, as a brother, has always been there to support me in all the situations. I further extend my thanks to all my friends (batchmates) Sanjib, Linthish, Tayyab, Gurudatt, Sita,

Vikram, Ujjwal, Kshitish, Ashwin, Arbind, Deepak for their love and unconditional support throughout. I can never forget the joyful days spent with them during the course work. A special thanks to Ashwin who always helped me whenever I had some difficulty in numerical programming. The numerical help I got from Linthish to begin my first problem is unforgettable. Gurudatt also deserves a special thanks for giving his valuable comments mainly on the introduction part and on one of the manuscripts. I am also very thankful to all my juniors Pravesh, Rameswer, Sushil, Sanat, Sayak, Aditya, Soumen, Iliyas, Vikram Dharodi, Veda, Sandeep, Shefali, Shailja and Sapna for making a good friendly environment at IPR hostel. Special thanks to Rameswer and Aditya for the quick proof reading of the thesis. I would also like to thank my seniors Neeraj, Jyotirmay, Anurag, Suraj, Pintu, Ritu, Rajneesh, Manas, Bhasker, Vikrant, Kishor, Maya, Satya, Shekhar, Sharad, Sunita and Jugal for their help and friendly attitude.

I further extend my sincere thank to Vikrant, Sita, Ujjwal, Gurudatt, Sanat and Bhavesh for giving their valuable time on numerical and physics discussions which have been helpful in widening my knowledge. A big thanks to our cook Jeevlal and his wife for providing the delicious food at IPR hostel.

I would also like to thank my beloved wife Neha for helping and supporting me specially during the thesis writing phase. Without her support my thesis could not have been submitted on time, I would say. I extend my thanks to my brother in law Mohit for his affection and ever encouraging attitude.

At last, I would say that the work I have presented in this thesis could not have been put together without the help I have received from a number of people. Its very difficult to name all those who have in one way or other made me to go through this very phase of life. I thank them all here for their overwhelming support throughout my Ph.D. tenure.

Prabal Singh Verma

LIST OF PUBLICATIONS

[1] **“Residual Bernstein-Greene-Kruskal-like waves after one-dimensional electron wave breaking in a cold plasma ”,**
Prabal Singh Verma, Sudip Sengupta, and Predhiman Kaw
Phys. Rev. E **86**, 016410 (2012)

[2] **“Breaking of Longitudinal Akhiezer-Polovin Waves ”,**
Prabal Singh Verma, Sudip Sengupta, and Predhiman Kaw
Phys. Rev. Lett. **108**, 125005 (2012)

[3] **“Bernstein-Greene-Kruskal waves in relativistic cold plasma ”,**
Prabal Singh Verma, Sudip Sengupta, and Predhiman Kaw
Phys. Plasmas **19**, 032110 (2012)

[4] **“Nonlinear oscillations and waves in an arbitrary mass ratio cold plasma ”,**
Prabal Singh Verma
Phys. Plasmas **18**, 122111 (2011)

[5] **“Nonlinear evolution of an arbitrary density perturbation in a cold homogeneous unmagnetized plasma ”,**
Prabal Singh Verma, Sudip Sengupta, and Predhiman Kaw
Phys. Plasmas **18**, 012301 (2011)

[6] **“Nonlinear oscillations in a cold dissipative plasma ”,**
Prabal Singh Verma, J. K. Soni, Sudip Sengupta, and Predhiman Kaw
Phys. Plasmas **17**, 044503 (2010)

[7] **“Spatio-temporal evolution and breaking of Double layers: A description using Lagrangian hydrodynamics ”,**
Predhiman Kaw, Sudip Sengupta, and Prabal Singh Verma
submitted

Abstract

In this thesis we studied nonlinear oscillations/waves in a cold plasma in various physical limits and investigated several novel aspects of wave breaking which have not been considered up till now. We have obtained an exact solution in the lab frame describing the space time evolution of an arbitrary perturbations in a cold homogeneous plasma and have shown that addition of a second harmonic increases the breaking amplitude of the fundamental mode. Later we verified this interesting observation in 1-D particle in cell simulation. We have further studied nonlinear oscillations in a cold viscous/hyperviscous and resistive plasma and obtained an expression describing the breaking criterion for Dawson like perturbation [102] for this case. Moreover, we have shown that the nonlinear effects as reported in a recent reference are independent of the model for viscosity chosen in the ref. [118]. We have numerically studied the breaking criterion of longitudinal Akhiezer-Polovin (AP) waves [119] in the presence of noise and found that they break at arbitrarily low amplitude through the process of phase mixing. Moreover, we have obtained longitudinal AP wave solution [119] from space time dependent solution of relativistic electron fluid equations for the cold homogeneous plasma [107]. We have also shown that it is not only the nonlinearly driven ponderomotive forces but the naturally excited zero frequency mode of the system may also be responsible for the phase mixing in an arbitrary mass ratio cold plasma. For example we have shown that the BGK waves in a cold electron plasma phase mix away and break at arbitrarily small amplitude via phase mixing if we allow ions to move. Here zero frequency mode of the system is found to be the only candidate responsible for phase mixing. We have also shown that there exist nonlinear traveling wave solutions in an arbitrary mass ratio cold plasma which do not exhibit phase mixing. Further, we have studied electron plasma oscillations beyond wave breaking using 1-D particle in cell simulation and found that a fraction of energy, decided by Coffey's limit in warm plasma [121], always remains with the wave in the form of the superposition of two BGK waves. This result is in contrast to the accepted fact that after the wave breaking all energy of the wave goes to random kinetic energy of the particles [102, 122]. The final distribution function is found to be non-Maxwellian. Lastly we studied development and collapse of double layers in the long scale length limit using method of Lagrange variables.

Contents

List of Figures

Chapter 1

Introduction

The entire thesis is based on the study of breaking and evolution of nonlinear oscillations/waves in a cold plasma. In this chapter we furnish the motivation for such studies, a review of earlier works and a summary of the important results obtained in this thesis.

1.1 Motivation

Plasma is a combination of charged particles which exhibit collective behavior due to the long range Coulomb forces. A key feature of a plasma is its ability to support various kinds of waves or collective modes of oscillation. In the simplest case, plasma waves correspond to longitudinal charge density fluctuations along with their associated electric fields. These plasma waves can be excited in the wake of the ultra-short, ultra-intense laser/beam pulse when it goes through underdense plasma [1]. When a particle comes in resonance with these plasma waves, it sees a DC electric field and gets accelerated to a high energy in a very short distance, a feature which is sometimes desirable and sometimes not. For example, in accelerator applications [2-30], one aims to produce efficient acceleration by an intentionally excited plasma wave. These accelerated (energetic) particles are being used in a wide variety of fields, ranging from medicine and biology to high-energy physics. These energetic particles are also desirable for producing a hot spot to initiate ignition in an already compressed pellet for fast ignition applications of laser fusion [35-85] Hence, one promotes generation of accelerated particles by plasma waves. On the other hand, these energetic electrons can prematurely heat the fuel in a capsule and make efficient implosions difficult in compression applications for inertial fusion [86-101]. Hence one tries to avoid exciting plasma waves. Note here that larger the amplitude of plasma wave, maximum the acceleration would be . But, we can not increase the amplitude of the plasma wave beyond a critical limit which is mainly decided by number density of the particles. When a coherent plasma wave's amplitude exceeds this critical value, coherent oscillation of plasma particles gets converted to random motion and the wave gets damped as it delivers its energy to the particles constituting the wave. This phenomenon is known as wave breaking [102]. When the plasma wave breaks, it is no more able to provide us maximum acceleration due to reduction in the amplitude. Physically, wave breaking occurs whenever there is a trajectory crossing between neighboring particles which results in density bursts. In the fluid picture, trajectory crossing leads to multistream motions and random acceleration of fluid particles. In a kinetic picture, trajectory crossing and density bursts lead to the production of very short wavelengths which can then resonantly interact with very cold particles accelerating them to high velocities. Breaking of plasma waves can also occur slowly, at and amplitude much lower than the critical value via a novel phenomena called phase mixing [102-109]. Phase mixing occurs when the plasma frequency for some physical reason acquires a spatial dependence. It may occur either due to inhomogeneity in the ion background [102-105] or due to relativistic effects [107-109] It may also occur in a homogeneous plasma as ion background selfconsistently becomes inhomogeneous in response to the low frequency forces [106]. Phase mixing of a plasma wave implies decay of the wave by fine scale mixing of various parts of the oscillation due to temporal dependence of the phase difference between individual oscillators constituting the wave. In the phase mixing process initial energy goes into higher harmonics which form a density peak and finally lead to density bursts (wave breaking).

Till now we have discussed breaking of plasma waves in the 1D geometry. The process of wave breaking in 2D and 3D plasma waves is expected to exhibit more complicated properties. A 2D wakefield plasma wave excited by a finite width, short laser pulse, or by a pulse with a sharp leading edge in an underdense plasma has a specific "horseshoe" (or "D shape") structure where the curvature of the constant phase surfaces increases with the distance from the pulse. The curvature radius "R" decreases until it is comparable to the electron displacement in the nonlinear plasma wave leading to a new type of self-intersection of the electron trajectories. This is called transverse wave breaking [110] which occurs at much lower wave amplitudes than the conventional one-dimensional wave break.

Wave breaking actually is a nonlinear mechanism for dissipating coherent wave energy in a plasma and delivering it to particles. On the face of it, wave breaking appears similar to Landau damping [111] converting coherent wave motions into randomized kinetic energy of particles. However, there are important differences between the two which are discussed in the following subsection.

Wave breaking versus Landau damping

Landau damping is a linear phenomenon of a warm plasma and has no thresholds. It only requires a negative slope of the distribution at the wave phase velocity such that the number of particles giving energy to the wave is smaller than the number of particles taking energy from the wave. It also requires that the wave amplitude be small so that the bounce frequency of the particle in the wave trough is smaller than the Landau damping rate ; in other words, Landau damping works if the damping rate is faster than the bounce frequency so that the wave disappears before the particles have a chance to bounce [112]. Otherwise, one gets a BGK mode with trapped particles [113], which do not suffer Landau damping. In contrast wave breaking is a nonlinear phenomenon in which the wave phase velocity typically does not resonate with the particle thermal velocities, which are assumed to be small. When the wave amplitude crosses the threshold for wave breaking, it basically accelerates the particles enough so that they come into temporary resonance with the wave, get accelerated by it and generate final velocities up to twice the phase velocity. It also generates high spatial harmonics through density bursts, which can more easily interact with the particles because they move with lower velocities and need lower amplitudes to nonlinearly resonate with the cold particles.

An another difference between wave breaking and Landau damping [111] is as follows. Landau damping is a reversible phenomena,i.e.; the energy lost by the wave can be obtained back by the application of secondary wave. Here the direction of the phase evolution of the perturbed distribution function due to dissipation of the primary wave can be reversed by the application of a second electric field.

This results in the subsequent reappearance of a macroscopic field, many Landau-damping periods after the application of the second pulse. This phenomena is called plasma wave echo [114, 115]. Thus we note here that the phenomena of Landau damping is a reversible in nature. However, in the wave breaking, energy lost by the wave can not be recovered back by any mean.

Now, as we have discussed earlier that in the phase mixing leading to wave breaking process, initial energy goes to higher and higher harmonics as time progresses. This can be understood as the damping of primary wave due to excitation of higher modes and can be explained by the mode coupling effect. Here, the primary wave is getting damped but its energy is not going to particles which makes this damping phenomena different from the Landau damping. Thus we see that damping of plasma wave due to wave breaking is very much different from the Landau damping.

In all the applications we have discussed here, it is important to understand the nonlinear effects which determine how large and how coherent a plasma wave can be excited with and without breaking. In this thesis we report on several novel aspects of 1D wave breaking in cold plasma which have not been discovered yet.

1.2 Discussion of earlier work

1.2.1 Breaking of nonlinear non-relativistic oscillations with static ion background

Concept of nonlinear oscillations and wave breaking in plasma was first introduced by Dawson[102], for the cold plasma model, where thermal motion may be neglected. The author proposed that, in a cold homogeneous plasma where ions are assumed to be static, as we increase amplitude of the perturbation, oscillations become nonlinear and lead to the excitation of higher ‘k’ modes. However, we can not increase the perturbation amplitude beyond a critical limit (known as wave breaking amplitude) as trajectory crossing takes place between neighboring electrons. As a result, there will be fine scale mixing of various parts of the oscillation which destroys the oscillations. Moreover, the author had shown that if we take an inhomogeneous ion background to begin with, plasma frequency becomes a function of position. As a result, at different positions electrons oscillate at different local frequency. Because of this effect oscillations in an inhomogeneous plasma will always break through phase mixing at arbitrarily low amplitude[102]. Kaw et al. [103] explained the phenomenon of phase mixing as mode coupling where energy goes form longer to shorter and shorter wavelengths. These authors have demonstrated it by taking an example of small sinusoidal inhomogeneity in static ion background. A couple of years later Infeld et al. [104] reported an exact solution describing the space time evolution of nonlinear cold electron plasma oscillations against the fixed sinusoidal ion background and found that all initial conditions lead to density burst (wave breaking).

Davidson and Schram [116, 117] have investigated the wave breaking problem by obtaining the exact solution of nonrelativistic cold electron fluid equations with infinitely massive ions using the method of Lagrange coordinates. The authors have obtained a general wave breaking condition where they have shown that if the minima of normalized initial density crosses 0.5 at any point in space, it will break within one plasma period. The authors have considered the initial density distribution to be sinusoidal and have given the solution in the lab frame also, by an inversion process. In the lab frame, feature of the solution becomes clear and we see surprising physical effect that whatever energy we load on the fundamental mode, it gets distributed over nonlinearly generated several number of modes and comes back to the original mode within one plasma period. Mathematically, the inversion process from Lagrange solution to lab frame solution can however be carried out only below a critical amplitude of the initial disturbance as beyond this critical amplitude the Jacobian of the transformation from Eulerian to Lagrangian coordinates goes to zero and the transformation is no longer unique.

Beyond this amplitude multistream motion results due to wave particle interaction and the disturbance leads to wave breaking. For a pure sine wave, oscillations break within one plasma period when electric field "$keE/(m\omega_{pe}^2)$" becomes greater than or equal to 0.5 [116, 117]. In realistic case, it is natural to expect that any exciting mechanism creating the initial density disturbance will excite a bunch of modes. Therefore it is interesting to know the space time evolution and the breaking of such a general disturbance.

Davidson and Schram [116, 117] also studied the effect of collisonal drag term (resistivity) on nonlinear oscillations in cold plasma. The solution to the equations exhibit damped oscillations and the density may be shown to damp to the value of the uniform background density, n_0. This asymptotic time behavior is valid for any initial conditions that do not lead to multistream flow. Recently Infeld et al. [118] studied the nonlinear oscillations for a more general damping mechanism, where the authors have included viscosity term along with the resistive term. The authors observed that nonlinear oscillations, initiated by a sinusoidal initial density perturbation, do not break even beyond the critical amplitude. However, the authors have not made any comment on how the breaking condition modifies in the presence of viscosity and resistivity. Moreover, the authors found a new nonlinear effect in the form of splitting of density peak for larger value of viscosity coefficient. The physical reason behind this effect needs to be investigated. The most important point to be noted here is that the authors have modeled the viscosity coefficient as inverse of electron number density "$n_e(x,t)$" to solve the fluid equations analytically. However in realistic case, viscosity coefficient has a relatively weak dependence on density through Coulomb logarithm. Therefore it will be interesting to investigate whether the new nonlinear effects as reported in ref. [118] persist for the realistic case.

1.2.2 Breaking of nonlinear relativistic plasma oscillations with static ion background

It is well known that in order to study very large amplitude plasma waves, one must include relativistic corrections in the cold electron fluid equations. The longitudinal traveling wave solutions in relativistic cold plasma were first obtained by Akhiezer and Polovin [119]. The authors found that the breaking amplitudes of these waves is very high which can be expressed as "$E_{wb}/E_0 = \sqrt{2}(\gamma_{ph} - 1)^{1/2}$" [119].Here $\gamma_{ph} = 1/\sqrt{1-(v_{ph}/c)^2}$ is the relativistic factor associated with the phase velocity v_{ph} of the AP wave. Note here that as $v_{ph} \to c$, $\gamma_{ph} \to \infty$, this implies $E_{wb} \to \infty$. Thus we see that if the phase velocity of the relativistic plasma waves is very close to speed of light, their breaking amplitude will be very high.

This wave breaking formula has been used extensively in many particle acceleration experiments/simulations [28, 29], to gain insight into the the observed experimental/numerical results, after it is shown analytically that the waves which get excited in the wake of the laser pulse when it goes through under dense plasma are nothing but longitudinal Akhiezer-Polovin waves [1]. It has also been proposed that a relativistic plasma oscillations always phase mix and break at arbitrarily small amplitude as relativity brings in spatial dependence in the frequency of the system [107, 108]. Therefore it will be interesting to explore whether ideal wave breaking criterion of longitudinal AP waves holds in the presence of the perturbations as in realistic experiments there is always some noise associated with the wake wave (AP wave).

As we have discussed that longitudinal AP waves are the time stationary solution of relativistic electron fluid equations in a cold homogeneous plasma [119]. In 1989, Infeld and Rowlands reported an exact space and time dependent solution for the relativistic electron fluid equations in Lagrange coordinates which shows an explosive behavior for almost all initial condition. It is also commented by these authors that Akhiezer-Polovin (AP) waves are very special type of modes which do not show explosive behavior as these structures are functions of just one variable, $x - v_{ph}t$. It was also emphasized that AP waves need very special set of initial conditions to set them up, and for other initial conditions there would be relativistic bursts (wave breaking)[107]. It is to be noted here that if we take small amplitude limit of longitudinal AP waves, we land up with nonrelativistic cold plasma BGK waves [120]. The space time dependent solution of Davidson and Schram [116] lead to these waves [120] if one chooses a special set of initial conditions. Therefore, for the completeness it will also be interesting to get the initial conditions in the space time dependent solution of Infeld and Rowlands [107] so as to excite relativistic traveling AP waves [119].

1.2.3 Breaking of nonlinear plasma oscillations with ion motion

In all the works, we have discussed till now, ions are assumed to be infinitely massive i.e.; they are just providing a neutralizing background to the electrons. In other words we can say that till now we have looked at the phenomena which occur at very fast time scale such that we can ignore ion response which is comparatively very slow. It is interesting to know what will happen to the plasma oscillations if we work on the time scale where ion response can not be neglected.This behavior was first studied by Nappi et al. [105] with inhomogeneous sinusoidal ion background. The authors found that ion background gets modified significantly due to ponderomotive forces, before wave breaking (due to phase mixing [102]). Later Sengupta et al. have shown that phase mixing of plasma oscillations can occur even if we start with homogeneous but mobile ions [106]. The authors have shown that ion distribution becomes inhomogeneous in response to low frequency force (ponderomotive force) and hence plasma oscillations phase mix away and break at arbitrarily small amplitude [106]. These authors have taken the example of sinusoidal electron density perturbation which in the absence of ion motion breaks when "$\delta n_e/n_0$" becomes greater than or equal to 0.5. However, with ion motion it breaks via phase mixing at arbitrarily small amplitude and the survival time of the oscillations is decided by the electron-ion mass ratio and the amplitude of the perturbation. It has also been shown that damping of plasma oscillations occur as the energy which is loaded on the fundamental mode, goes irreversibly into higher harmonics [106] and it can be interpreted as mode coupling effect [103]. It is the understanding till now that phase mixing occurs only due to ponderomotive forces. However, phase mixing of oscillations can be seen even if one ignores the ponderomotive force effect [106]. Therefore it will be interesting to explore the physical reason behind this.

Thus we see that nonlinear standing oscillations, in an arbitrary mass ratio cold plasma always, phase mix away and break at arbitrarily small amplitude. This phenomenon has got a very much similarity to phase mixing of standing oscillations in the relativistic cold plasma with infinitely massive ions. However, we know that there exist nonlinear traveling wave solutions for the relativistic case, which do not show phase mixing. Therefore, it is interesting to explore whether such solutions, which do not exhibit phase mixing, exist for the nonrelativistic arbitrary mass ratio cold plasma.

As we have discussed earlier that cold plasma BGK waves [120] are the time stationary solutions for electron plasma oscillations with static ion background. Therefore it will also be interesting to explore the effect of ion motion on these waves.

1.2.4 Wave breaking at critical amplitude

In cold homogeneous plasma with static ions, electron plasma oscillations break if we increase the amplitude of the initial perturbation beyond a critical limit [102, 116]. However, thermal effects reduce the maximum amplitude require for wave breaking for two reasons. Firstly, the tendency of the plasma density to increase to infinity is opposed by plasma pressure. Secondly, the thermal velocity of particles moving in the direction of the wave enables them to be trapped at a lower amplitude than if they were initially at rest. Thermal corrections were not obtained until 1971 when Coffey [121], using a 1-D until 1971 when Coffey [121], using a 1-D waterbag fluid description, obtained the fluid description, obtained the nonrelativistic formula $eE_{max}/(m\omega_{pe}v_{ph}) = (1 - \beta/3 - 8\beta^{1/4}/3 - 2\beta^{1/2})^{1/2}$, where $\beta = 3T/mv_{ph}^2$.

Wang et al. [122] extended the study of nonlinear plasma oscillations beyond breaking by solving the fluid equations numerically using the Lagrange description for the electrons and have seen multistream flow and generation of fast electrons when the initial amplitude of the perturbation becomes greater than the so called wave breaking amplitude. It is to be emphasized that though the authors did not study long time evolution of plasma oscillations in the breaking regime, they predicted that after the wave breaking coherent oscillation energy transform into disordered electron kinetic energy. Thus it is generally believed that after the wave breaking, plasma gets heated and all energy of the wave goes to the randomized kinetic energy of particles. There is also a possibility that in a warm plasma some particles might get trapped in the wave and lead to the selfconsistent generation of BGK type waves [113]. It may therefore be interesting to explore the physics of nonlinear plasma oscillations beyond wave breaking.

We know that nonlinear plasma waves can be used in particle acceleration and the phenomenon of wave breaking leads to conversion of wave energy into random kinetic energy of the particle. Both the features can be seen in cold plasma electrostatic instability, known as Buneman instability which involves streaming of electron with respect to ions. It is associated with novel physical effects like double layer formation, anomalous resistivity etc. [123, 124]. Double layers can be used in particle acceleration and potential explosion, due to collapse of double layers, converts collective energy into thermal energy. It would be interesting if one could use the above methods (Lagrange variables) to get an exact description of the formation and collapse of double layers.

1.3 Scope of the thesis

Rest of the chapters of this thesis are organized as follows. Chapter 2, deals with the space time evolution of large amplitude plasma oscillations initiated by an arbitrary density perturbation which can be expressed as the Fourier series in "x" in a cold homogeneous plasma. We also show in this chapter the usefulness of our solution by describing the space time evolution of square wave, triangular wave and Dawson like initial density perturbations. We obtain wave breaking condition for square wave and triangular wave profiles and recover wave breaking limit for Dawson like profile using the inequality proposed by Davidson et al. [116]. A special two mode case (where the initial energy is distributed only over two commensurate mode) is also studied in this chapter and 1-D particle in cell has been done to verify the evolution and breaking for this case. Moreover, we study in this chapter the evolution and breaking of more general two mode case, where the second mode need not be an integral multiple of the fundamental mode and recover the case of Davidson et al. [116] and commensurate two mode case for different set of initial conditions. In chapter 3, we study the behavior of nonlinear oscillation in a cold dissipative homogeneous plasma. Here we first present the results from the fluid simulation for viscous and resistive cold plasma and reproduce earlier results [118]. We further show that the results remain unchanged even for the realistic case where viscosity coefficient is chosen to be independent of density. Moreover we study the behavior of nonlinear oscillation in cold plasma for another dissipative mechanism by substituting viscosity with hyper-viscosity along with the resistivity and find the same results as reported in Ref. [118]. We also discuss, in this chapter, the physics behind the nonlinear effects and introduce a simple relation between the breaking amplitude of nonlinear oscillations and the viscosity/hyper-viscosity coefficients. Chapter 4 deals with the excitation and breaking of longitudinal relativistic plasma waves (Akhizer-Polovin waves). In this chapter we first construct the longitudinal traveling wave solution of Akheizer and Polovin [119] from the exact space and time dependent solution of relativistic cold electron fluid equations due to Infeld and Rowlands [107]. Moreover, we suggest an alternative derivation of the Akheizer Polovin solution after making the standard traveling wave ansatz. Furthermore, we load AP type initial conditions in the relativistic sheet code and show their propagation in all physical variable with out any dissipation up to 1000's of plasma periods. We next show in this chapter that if we add a very small amplitude longitudinal perturbations to these waves, they show an explosive behavior after some time (decided by amplitudes of the AP wave and the perturbation) due to phase mixing effect. We also show that the scaling of phase mixing can be interpreted from Dawson's formula for phase mixing in inhomogeneous plasma [102]. In chapter 5, we study the nonlinear oscillation and waves in an arbitrary mass ratio cold plasma. Here we first make a choice of initial conditions such that we see pure oscillations at the linear level and phase mixing comes nonlinearly due to ponderomotive forces only. We also demonstrate the existence of nonlinear electron-ion traveling waves in an arbitrary mass ratio cold plasma which do not exhibit phase mixing due to absence of ponderomotive forces and zero frequency mode. Lastly in this chapter we show that cold plasma BGK waves [116, 120] phase mix away when ions are allowed to move and the scaling of phase mixing is found to be different from earlier work [106]. In this case zero frequency mode is found to be the only candidate responsible for phase mixing as ponderomotive force for waves is zero. Chapter 6 describes the study of plasma oscillations beyond wave breaking which is done by using 1-D particle in cell simulation and it is shown that after the wave breaking all energy of a standing plasma oscillation does not end up as the random kinetic energy of particles but some fraction always remains with two oppositely propagating coherent BGK like modes with supporting trapped particle distributions. The randomized energy distribution of untrapped particles is found to be characteristically non-Maxwellian with a preponderance of energetic particles. Chapter 7 deals with the development and collapse of double layers which is studied using method of Lagrange variables. Finally in chapter 8, we summarize all the problems addressed in this thesis.

Chapter 2

Nonlinear evolution of an arbitrary density perturbation in a cold homogeneous unmagnetized plasma

In the present chapter exact and general analytical solutions describing the nonlinear evolution of a large amplitude plasma oscillation initiated by arbitrary density perturbations are found. Analytical results have been verified using 1-D PIC simulation.

2.1 Introduction

The basic physics of nonlinear evolution of large amplitude plasma oscillations is well illustrated by the exact solution of cold plasma fluid equations by Davidson *et al.* [116, 117]. The solution strategy involves transforming the fluid equations to a co-moving coordinate frame (Lagrange coordinates) where the equations become linear, and hence are easily solved. The general features of the solution becomes clear when the solution in Lagrange coordinates is transformed back to the lab frame (Eulerian frame) for a model set of initial condition where all the electrostatic energy (ESE) is loaded on a single long wavelength mode. This solution shows coherent oscillations at the plasma frequency with the energy sloshing back and forth between the initial mode and higher nonlinearly excited modes, provided the initial normalized density perturbation $\delta n/n_0 \leq 0.5$. Beyond this limit the oscillations break and energy contained in coherent motion gets converted into random motion.

The above conclusion, as mentioned before, has been derived with an initial condition where only a single well defined mode (“k”) is excited. In present day laser/beam-plasma experiments where $E^2/(8\pi nT) >> 1$, it is natural to expect that the exciting mechanism (laser, electron beam, electrical pulse etc.) will in general excite a wave packet with energy distributed over several modes. Such a kind of excitation of wave packets has also been seen in simulation [125, 126]. Therefore, both from the point of view of experiments and simulations, it is of utmost importance to study the spatio-temporal evolution of a wave packet, where the initial electrostatic energy is distributed over multiple modes.

In this chapter, we report a general solution in the lab frame describing the nonlinear oscillations initiated by an arbitrary density perturbation which can be expressed as a Fourier series. This general solution thus, in principle describes the evolution of different type of periodic density perturbations. We first use this solution to reproduce the earlier results of Davidson-Schram [116, 117] and Dawson [102] using appropriate initial conditions. We next show the usefulness of our solution by deriving, as examples, the space time evolution for a square wave and a triangular wave. Furthermore, we present a very special case where the total ESE is loaded over two commensurate modes (say “k” and 2“k”). Here we get two wave breaking limits depending on how the total ESE is distributed over these two modes. One of them shows, that addition of a second harmonic increases the wave breaking limit of the fundamental mode. This may have relevance for particle acceleration studies of breaking wake fields.

Furthermore, we study more general two mode case and obtain an exact solution for the space time evolution of two incommensurate modes, where second mode need not be an integral multiple of the fundamental mode. We recover earlier single mode [116, 117] and two mode cases for $\Delta_2 = 0$, $\Delta k = k$ respectively.

In section.(2.2), we first, present the basic cold plasma fluid equations and the general solution in Lagrangian coordinates for an arbitrary initial density profile, which is actually a Fourier series in “x” with zero initial velocity profile. The general solution is inverted from Lagrangian coordinates to Eulerian coordinates following the method of Davidson *et al.* [116]. In subsections.(2.2.1) and (2.2.2), we respectively recover the earlier results of Davidson & Schram [116] and Dawson

[102] from our general solution. In addition, we recover the wave breaking limit given in Ref. [102]. In section.(2.3), we present, as examples, the evolution and wave breaking limit for a square wave and a triangular wave as initial density profiles. In section.(2.4), we study a very special case where the initial ESE is loaded over first two modes. Section.(2.5) contains 1-D PIC simulation [128] results for this special case. In section.(2.6), we study evolution of two incommensurate modes and recover Davidson's, commensurate mode solutions for special choice of Δ_2 and Δk. At the end, our results are summarized in section.(2.7).

2.2 Governing equations and the General solution

The basic equations describing the evolution of an arbitrary electrostatic perturbation in an unmagnetized cold homogeneous plasma with immobile ions are

$$\frac{\partial v_e}{\partial t} + v_e \frac{\partial v_e}{\partial x} = -\frac{eE}{m} \tag{2.1}$$

$$\frac{\partial n_e}{\partial t} + \frac{\partial (n_e v_e)}{\partial x} = 0 \tag{2.2}$$

$$\frac{\partial E}{\partial x} = 4\pi e(n_0 - n_e) \tag{2.3}$$

where the symbols have their usual meaning. Exact solution of the above set of equations is well known [116] and can be written in terms of Lagrange coordinates (x_0, τ) as

$$v_e(x_0, \tau) = V(x_0)\cos(\omega_{pe}\tau) + \omega_{pe} X(x_0)\sin(\omega_{pe}\tau) \tag{2.4}$$

$$E(x_0, \tau) = -\frac{m}{e}\omega_{pe}\left[\omega_{pe} X(x_0)\cos(\omega_{pe}\tau) - V(x_0)\sin(\omega_{pe}\tau)\right] \tag{2.5}$$

$$n_e(x_0, \tau) = \frac{n_e(x_0, 0)}{\left[1 + \frac{1}{\omega_{pe}}\frac{\partial V}{\partial x_0}\sin(\omega_{pe}\tau) + \frac{\partial X}{\partial x_0}(1 - \cos\omega_{pe}\tau)\right]} \tag{2.6}$$

where Lagrange and Euler coordinates (x, t) are related by

$$x = x_0 + \frac{1}{\omega_{pe}} V(x_0) \sin(\omega_{pe}\tau) + X(x_0)(1 - \cos\omega_{pe}\tau),\ t = \tau \tag{2.7}$$

It is to be noted that the solution depends on two arbitrary functions of x_0 viz. $X(x_0)$ and $V(x_0)$ which are related to the initial density and velocity profile as

$$\frac{\partial X}{\partial x_0} = \frac{n_e(x_0, 0)}{n_0} - 1,\ V(x_0) = v_e(x_0, 0) \tag{2.8}$$

The general wave breaking condition, can be easily obtained by using the fact that density is a physical parameter and can never be negative, which is

$$n_e(x_0, 0) > \frac{n_0}{2} \tag{2.9}$$

This inequality was first derived by Davidson *et al.* [116, 117]. Physically, circumstances in which this inequality is violated for some range(s) of x_0, lead to the development of multi-stream flow within half the period of a plasma oscillation as oscillation breaks. A point to be noted here is that wave breaking condition is actually extracted from the initial density profile where the Euler and the Lagrange coordinates are identical.

Let us now take the initial density and velocity profiles as $n_e(x_0, 0) = n_0 \Bigg[1 + \sum_{n=1}^{\infty} a_n cos(nkx_0)\Bigg]$, $v_e(x_0, 0) = 0$. Therefore the set of Eqs.(2.4)-(2.7) will become

$$v_e(x_0, \tau) = \frac{\omega_{pe}}{k} \sin(\omega_{pe}\tau) \sum_{n=1}^{\infty} \frac{a_n}{n} sin(nkx_0) \tag{2.10}$$

$$E(x_0, \tau) = -\frac{m\omega_{pe}^2}{ek} \cos(\omega_{pe}\tau) \sum_{n=1}^{\infty} \frac{a_n}{n} sin(nkx_0) \tag{2.11}$$

$$n_e(x_0, \tau) = \frac{n_e(x_0, 0)}{1 + 2\sin^2(\omega_{pe}\tau/2) \sum_{n=1}^{\infty} a_n cos(nkx_0)} \tag{2.12}$$

$$kx = kx_0 + \alpha(\tau)\sum_{n=1}^{\infty}\frac{a_n}{n}sin(nkx_0), \qquad t = \tau \tag{2.13}$$

Here $\alpha(\tau) = 2\sin^2(\omega_{pe}\tau/2)$. Thus, set of Eqs.(2.10)-(2.13) give the evolution of an arbitrary density perturbation in terms of Lagrange coordinates. Now we transform from Lagrangian to Eulerian coordinates (Fluid frame of reference to Lab frame of reference) following the method of Ref. [116]. We define $f(kx_0) = \sum_{n=1}^{\infty}\frac{a_n}{n}sin(nkx_0)$. So the transcendental Eq.(2.13) becomes $kx(x_0,\tau) = kx_0 + \alpha(\tau)f(kx_0)$. Since $f(kx_0)$ is a periodic function of x, therefore it can be expressed as a Fourier series in x i.e. $f(kx_0) = \sum_{m=1}^{\infty}b_m(t)sin(mkx)$, where $b_m(t)$ is found to be

$$\begin{aligned} b_m(t) = \prod_{s=1}^{\infty}\sum_{l_s=-\infty}^{+\infty}J_{l_s}(\frac{m\alpha a_s}{s})\Bigg[\sum_{n=1}^{\infty}\frac{a_n}{n}\Big\{\delta_{m-n+\sum_{p=1}^{\infty}pl_p,0} \\ -\delta_{m+n+\sum_{p=1}^{\infty}pl_p,0}\Big\} + \frac{\alpha}{2}\sum_{n=1}^{\infty}\frac{a_n}{n}\sum_{q=1}^{\infty}a_q \\ \Big\{\delta_{m-n+q+\sum_{p=1}^{\infty}pl_p,0} + \delta_{m-n-q+\sum_{p=1}^{\infty}pl_p,0} \\ -\delta_{m+n+q+\sum_{p=1}^{\infty}pl_p,0} - \delta_{m+n-q+\sum_{p=1}^{\infty}pl_p,0}\Big\}\Bigg] \end{aligned} \tag{2.14}$$

Now from Eqs.(2.10) and (2.11) we can easily write velocity and electric field in Lab frame as

$$v_e(x,t) = \frac{\omega_{pe}}{k}\sin(\omega_{pe}t)\sum_{m=1}^{\infty}b_m(t)\sin(mkx) \tag{2.15}$$

$$E(x,t) = -\frac{m\omega_{pe}^2}{ke}\cos(\omega_{pe}t)\sum_{m=1}^{\infty}b_m(t)\sin(mkx) \tag{2.16}$$

and using Eq.(2.16) in Poisson's equation (5.5), electron density can be expressed as

$$n_e(x,t) = n_0[1 + \cos(\omega_{pe}t)\sum_{m=1}^{\infty}mb_m(t)\cos(mkx)] \tag{2.17}$$

We have thus obtained a general solution in the lab frame for an arbitrary perturbation. This solution which gives the density profile as a function of space and time, besides being of intrinsic interest is also superior than numerically interpolating the real space-Lagrangian formula [Eqs.(2.7),(2.13)] to obtain spatio-temporal evolution of of density profile. This is because, near the wave breaking point calculation of "x_0" for a given "x" by numerically inverting Eqs.(2.7),(2.13) may lead to singularities. By choosing different form of a_n's, it is possible to obtain the earlier results of Davidson & Schram [116], where electron density is perturbed sinusoidally and Dawson [102] where the particle position is perturbed sinusoidally (as shown in subsections.(2.2.1) and (2.2.2)), and the evolution of other periodic disturbances like a triangular wave and a square wave (as shown in section.(2.3)).

We note here that in a recent publication, Infeld *et al.* [118] have analytically solved for nonlinear oscillations excited by an arbitrary initial density perturbation in a cold, viscous and resistive plasma. The authors have left their solution in Lagrange coordinates and did not give inversion in the Lab frame. A close look at Eqs.(21a)-(21b) of ref. [118] reveals that inversion of their solution in the Lab frame is included in our solution just by reading $a_n\alpha(\tau)/n$ as $-A_nG_n(t)$.

2.2.1 Sinusoidal perturbation in the density

Assuming all a_n's, except a_1, to be zero, and therefore putting $n=1$, $s=1$ $p=1$, $q=1$ in Eq.(2.14) and using the recurrence relation $2nJ_n(z)=z[J_{n+1}(z)+J_{n-1}(z)]$, we get $b_m(t)=\frac{(-1)^{m+1}}{m}\frac{2}{\alpha(t)}J_m[m\alpha a_1]$. This together with set of Eqs.(2.15)-(2.17) gives the evolution of sinusoidal density perturbation [116, 117]. The general wave breaking condition (2.9), in this case gives $a_1<0.5$ [116, 117].

2.2.2 Sinusoidal perturbation in the particle position

In this case, the initial conditions are given in terms of displacements; $\xi(x_{eq},0)$, of the particles from their equilibrium positions, x_{eq}. Here the initial conditions are chosen to be $\xi(x_{eq},0)=A\sin(kx_{eq})$, $v_e(x_{eq},0)=0$, where "A" has dimension of length. Therefore at t=0 the Euler position of the electron and electric field are respectively expressed as $kx_0=kx_{eq}+kA\sin(kx_{eq})$ and $E=4\pi en_0A\sin(kx_{eq})$. Here $\sin(kx_{eq})$ can be written as a Fourier series in x_0 i.e. $\sin(kx_{eq})=\sum_{n=1}^{\infty}c_n\sin(nkx_0)$

with $c_n = \frac{(-1)^{n+1}}{n}\frac{2}{kA}J_n[nkA]$. Thus, using the expression for electric field in terms of x_0 and Poisson's equation, the initial electron density is found to be $n_e(x_0, 0) = n_0\Big[1 + 2\sum_{n=1}^{\infty}(-1)^n J_n[nkA]\cos(nkx_0)\Big]$. From this it is clear that space and time evolution of this density profile is given by set of Eqs. (2.14)-(2.17) with $a_n = 2(-1)^n J_n[nkA]$.

We now use the inequality (2.9) to recover the Dawson's wave breaking limit i.e. $-\sum_{n=1}^{\infty}(-1)^n J_n(nkA)\cos(nkx_0) < \frac{1}{4}$. Here we see that this series will have a maxima only at $kx_0 = 2m\pi$, m = 0,1,2..and so on. Therefore putting $kx_0 = 0$ and using the identity $\sum_{n=1}^{\infty} J_n(n\beta) = \frac{\beta}{2(1-\beta)}$ we get $kA < 1$.

2.3 Evolution and breaking of square and triangular wave profiles

We now present as an example space time evolution and breaking limit of a square wave density profile, with height δ and wavelength 2π, which can be expressed as a Fourier series in x as $n_e(x_0, 0) = n_0\big[1 + \frac{4\delta}{\pi}\sum_{n=1}^{\infty}\frac{(-1)^{n+1}}{n}\sin(\frac{n\pi}{2})\cos(nkx_0)\big]$. It is clear that the square wave is nothing but a particular form of our general density profile with very special a_n's. Now from the inequality (2.9) we find $\frac{4\delta}{\pi}\sum_{n=1}^{\infty}\frac{(-1)^n}{n}\sin(\frac{n\pi}{2})\cos(nkx_0)\big] < \frac{1}{2}$. This series will have a maxima only at $kx_0 = \pi$, therefore we have $\frac{4\delta}{\pi}\sum_{n=1}^{\infty}\frac{1}{n}\sin(\frac{n\pi}{2}) < \frac{1}{2}$. L.H.S. of this inequality is the well known Leibniz series and its value is $\pi/4$. Thus we conclude that a square wave profile will not break as long as $\delta < 0.5$ and oscillate like a sine wave as predicted in Ref. [127].

We next present as a second example, evolution of a triangular wave profile with height δ and wavelength 2π, which can be written as a Fourier series in 'x' i.e. $n_e(x_0, 0) = n_0\Bigg[1 + \frac{8\delta}{\pi^2}\sum_{n=1,3,5..}^{\infty}\frac{1}{n^2}\cos(nkx_0)\Bigg]$. This profile will also evolve in space and time as given by Eqs.(2.14) to (2.17) and the wave breaking limit can be obtained using the inequality (2.9) i.e. $-\frac{8\delta}{\pi^2}\sum_{n=1,3,5..}^{\infty}\frac{1}{n^2}\cos(nkx_0) < \frac{1}{2}$. This series has a maxima at $kx_0 = \pi$. Now using the identity $\sum_{n=1,3,5..}^{\infty}\frac{1}{n^2} = \frac{\pi^2}{8}$ and putting $kx_0 = \pi$ we get $\delta < \frac{1}{2}$. Thus we see that a triangular wave profile will also not break if its height δ is less than 0.5.

It is to be noted that for the triangular and the rectangular case, the wave breaking condition can also be obtained even without the Fourier series representation. In fact, wave breaking points for both profiles can also be seen from their respective graphical plots. Here we have used the Fourier representation for illustrative purpose.

2.4 First two modes are non-zero

Let us now consider a case where all a_n's are zero for $n > 2$; then the density profile can be expressed as $n_e(x_0, 0) = n_0[1+a_1\cos(kx_0)+a_2\cos(2kx_0)]$. Now in Eq.(2.14) expanding n, s, p and q from 1 to 2 and doing some algebra we get the evolution of two modes in space and time. Using the wave breaking condition (2.9) we get $-a_1\cos(kx_0) - a_2\cos(2kx_0) < 1/2$. Let $G(kx_0) = -a_1\cos(kx_0) - a_2\cos(2kx_0)$. In order to get the wave breaking limits we need to evaluate the maxima's of $G(kx_0)$. For $a_1 > 4a_2$, $G(kx_0)$ has a maxima at $kx_0 = \pi$ and for $a_1 < 4a_2$ $G(kx_0)$ has a maxima at $kx_0 = \cos^{-1}(-1a_1/4a_2)$. Using these, the two wave breaking limits are (i) $(a_1 - a_2) < 0.5$ for $a_1 > 4a_2$, (ii) $(\frac{a_1^2+8a_2^2}{8a_2}) < 0.5$ for $a_1 < 4a_2$. When compared with the results of Davidson *et al.* [116, 117], the first wave breaking limit presents a very interesting situation. If all the initial ESE is loaded on the fundamental mode (i.e. $a_2 = 0$), the wave will break if the amplitude of the fundamental mode $a_1 \geq 0.5$. But if we add a very small perturbation to the next higher mode, wave does not break even when $a_1 > 0.5$. We have verified this interesting observation using 1-D PIC simulation [128], which we present in the next section.

2.5 Results from the simulation

We have done a electrostatic 1-D PIC simulation [128] using the following parameters : total number of particles (N) $\sim 3 \times 10^5$, number of grid points (NG) $\sim 3 \times 10^4$, time step $\Delta t \sim \pi/50$ and system length (L) $\sim 2\pi$. We have used periodic boundary conditions and all physical quantities are normalized as $x \to kx$, $t \to \omega_{pe}t$, $n_e \to n_e/n_0$, $v_e \to v_e/(\omega_{pe}k^{-1})$ and $E \to keE/(m\omega_{pe}^2)$, where ω_{pe} is the plasma frequency and 'k' is the wave number of the longest (fundamental) mode.

Fig.(2.1) shows the spatial profile of the electron number density at various time steps for $a_1 = 0.6$ and $a_2 = 0.0$. This value for a_1 is clearly beyond the wave breaking point for the single mode case. The appearance of sharp spikes (blue

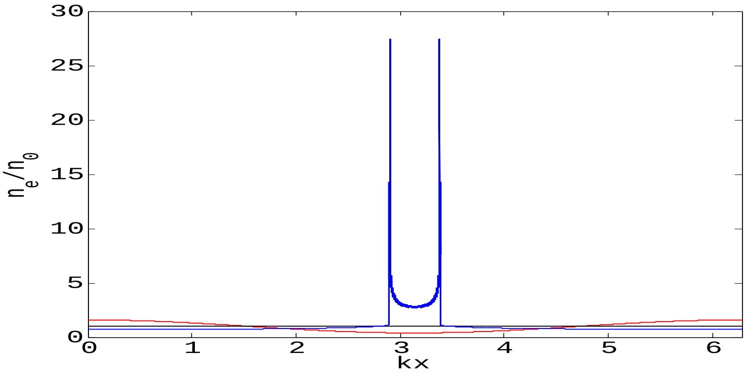

Figure 2.1: Numerical plot of electron density at $a_1 = 0.6$ and $a_2 = 0.0$ where red line shows the profile at $\omega_{pe}t = 0$, black line at $\omega_{pe}t = \pi/2$ and blue line at $\omega_{pe}t = \pi$

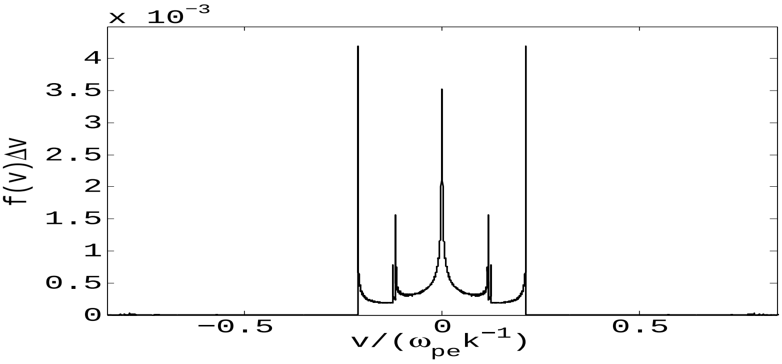

Figure 2.2: Velocity distribution of electrons at $a_1 = 0.6$, $a_2 = 0.0$ and $\omega_{pe}t = 2\pi$

lines) in the density profile at $\omega_{pe}t = \pi$, is a clear indicator of wave breaking. Physically, at the wave breaking point, the energy contained in the initial mode goes irreversibly into self-consistently excited high "k" modes. This generation of high “k” modes shows up in the density profile as sharp “spikes”. Resonant interaction of these high “k” modes with the particles causes the particles to accelerate, resulting in multistream flow (another signature of wave breaking [102]). This is shown in Fig.(2.2) for the same parameters as in Fig.(1) at $\omega_{pe}t = 2\pi$, which gives the probability of finding a particle with velocity lying between v and $v + \Delta v$, and is independent of total number of simulation particles. The magnitude of a streamer at a given value of “v” is thus determined by the fraction of total number of particles interacting resonantly with a mode “k” such that $v \sim \omega_{pe}/k$.

Fig.(2.3), which shows density profiles at different times with two modes, clearly shows coherent oscillations even when the amplitude of the fundamental mode is beyond the wave breaking limit for a single mode. It thus shows that addition of a second mode enhances the wave breaking limit of the fundamental mode. The points (‘*’) on the density profile are a result of analytical calculation. We see here a good agreement between our analytical calculation and numerical results.

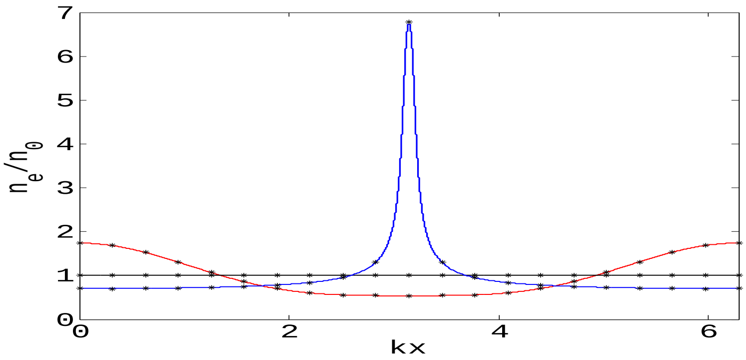

Figure 2.3: Numerical vs analytical (‘*’) plot of electron density at $a_1 = 0.6$ and $a_2 = 0.14$ where red line represents the profile at $\omega_{pe}t = 0$, black line at $\omega_{pe}t = \pi/2$ and blue line at $\omega_{pe}t = \pi$

Fig.(2.4) where we present the harmonic content of density profile for the single mode case ($\delta n/n_0 \sim 0.6$) and the two mode case [$(\delta n/n_0)_k \sim 0.6$,$(\delta n/n_0)_{2k} \sim 0.14$] beyond the wave breaking time ($\omega_{pe}t = 3\pi/2$) further supports the above mentioned fact. For the single mode case at $\omega_{pe}t = 3\pi/2$, the wave is already broken

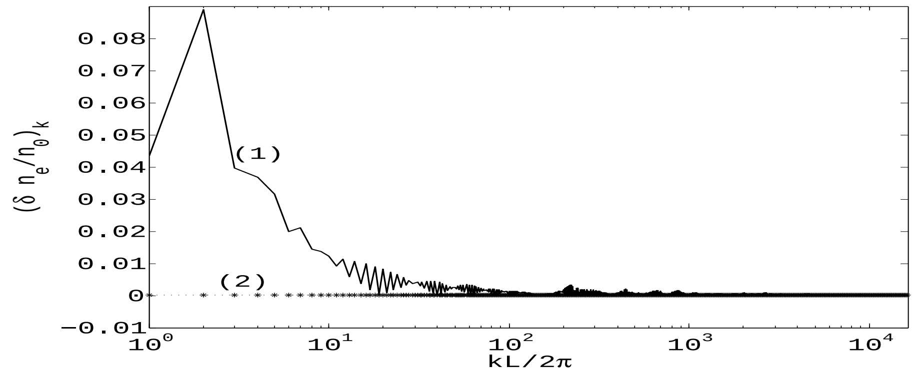

Figure 2.4: Number density vs mode number at $a_1 = 0.6$, $a_2 = 0.0$ shown by curve (1) (solid line'-') and at $a_1 = 0.6$, $a_2 = 0.14$ shown by curve (2) (line points '*') at $\omega_{pe}t = 3\pi/2$

and the energy is spread over several modes. This is shown by curve(1) in Fig.(4). For the two mode case at $\omega_{pe}t = 3\pi/2$, the density profile after exhibiting a peak at $\omega_{pe}t = \pi$, comes back to the equilibrium. The curve(2) in Fig.(4) thus shows negligible energy distribution over modes. Thus we observe that the addition of a second mode avoids breaking of wave even when the amplitude of the fundamental mode is as high as ~ 0.6. Physically, this happens because the addition of the "2k" perturbation to the fundamental mode ("k" perturbation) produces a destructive interference at the peak of the 'k' mode with the result that the wave breaking condition is not satisfied anywhere .

In the next section, we are now going to present the case of two incommensurate modes.

2.6 Evolution and breaking of incommensurate modes

Let us take the initial density and velocity profiles as below:

$$n_e(x_0, 0) = n_0[1 + \delta_1 \cos kx_0 + \delta_2 \cos(k + \Delta k)x_0], v_e(x_0, 0) = 0 \tag{2.18}$$

Now the set of Eqs.(2.4)-(2.7) will become

$$v_e(x_0,\tau) = \frac{\omega_{pe}}{k}\sin\omega_{pe}\tau[\delta_1 \sin kx_0 + \frac{k\delta_2}{k+\Delta k}\sin(k+\Delta k)x_0] \tag{2.19}$$

$$E(x_0,\tau) = -\frac{m\omega_{pe}^2}{ek}\cos\omega_{pe}\tau[\delta_1 \sin kx_0 + \frac{k\delta_2}{k+\Delta k}\sin(k+\Delta k)x_0] \tag{2.20}$$

$$n_e(x_0,\tau) = \frac{n_e(x_0,0)}{1+(1-\cos\omega_{pe}\tau)(\delta_1\cos kx_0 + \delta_2\cos(k+\Delta k)x_0)} \tag{2.21}$$

$$kx(x_0,\tau) = kx_0 + \alpha(\tau)f(x_0) \tag{2.22}$$

Here $\alpha(\tau)$ is given by

$$\alpha(\tau) = 2\sin^2\omega_{pe}\tau/2 \tag{2.23}$$

and $f(x_0)$ is expressed as :

$$f(x_0) = \delta_1 \sin kx_0 + \frac{k\delta_2}{k+\Delta k}\sin(k+\Delta k)x_0 \tag{2.24}$$

Again $f(x_0)$ can be written as the Fourier series of x:

$$f(x_0) = \sum_{n=1}^{\infty} a_n(t)\sin nkx \tag{2.25}$$

Now from Eqs.(2.19) and (2.20), we can easily express velocity and the electric field in the lab frame as

$$v_e(x,t) = \frac{\omega_{pe}}{k}\sin\omega_{pe}t\sum_{n=1}^{\infty} a_n(t)\sin nkx \tag{2.26}$$

$$E(x,t) = -\frac{m\omega_{pe}^2}{ek}\cos\omega_{pe}t\sum_{n=1}^{\infty} a_n(t)\sin nkx \tag{2.27}$$

Equation.(2.27) together with Poisson's equation gives an expression for electron density as

$$n_e(x,t) = n_0[1+\cos\omega_{pe}t\sum_{n=1}^{\infty} na_n(t)\cos nkx] \tag{2.28}$$

Now from Eq.(2.25), a_n can be written as

$$a_n(t) = \frac{k}{\pi}\int_0^{\frac{2\pi}{k}} f(x_0)\sin nkxdx \tag{2.29}$$

Solving Eq.(2.29) we get an exact expression for $a_n(t)$

$$\begin{aligned} a_n(t) = (-1)^n \sum_{m=-\infty}^{+\infty} J_m(\frac{z\delta_2}{k'\delta_1})[(-1)^{mk'}\delta_1\{J_{n+mk'+1} - J_{n+mk'-1}\} \\ -(-1)^{mk'}\frac{z\delta_1}{2n}\{J_{n+mk'-2} - J_{n+mk'+2}\} \\ +\frac{\delta_2}{k'}\{(-1)^{(m-1)k'}J_{n+(m-1)k'} - (-1)^{(m+1)k'}J_{n+(m+1)k'}\} \\ +\frac{z\delta_2^2}{2nk'\delta_1}\{(-1)^{(m-2)k'}J_{n+(m-2)k'} - (-1)^{(m+2)k'}J_{n+(m+2)k'}\} \\ +\frac{z\delta_2}{2n}(1+\frac{1}{k'})\{(-1)^{(m+1)k'}J_{n+1+(m+1)k'} - (-1)^{(m-1)k'}J_{n-1+(m-1)k'}\} \\ +\frac{z\delta_2}{2n}(1-\frac{1}{k'})\{(-1)^{(m-1)k'}J_{n+1+(m-1)k'} - (-1)^{(m+1)k'}J_{n-1+(m+1)k'}\}] \end{aligned} \tag{2.30}$$

Here $k' = \frac{k+\Delta k}{k}$, $J_s \equiv J_s[z]$ and z$=n\alpha(\tau)\delta_1$

Eq.(2.30) together with Eqs.(2.26)-(2.28) gives an exact solution for the evolution of incommensurate modes in cold plasma. We can easily recover single mode case [116] just by putting $\delta_2 = 0$ in Eq.(2.30). One can also recover earlier derived commensurate case just by substituting $\Delta k = k$. For incommensurate waves, breaking occurs when $\delta_1 + \delta_2 > 0.5$ for all Δks, except $\Delta k = 0.5k$ and k. As for these cases, both the waves superpose in such a way that wave breaking condition (2.9) is not satisfied even though $\delta_1 + \delta_2 > 0.5$.

2.7 Summary

In summary, we have given, in this chapter, the exact evolution of an arbitrary density profile which can be expressed as a Fourier series in x in the lab frame. This solution describes a realistic situation where a bunch of modes are excited initially. In our work, we have taken an initial density profile which is represented by a general Fourier series. In order to illustrate the calculation of wave breaking condition for series like profiles, we have presented examples of triangular wave, rectangular wave and Dawson like perturbations. For the specific case with two modes, we find that if all the initial ESE is loaded on the fundamental mode (i.e. $a_2 = 0$), the wave will break if the amplitude of the fundamental mode $a_1 \geq 0.5$ [116]. But if we add a very small perturbation to the next higher mode, wave does not break even when $a_1 > 0.5$. This interesting observation has been verified using 1-D PIC simulation. Moreover, we have studied a more general two mode case where second mode need not be an integral multiple of the fundamental mode. It would be interesting to carry out experiments that would follow the space time evolution and wave breaking limits as predicted by the theory and seen in the simulation.

In the next chapter, we are going to study the behavior of nonlinear oscillations if one includes dissipative (viscous/hyperviscous and resistive) effects in the cold plasma model.

Chapter 3

Nonlinear oscillations in a cold dissipative plasma

Recently, it has been shown that, when viscosity and resistivity is included in the cold plasma model, nonlinear plasma oscillations exhibit two new nonlinear effects. First one is that plasma oscillations do not break even beyond the critical amplitude and the second one is that the density peak splits into two [Infeld *et al.*, Phys. Rev. Lett. 102, 145005 (2009)]. Infeld *et al.* have analytically derived these results for a specific model of viscosity as $4/3\nu_e = \nu(n_0/n_e(x,t))$. In a realistic case however, electron viscosity has a relatively weak dependence on density through Coulomb logarithm. In this work, firstly Infeld's result is numerically extended for the more realistic case where electron viscosity is chosen to be independent of density and secondly an alternative electron dissipative mechanism is studied by substituting viscosity with hyper-viscosity. In both cases, results are found to be qualitatively similar to Infeld *et al.* . Moreover, we obtain an analytical expression describing the wave breaking criteria for both viscous and hyperviscous cases.

3.1 Introduction

The subject of large amplitude oscillations and waves in a cold homogeneous plasma has retained the interest of plasma physicists for a long time, mainly because of two reasons. Firstly, it belongs to a class of nonlinear problems which is exactly solvable analytically using the methods of Lagrangian hydrodynamics

[117] and secondly it serves as a useful paradigm to illustrate the physics of many plasma based experiments where large amplitude oscillations/waves are excited.

The problem which had defied an exact solution till recently was cold plasma nonlinear oscillation with the addition of viscous term to fluid-Maxwell equations. In the absence of viscosity and resistivity, Davidson-Schram solution [116] shows that when a cold homogeneous plasma is excited with energy loaded on a single mode, coherent nonlinear oscillations appear with the energy moving back and forth between the single initial mode and a large number of nonlinearly excited higher modes, and this entire process happens at the plasma frequency. The appearance of large number of higher modes results in the formation of a density peak which occurs once in a plasma period. Coherent nonlinear plasma oscillations occur only when the amplitude of the initial density perturbation $\delta n/n_0$ is kept below 0.5. Above this value the oscillations break and the energy loaded on the initial mode goes into random particle motion.

In a recent publication, it has been shown that when viscosity and resistivity are included in the cold plasma model, nonlinear plasma oscillations exhibit a new nonlinear effect in the form of splitting of density peak, and oscillations do not break even when the amplitude of the density perturbation $\delta n/n_0$ is greater than 0.5 [118]. In order to make the problem analytically tractable, the authors have modeled the viscous term in a way which makes the viscosity coefficient depend inversely on the local electron density $n_e(x,t)$. They have argued in their paper, that if n_e/n_0 (where n_0 is the equilibrium density) is "*not much different from unity and T_e (electron temperature) = constant*", then their modelling of viscosity coefficient is approximately consistent with equation (5a) of ref. [118]. In reality however, during the course of oscillation, specifically when the initial density perturbation is close to the breaking point, n_e/n_0 becomes considerably different from unity, which makes their modelling of viscosity coefficient inaccurate. A close look at equation (5a) of ref. [118] shows that viscosity coefficient actually has a relatively weak dependence on density through Coulomb logarithm.

Therefore in this work, we have first studied the nonlinear oscillations in a cold viscous and resistive plasma with a constant viscosity coefficient by neglecting the weak density dependence. Our aim here is to see whether the new nonlinear effects as seen in ref. [118] persist even in the absence of inverse density dependence of viscosity coefficient. With a constant viscosity coefficient, the cold plasma fluid

Maxwell's equations are not amenable to Lagrangian treatment. We have thus done a fluid simulation of the problem using a flux corrected transport code [129]. We observe that the same new nonlinear effect in the form of splitting of density peak persists although in a slightly different parameter regime, clearly indicating that this effect is not due to inverse dependence of viscosity coefficient on local electron density as chosen in ref. [118].

If there are some turbulence effects in the plasma, oscillations may damp faster than the normal dissipation due to viscosity and the plasma may be considered as hyper-viscous. Therefore, we have further studied the effect of hyper-viscosity on cold plasma nonlinear oscillations, where we have replaced the viscous term with a hyper-viscosity term. Here, following Infeld *et al.* [118] we have chosen the hyper-viscosity coefficient to depend inversely on the cube of local electron density. This has been done, so that the problem yields to Lagrangian methods. Here again, we find that the same nonlinear effect in the form of splitting of density peak appears.

In section.(3.2), we first present the basic governing equations, give a brief description of our code and present a validation of our code against the analytical results [118]. We next present our simulation results for the case where viscosity coefficient is independent of density. Section.(3.3), contains our analytical work on nonlinear cold plasma oscillations with hyper-viscosity. In section.(3.4) we derive an analytical relation which describes how wave breaking amplitude modifies in the presence of viscosity and hyperviscosity. Finally in section.(3.5) we present a summary of our results.

3.2 Nonlinear plasma oscillations with viscosity and resistivity

The basic equations governing the evolution of large amplitude oscillation in a cold homogeneous, unmagnetized, viscous and resistive plasma with immobile ions, are the continuity equation, momentum equation and Poisson's equation which in normalized form are

$$\frac{\partial n_e}{\partial t} + \frac{\partial (n_e v_e)}{\partial x} = 0 \tag{3.1}$$

$$\frac{\partial v_e}{\partial t} + v_e \frac{\partial v_e}{\partial x} = -E + \frac{1}{n_e}\frac{\partial}{\partial x}\left(\nu_e \frac{\partial v_e}{\partial x}\right) - \eta v_e \tag{3.2}$$

$$\frac{\partial E}{\partial x} = 1 - n_e \tag{3.3}$$

Where the dimensionless form is obtained by $x \to k^{-1},\ t \to \omega_{pe}^{-1},\ n_e \to n_0,\ E \to \frac{m\omega_{pe}^2}{ke},\ v_e \to \frac{\omega_{pe}}{k},\ \nu_e \to \frac{3mn_0\omega_{pe}}{4k^2},\ \eta \to \frac{m\omega_{pe}}{n_0 e^2}$. Here ν_e is the electron viscosity, η is the plasma resistivity; the other symbols have their usual meaning. We now model $\nu_e(x,t)$ as $\nu_e = \nu\Big(\frac{1}{\bar{n}_e(x,t)}\Big)^{\alpha},\ \nu \to \frac{mn_0\omega_{pe}}{k^2}$ is a constant, where $\alpha = 1$ corresponds to the ref. [118].

We now solve equations (3.1)-(3.3) using a fluid code (LCPFCT) based on a flux corrected transport scheme [129] which is a generalization of the two step Lax-Wendroff scheme [130]. Equations (3.1)-(3.3) are solved using periodic boundary conditions with initial conditions as

$$n_e(x,0) = 1 + \Delta\cos x,\ v_e(x,0) = 0,\ E(x,0) = -\Delta\sin x \tag{3.4}$$

We now present results for $\alpha = 1$ [118] and $\alpha = 0$ which is the constant viscosity case.

3.2.1 $\alpha = 1$ (viscosity coefficient inversely depends on density)

In this subsection, the evolution of a sinusoidal density profile in space and time, for $\alpha = 1$, is presented, for the same parameters as were used in ref. [118], this is done to validate our code against the analytical results.

Fig.(3.1) shows the space-time evolution of density profile for $\alpha = 1$, and for the same parameters as were used in ref. [118] *i.e.* $\Delta = 0.55$, $\nu = 0.03$ and $\eta = 2 \times 10^{-5}$. As time progresses, the damping of nonlinear oscillations is clearly observed, as predicted in ref. [118]. Fig.(3.2) shows the evolution of electron density for $\Delta = 0.55$, $\nu = 0.2$ and $\eta = 2 \times 10^{-4}$ and we find bifurcation in the density peak as was shown in ref.[118]. In both the figures, the lines show the numerical results and the points ('*') show the analytical profile. It is clear from these figures that our code reproduces the analytical results [118] quite well.

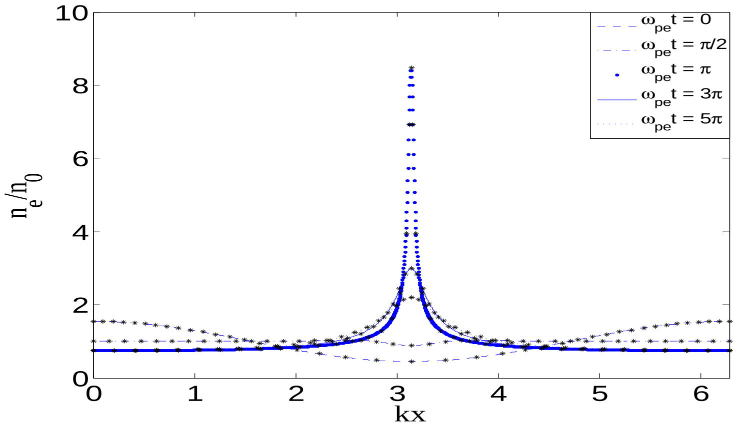

Figure 3.1: Numerical versus analytical ('*') plot of $n_e(x,t)$ in a viscous and resistive plasma with $\alpha = 1$, $\Delta = 0.55$, $\nu = 0.03$, $\eta = 2 \times 10^{-5}$ at various time steps

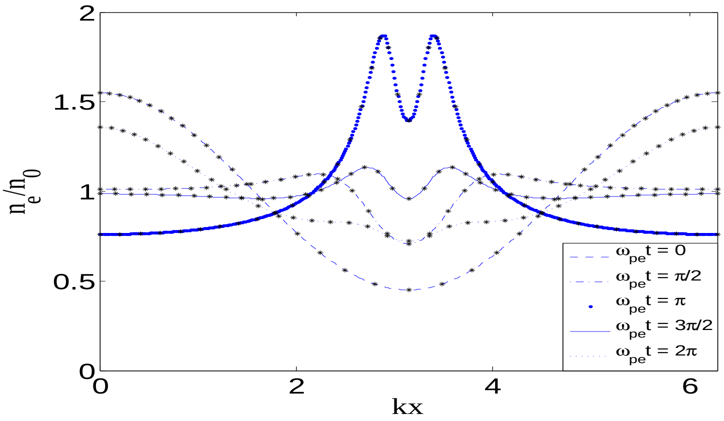

Figure 3.2: Numerical versus analytical ('*') plot of $n_e(x,t)$ in a viscous and resistive plasma with $\alpha = 1$, $\Delta = 0.55$, $\nu = 0.2$, $\eta = 2 \times 10^{-4}$

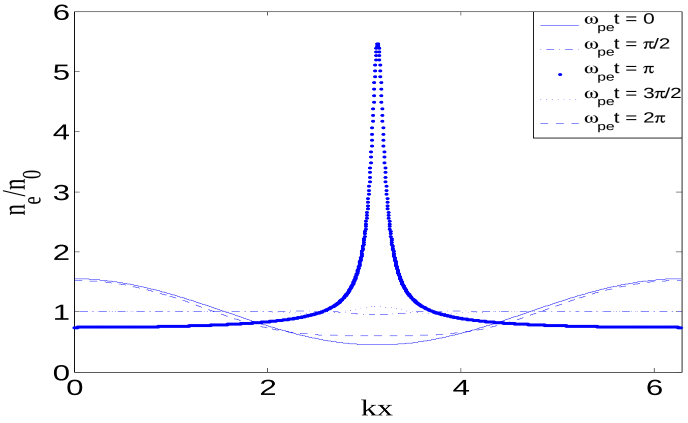

Figure 3.3: Numerical plot of $n_e(x, t)$ in a viscous and resistive plasma for one plasma oscillation with $\alpha = 0$, $\Delta = 0.55$, $\nu = 0.03$, $\eta = 2 \times 10^{-5}$

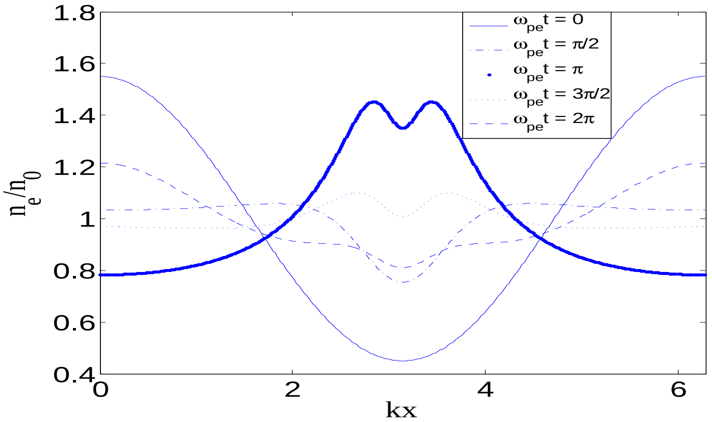

Figure 3.4: Numerical plot of $n_e(x, t)$ in a viscous and resistive plasma for one plasma oscillation with $\alpha = 0$, $\Delta = 0.55$, $\nu = 0.35$, $\eta = 2 \times 10^{-3}$

3.2.2 $\alpha = 0$ (viscosity coefficient is constant)

In this subsection, the evolution of electron density is presented for constant viscosity coefficient *i.e.* for this case, where electron viscosity is not a function of density. Fig.(3.3) shows evolution of density profile for $\alpha = 0$, and parameters $\Delta = 0.55$, $\nu = 0.03$ and $\eta = 2 \times 10^{-5}$; and again we observe nonlinear damped oscillations similar to that as seen in ref. [118]. Fig.(3.4) again shows the bifurcation in the density peak for $\Delta = 0.55$, $\nu = 0.35$ and $\eta = 2 \times 10^{-3}$. Thus it is clear that the new nonlinear effects, *i.e.* the observed bifurcation of density peak and the non-breaking of plasma oscillations even beyond the critical amplitude are not restricted to the viscosity model of ref. [118] as they are seen even for the constant viscosity coefficient.

3.3 Nonlinear Plasma Oscillations with hyper-viscosity and resistivity

We, now investigate the effects of hyper-viscosity on cold plasma oscillations by replacing viscosity with hyper-viscosity. For hyper-viscous case, the momentum equation in normalized form can be written as

$$\frac{\partial v_e}{\partial t} + v_e \frac{\partial v_e}{\partial x} = -E - \frac{1}{n_e} \frac{\partial}{\partial x} \left(\nu_{hy} \frac{\partial^3 v_e}{\partial x^3} \right) - \eta v_e \tag{3.5}$$

Equation (3.5) together with equations (3.1) and (3.3) describes the evolution of large amplitude oscillations in a hyper-viscous and resistive plasma. Here ν_{hy} is the electron hyper-viscosity coefficient and η is the plasma resistivity.

In order to solve above equations analytically, we model $\nu_{hy}(x,t)$ as $\nu_{hy} = \nu_h / n_e^3(x,t)$; $\nu_h =$ constant. This choice of "n_e" dependence may be consistent with some turbulence models of anomalous hyperviscosity.

Let us now choose the Lagrange coordinates as

$$x = x_{eq} + \xi(x_{eq}, \tau), \;\; t = \tau.$$

Here "x_{eq}" is the equilibrium position of an electron fluid element (*i.e.* the position when the electrostatic force on the fluid element is zero) and $\xi(x_{eq}, \tau)$ is the displacement from the equilibrium position. In terms of Lagrange coordinates, the convective derivative becomes $\frac{\partial}{\partial\tau} = \frac{\partial}{\partial t} + v_e \frac{\partial}{\partial x}$ and the continuity equation becomes

$$\frac{\partial x_{eq}}{\partial x} = n_e(x,t) \tag{3.6}$$

and therefore momentum equation (3.5) can finally be written as

$$\frac{\partial v_e}{\partial \tau} = -E - \nu_h \frac{\partial^4 v_e}{\partial x_{eq}^4} - \eta v_e \tag{3.7}$$

Further, Poisson's equation combined with Ampere's law, in Lagrange coordinates, gives

$$\frac{\partial E}{\partial \tau} = v_e \tag{3.8}$$

Now differentiating equation (3.7) with respect to "τ" and using equation (3.8) we get

$$\frac{\partial^2 v_e}{\partial \tau^2} + \nu_h \frac{\partial^4}{\partial x_{eq}^4}\frac{\partial v_e}{\partial \tau} + \eta \frac{\partial v_e}{\partial \tau} + v_e = 0 \tag{3.9}$$

which is a linear partial differential equation for $v_e(x_{eq},\tau)$ with constant coefficient. Writing the solution of equation (3.9) as a sum of normal modes of the form $exp[i(nx_{eq} - \omega\tau)]$, we get

$$v_e = \sum_{n=1}^{\infty} A_n exp(-\alpha_n \tau)\sin(\omega_n \tau)\sin(nx_{eq}) \tag{3.10}$$

where A_n is the amplitude of a normal mode and $\omega = -i\alpha_n \pm \omega_n$, with $\alpha_n = \frac{1}{2}(n^4\nu_h + \eta)$ and $\omega_n = \sqrt{1-\alpha_n^2}$. Here we have chosen $v_e(x_{eq},0) = 0$ and $v_e(0,\tau) = 0$. Using equation (3.8) and (3.10), the electric field can now be written as

$$E(x_{eq},\tau) = -\sum_{n=1}^{\infty} A_n G_n(\tau)\sin(nx_{eq}) \tag{3.11}$$

where

$$G_n(\tau) = exp(-\alpha_n \tau)\Big[\alpha_n \sin(\omega_n \tau) + \omega_n \cos(\omega_n \tau)\Big] \tag{3.12}$$

To calculate the electron density, we write Poisson's equation in Lagrange variables as $\frac{\partial E}{\partial x_{eq}} = \frac{1}{n_e} - 1$ which finally gives

$$n_e(x_{eq}, t)^{-1} = 1 - \sum_{n=1}^{\infty} nA_n G_n(t) \cos(nx_{eq}) \tag{3.13}$$

The relation between the Lagrange variable "x_{eq}" and the Euler variable "x" can be found from equation (3.6) and Poisson's equation as

$$x = x_{eq} + E(x_{eq}, \tau) \tag{3.14}$$

Using equations (3.11) and (3.14) the coefficients A_n's can be related to the initial electric field as

$$A_n = -\frac{1}{n\pi} \int_0^{2\pi} \cos[nx_0 - nE(x_0, 0)]dx_0 \tag{3.15}$$

where $x_0 = x_{eq} + \xi(x_{eq}, 0) = x_{eq} + E(x_{eq}, 0)$ is the initial Euler coordinate of a fluid element. The set of equations (3.10)-(3.12) and (3.13) describes the space-time evolution of an electron fluid, in terms of Lagrange coordinates for an arbitrary initial density perturbation, in a cold hyper-viscous and resistive plasma. The relation between Euler and Lagrange coordinate is given by equation (3.14).

Now we present, as an example, evolution of a sinusoidal initial density perturbation as $n_e(x_0, 0) = 1 + \Delta \cos x_0$. From Poisson's equation (3.3), electric field, in the lab frame, at t = 0 can be expressed as $E(x_0, 0) = -\Delta \sin x_0$ and therefore equation (3.15) takes the form $A_n = (-1)^{n+1} \frac{2}{n} J_n[n\Delta]$. This expression of A_n together with set of equations (3.10)-(3.14) gives the evolution of a pure sinusoidal density perturbation in a cold, hyper-viscous and resistive plasma. Fig.(3.5) shows the space time evolution of a sinusoidal density profile in the lab frame (Euler coordinates) for $\nu_h = 0.002$, $\eta = 2 \times 10^{-6}$ and $\Delta = 0.55$. Fig.(3.6) shows the same for a different set of parameters *viz.* $\nu = 0.03$, $\eta = 2 \times 10^{-5}$ and $\Delta = 0.55$. The splitting of the density peak is clearly seen in this case.

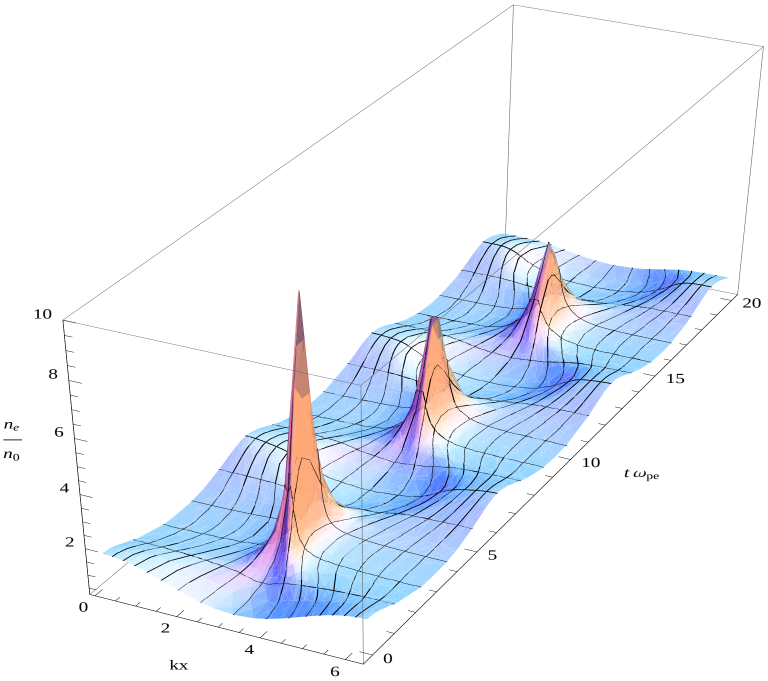

Figure 3.5: Analytical plot of $n_e(x,t)$ a hyper-viscous and resistive plasma with $\Delta = 0.55$, $\nu_h = 0.002$, $\eta = 2 \times 10^{-6}$

3.4 Relation between breaking amplitude and viscous/hyper-viscous coefficient

For Dawson like initial condition [102] equation (3.11) at $t = 0$ takes the form as

$$\xi(x_{eq}, 0) = -A_1\omega_1 \sin x_{eq}$$

Now the general breaking condition [102]

$$\frac{\partial\xi}{\partial x_{eq}} > -1$$

gives $A_1\omega_1 < 1$, i.e. $A_1 < 1/\omega_1$, where $\omega_1 = \sqrt{1-\alpha_1^2} = \sqrt{1-(\nu_h+\eta)^2/4}$. i.e. $A_1 < 1/(\sqrt{1-(\nu_h+\eta)^2/4})$. Due to absence of '$n$' this relation is true for both

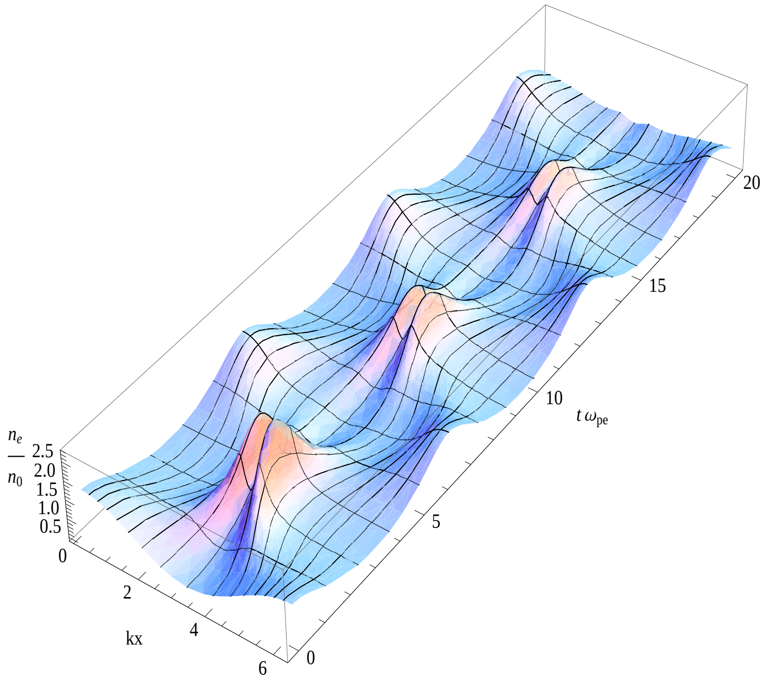

Figure 3.6: Analytical plot of $n_e(x,t)$ in a hyper-viscous and resistive plasma with $\Delta = 0.55$, $\nu_h = 0.03$, $\eta = 2 \times 10^{-5}$

viscous and hyper-viscous case, therefore we drop the subscript *'h'* i.e.,

$$A_1 < \frac{1}{\sqrt{1 - (\nu + \eta)^2/4}} \tag{3.16}$$

Above equation, in terms of actual plasma parameters, modifies as

$$kA_1 < \frac{1}{\sqrt{1 - [4\nu_e k^2/(3m_e n_0 \omega_{pe}) + \eta n_0 e^2/(m_e \omega_{pe})]^2/4}} \tag{3.17}$$

Thus we see that nonlinear oscillations in the cold dissipative plasma initiated by Dawson like initial condition, do not break as long as above inequality is satisfied. Note here that if there is no viscosity/hyper-viscosity and resistivity in the plasma i.e.; $\nu_e = \eta = 0$, breaking condition modifies as $kA_1 < 1$, which is the wave breaking criteria obtained by Dawson [102] for the cold homogeneous plasma model. Thus we see that the wave breaking condition in the cold dissipative plasma is consistent with the wave breaking condition in the non-dissipative plasma [102]. It is also to be noted here that the inclusion of even a small dissipation in the cold plasma enhances the critical (wave breaking) amplitude significantly.

3.5 Summary

In summary, we have numerically studied nonlinear plasma oscillations in a cold, viscous and resistive plasma, where the electron viscosity coefficient is chosen to be independent of density. This is in contrast to the study carried out in a recent publication [118] where authors have chosen the electron viscosity coefficient to depend inversely on density, to allow for analytical treatment. Our studies are closer to the realistic case where electron viscosity has a weak dependence on density through Coulomb logarithm. We observe that our results are similar to that of ref.[118], and hence conclude that that new nonlinear effect (splitting of density peak) observed in ref. [118] is independent of the model for viscosity coefficient. We have further analytically studied an alternative electron dissipative mechanism by substituting viscosity with hyper-viscosity, using Lagrangian methods. We observe that in a certain parameter regime, the same nonlinear effect *i.e.* splitting of the density peak is seen. This new nonlinear effect *i.e.* bifurcation of the density peak may be explained on the basis of interference between initial mode and nonlinearly excited modes during the course of oscillation. It is clear from the linear dispersion relation that viscosity affects different modes differently by introducing wave number dependent damping and frequency shifts, the latter leading to shifts in their relative phases. Some of these modes interfere destructively with the initial mode and produce a dip at the center. It is to be noted that resistivity alone does not produce any splitting or interference effects because the frequency shift introduced is wave number independent. We have confirmed this concept further by incorporating a small thermal correction to the non-dissipative cold plasma model and verifying that the wavelength dependent thermal frequency shifts again lead to interference and peak splitting effects. Moreover, we obtain a wave breaking criterion for Dawson like initial condition which clearly show that if we include dissipative (viscous or hyperviscous) terms, it does not remove the phenomenon of wave breaking completely but increases the critical amplitude.

In all studies presented up to this chapter,motion of the electron fluid was hitherto treated as nonrelativistic. However, in order to study very large amplitude plasma waves/oscillations we need to include the relativistic corrections in the equation of motion. In the next chapter we are going to study relativistic electron plasma waves/oscillations in a cold plasma.

Chapter 4

Breaking of longitudinal Akhiezer-Polovin waves

It is well known that breaking amplitude of longitudinal Akhiezer-Polovin (AP) waves approaches to infinity when their phase velocity is close to speed of light [119]. However, Infeld and Rowlands [107] have shown that relativistic plasma oscillations break at arbitrarily small amplitude as frequency acquires a spatial dependence for almost all initial conditions. In order to show a connection between both the theories, we first obtain the initial conditions which excite traveling AP waves, once substituted in the exact solution of Infeld and Rowlands [107]. Later, we demonstrate using the 1-D simulation based on Dawson sheet model, that AP waves break at arbitrarily small amplitude through the process of phase mixing when subjected to very small perturbation. Results from the simulation show a good agreement with the Dawson phase mixing formula for inhomogeneous plasma.This result may be of direct relevance to the laser/beam plasma wakefield experiments.

4.1 Introduction

The problem of propagation of relativistically intense nonlinear plasma waves traveling close to the speed of light has been a problem of great interest from the viewpoint of plasma methods which may be used for accelerating particles to very high energies. An exact solution for relativistic traveling waves in cold plasma was first reported by Akhiezer and Polovin [119]. It is to be noted here that Akhiezer and Polovin demonstrated the existence of these waves without worrying about how they can be excited in real plasma. Later it has been shown analytically [1] that when an ultra-short, ultra-intense laser pulse propagates through underdense plasma, the waves which get excited in the wake of the laser pulse are nothing but AP waves. One of the important properties of these waves is that their frequency depends on their amplitude in such a way that larger the amplitude, smaller the frequency will be. This happens due to increase in the mass of the electrons because of relativistic effects. Second important property of these waves is that their breaking amplitude is very high and can be expressed as $eE_{wb}/(m\omega_{pe}c) = \sqrt{2}(\gamma_{ph}-1)^{1/2}$, here $\gamma_{ph} = 1/\sqrt{(1-v_{ph}^2/c^2)}$ is the relativistic factor associated with the phase velocity v_{ph} of the AP waves. Note here that as $v_{ph} \to c$, $\gamma_{ph} \to \infty$, this implies $E_{wb} \to \infty$. In other words we can say that for highly relativistic plasma waves breaking amplitude becomes too high to break. Breaking property of the relativistic plasma oscillations has also been studied by Infeld and Rowlands by obtaining an exact space and time dependent solution for the relativistic fluid equations in Lagrange coordinates. In contrast to the wave breaking criteria as suggested by Akhiezer and Polovin [119], the authors [107] have shown that their solution shows an explosive behavior (wave breaking) for almost all initial conditions. The authors have shown that relativistic effects bring position dependence in the plasma frequency, as a result plasma oscillations phase mix away and break at arbitrarily small amplitude. On the other hand, the authors accepted that AP waves are very special case of their solution as these waves do not show explosive behavior and need a special set of initial conditions to set them up. However, the authors have not shown how their solution leads to class of traveling waves (do not show explosive behavior), i.e., what initial conditions should be chosen in their solution so as to get AP waves. Elucidation of initial conditions leading to AP traveling waves might show the connection between the theories of Akhiezer & Polovin [119] and Infeld & Rowlands [107]. Besides one may need to worry about sensitivity to initial conditions because the manner AP waves are excited in the plasma may introduce some noise (due to group velocity dispersion of the pulse, thermal effects etc) along with the AP waves.

Therefore, in this chapter we first show what initial conditions we should choose in the solution of Infeld and Rowlands such that we get AP wave solution. We next perform relativistic sheet simulation [108] in order to study the sensitivity of large amplitude AP waves due to small perturbations. We find that AP waves are very sensitive and their breaking criterion as given in ref.[119] does not really hold in the presence of perturbations. Physically, it happens due to phase mixing effect [108] as frequency of the system which is constant for pure AP waves, acquires a position dependence in the presence of perturbations.

In the section.(4.2) we obtain traveling AP wave solution from space time dependent solution of Infeld and Rowlands [107]. Section.(4.5) contains an alternative derivation of AP wave solution. In section.(4.3) we present results from the simulation. In section.(4.4) we show a good match between analytical and numerical scaling of phase mixing time. Finally in section(4.5) we summarize all the results.

4.2 Relativistic fluid equations and Lagrange solution

The basic equations describing the evolution of an arbitrary electrostatic perturbation in an unmagnetized cold homogeneous plasma with immobile ions are

$$\Big(\frac{\partial}{\partial t}+v\frac{\partial}{\partial x}\Big)p=-eE \tag{4.1}$$

$$\frac{\partial n}{\partial t}+\frac{\partial (nv)}{\partial x}=0 \tag{4.2}$$

$$\frac{\partial E}{\partial x}=4\pi e(n_0-n) \tag{4.3}$$

$$\frac{\partial E}{\partial t}=4\pi env \tag{4.4}$$

where $p=\gamma mv$ is momentum and $\gamma=1/\sqrt{1-v^2/c^2}$ is relativistic factor, n_0 is the back ground ion density and other symbols have their usual meaning.

We now introduce Lagrange coordinates (x_{eq},τ) which are related to Euler coordinates as

$$x=x_{eq}+\xi(x_{eq},\tau), \quad t=\tau \tag{4.5}$$

here ξ is the the displacement from the equilibrium position x_{eq} of the electron fluid (sheet). Using Eq.(4.5),set of Eqs.(4.1)-(4.4) again can be combined as

$$\frac{d^2p}{d\tau^2} + \omega_{pe}^2 \frac{p}{[1 + p^2/(m^2c^2)]^{1/2}} = 0 \tag{4.6}$$

Integrating once Eq.(4.6) we get

$$\frac{dp}{d\tau} = \pm\sqrt{2}m\omega_{pe}c\big[a(x_{eq}) - [1 + p^2/(m^2c^2)]^{1/2}\big]^{1/2} \tag{4.7}$$

Here 'a' is the first integration constant which is a function of position 'x_{eq}'. Let us again substitute

$$a - [1 + p^2/(m^2c^2)]^{1/2} = (a - 1)\sin^2\alpha \tag{4.8}$$

Solution of Eq.(4.7) can be expressed as

$$\omega_{pe}\tau = \sqrt{2(a+1)}E(\alpha,\kappa) - \sqrt{\frac{2}{a+1}}F(\alpha,\kappa) + \Phi(x_{eq})$$

$$\omega_{pe}\tau = \frac{2}{\kappa'}E(\alpha,\kappa) - \kappa' F(\alpha,\kappa) + \Phi(x_{eq}) \tag{4.9}$$

Here Φ is the second integration constant which is also a function of x_{eq} and

$$\kappa = \left[\frac{a-1}{a+1}\right]^{1/2}, \quad \kappa' = \sqrt{1-\kappa^2} \tag{4.10}$$

Thus set of Eqs.(4.8)-(4.10) together with Eq.(4.5) gives the space-time evolution of relativistic Langmuir waves initiated by an arbitrary perturbation. This exact solution was first obtained by Infeld and Rowlands [107]. The frequency of the wave is obtained by integrating equation (4.9) over "α" from 0 to $\pi/2$, as

$$\omega = \omega_{pe}\frac{\pi}{2}\frac{\kappa'}{[2E(\kappa) - \kappa' K(\kappa)]} \tag{4.11}$$

Note here that the equations (4.10)-(4.11) together with equation (4.5) give an exact dependence of frequency on the initial spatial position of sheets. We are now going to construct plane wave solution from this non-trivial space-time dependent solution. We know that

$$p = \gamma m v = \frac{\dot{\xi}}{\sqrt{1 - \dot{\xi}^2/c^2}} \tag{4.12}$$

From Eqs.(4.8) and (4.12) we can easily get an expression for $\dot{\xi}$ and ξ as

$$\dot{\xi} = c\frac{(2\kappa/\kappa'^2)\cos\alpha[1 - \kappa^2\sin^2\alpha]^{1/2}}{[1 + 2(\kappa^2/\kappa'^2)\cos^2\alpha]} \tag{4.13}$$

$$\xi = \frac{c}{\omega_{pe}}\frac{2\kappa}{\kappa'}\sin\alpha \tag{4.14}$$

Now subtract $\omega_{pe}x/\beta$ on both sides of Eq.(4.9) and using Eqs.(4.5),(4.14) we get

$$\begin{aligned} \omega_{pe}(t - x/\beta) = {} & \frac{2}{\kappa'}E(\alpha,\kappa) - \kappa' F(\alpha,\kappa) \\ & -\omega_{pe}\frac{x_{eq}}{\beta} - \frac{c}{\beta}\frac{2\kappa}{\kappa'}\sin\alpha + \Phi(x_{eq}) \end{aligned} \tag{4.15}$$

Now we first choose 'a' to be independent of 'x_{eq}' and $\Phi(x_{eq})$ as follows

$$\Phi(x_{eq}) = \omega_{pe}\frac{x_{eq}}{\beta} \tag{4.16}$$

then Eq.(4.15) becomes

$$\begin{aligned} \omega_{pe}(t - x/\beta) = {} & \frac{2}{\kappa'}E(\alpha,\kappa) - \kappa' F(\alpha,\kappa) \\ & -\frac{c}{\beta}\frac{2\kappa}{\kappa'}\sin\alpha \end{aligned} \tag{4.17}$$

Thus we have obtained longitudinal plane wave solution from non-trivial space-time dependent solution with special choice of integration constants. One can note from Eq.(4.9) that, the frequency of the system will have a position dependence if "a" is a function of position and the solution will show an explosive behavior according to Infeld et al. [107]. However, we know that AP waves do not show explosive behavior, therefore "a" must be independent of 'x_{eq}' to excite AP wave. Moreover to make 'α' (or momentum) a function of $(t - x/\beta)$ alone restricts us to choose $\Phi(x_{eq})$ as $\omega_{pe}\frac{x_{eq}}{\beta}$. Thus, assuming 'a' to be independent of 'x_{eq}', Eqs.(4.9) and (4.16) together with Eqs.(4.13) and (4.14) give the velocity and displacement profiles of particles in the transcedental form which can be loaded easily in the relativistic PIC or sheet code to excite class of AP waves. On the other hand if initial conditions are not perfectly loaded but have some perturbations on them,the frequency may become a function of "x_{eq}" giving the possibility of bursty solutions and phase mixing effect. This is what we need to explore next.

4.3 Results from the simulation

In this section we perform relativistic sheet simulation based on Dawson sheet model in order to study the sensitivity of large amplitude AP waves to small amplitude longitudinal perturbations. For this purpose, we have used a relativistic sheet simulation code [108] where we solve the relativistic equation of motion for $\sim$ 10000 sheets, using fourth-order Runge-Kutta scheme for a specific choice of initial conditions (pure AP waves and AP waves with perturbations). Ordering of the sheets for sheet crossing is checked at each time step. Phase mixing/wave breaking time is measured as the time taken by any two of the adjacent sheets to cross over.

We first load AP type initial conditions (as discussed earlier in this chapter) in the relativistic sheet code and have seen smooth traveling structures in all physical variables (quantities) up to 1000's of plasma periods. Then we add a very small amplitude perturbation to the nonlinear AP wave and find that the structure breaks at a time decided by the "u_m" and "δ" (where "u_m" and "δ" are respectively the amplitude of the AP wave and the perturbation). In this way we show that AP waves are very sensitive to longitudinal perturbations and the wave breaking criterion does not hold in the presence of perturbations. In all the simulation runs we keep the phase velocity of AP waves close to speed of light i.e. $v_{ph} \sim 0.9995c$. Moreover, time is normalized to "ω_{pe}^{-1}" and distances are normalized to "$c\omega_{pe}^{-1}$". Figure.(4.1) shows the space-time evolution for the density profile of AP wave with maximum velocity amplitude $u_m \sim 0.81$. Thus we see that there is no numerical dissipation in our code and relativistic shift in the frequency is clearly visible. Now we add a sine wave (very small amplitude AP wave) to this large amplitude AP wave with wavelength same as the large amplitude AP wave and maximum velocity amplitude $\delta = 0.001$. Figure(4.2) shows the space and time evolution of the density

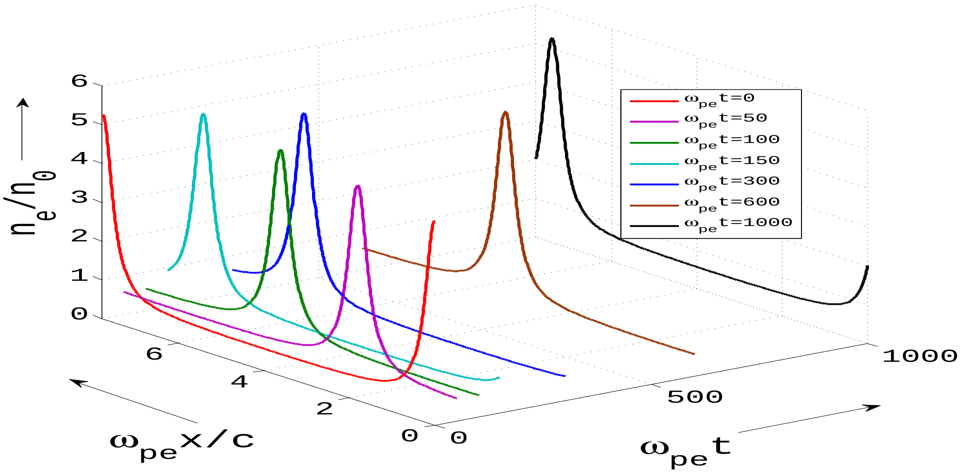

Figure 4.1: Space time evolution of electron density for pure AP wave of maximum velocity amplitude ($u_m = 0.81$) up to 1000's of plasma periods.

profile of the resultant structure up to the breaking point. As time progresses density peak becomes more and more spiky as energy is going irreversibly into the higher harmonics (a signature of phase mixing leading to wave breaking [108]) and the time at which neighboring sheets cross (wave breaking point) density burst can be seen.

Figure(4.3) shows the Fourier spectrum of pure AP wave and AP wave at the time of breaking. It is clear from the figure that a significant amount of energy has gone to the higher harmonics which is another signature of wave breaking. Thus we see that though breaking amplitude of AP wave for our choice of parameters is very high i.e., $eE_{wb}/(m\omega_{pe}c) \sim 7.8$, it breaks at a lower amplitude when perturbed slightly. Figure(4.4) contains the space-time evolution of electric field which clearly shows that maximum amplitude of the electric field is much less than 7.8 even at the time of breaking. In order to get a dependence of phase mixing time on the amplitude of the perturbation we repeat the numerical experiment such that maximum velocity amplitude of AP wave is kept fixed at $u_m = 0.55$ and amplitude of the perturbation δ is varied. In figure(4.5) points ('*') represent the results from the simulation which clearly indicate that as amplitude of the perturbation is

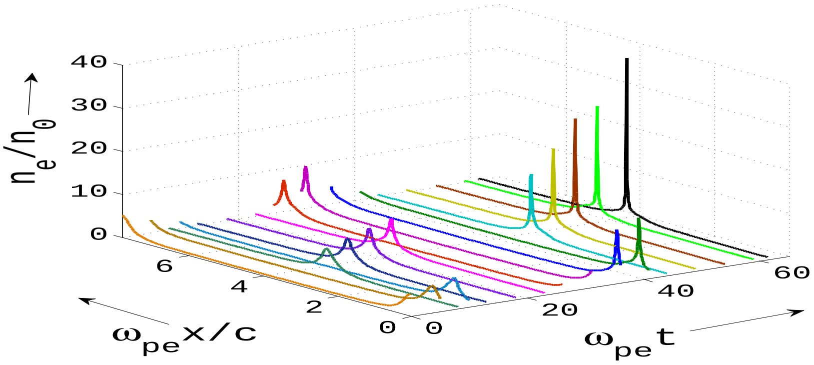

Figure 4.2: Space time evolution of electron density for AP wave of maximum velocity amplitude ($u_m = 0.81$) with perturbation amplitude $\delta = 0.001$.

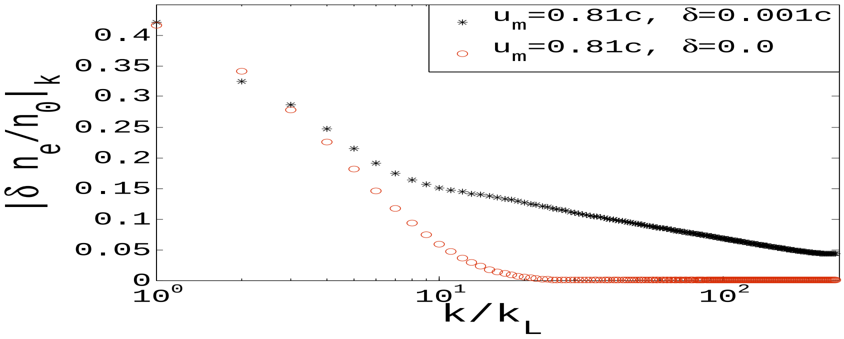

Figure 4.3: Fourier spectrum of pure AP wave ($u_m = 0.81$) and AP wave at the time of breaking due to perturbations ($\delta = 0.001$). Here "k_L" is the lowest wave number.

increased, phase mixing time of AP wave decreases. We perform another numerical

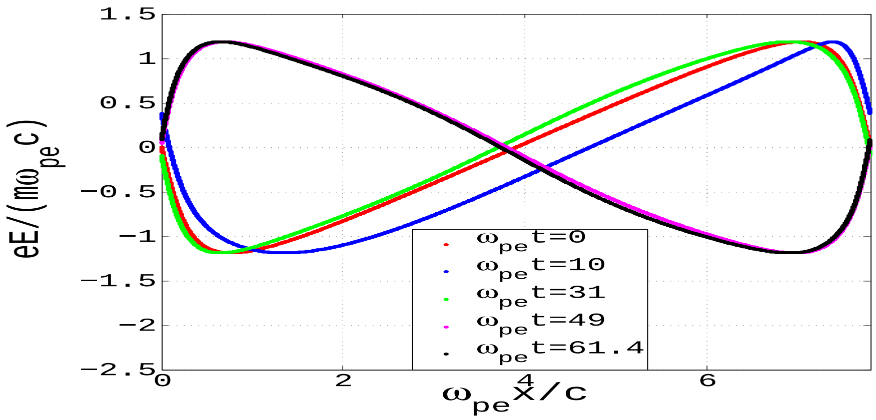

Figure 4.4: Space time evolution of electric field for AP wave of maximum velocity amplitude ($u_m = 0.81$) with perturbation amplitude $\delta = 0.001$.

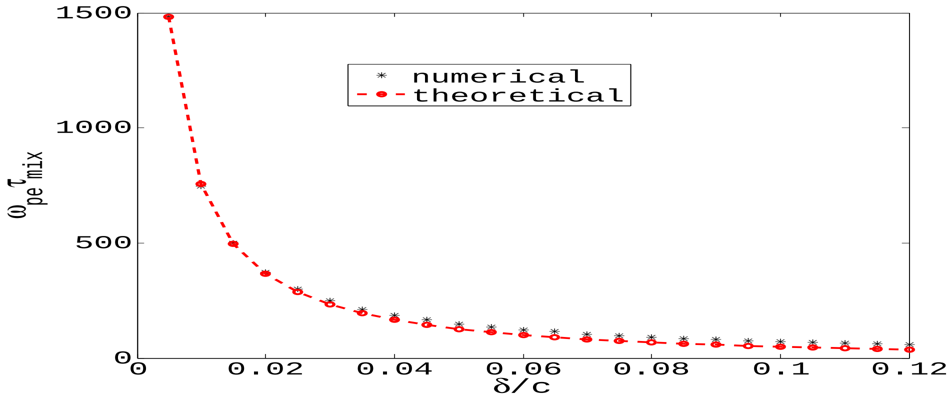

Figure 4.5: Theoretical ('-o') and numerical ('*') scaling of phase mixing time for a finite amplitude AP wave ($u_m = 0.55$) as a function of perturbation amplitudes δ.

experiment where amplitude of the perturbation is kept fixed at $\delta = 0.01$ and amplitude of the AP wave is varied. This case is presented in figure(4.6) by points

('*') which shows that for a finite longitudinal perturbation, smaller the amplitude of AP wave, longer is the phase mixing time.

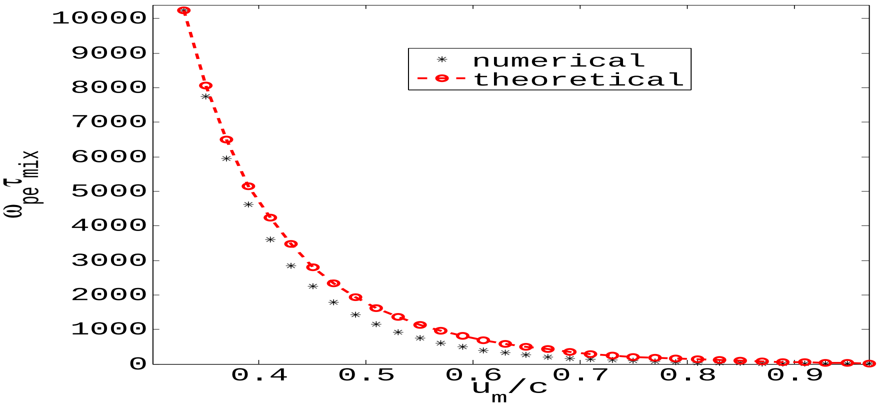

Figure 4.6: Theoretical ('-o') and numerical ('*') scaling of phase mixing time as function of amplitude of AP waves (u_m) in the presence of finite perturbation amplitude $\delta = 0.01$.

We know that relativistic plasma waves cannot accelerate particles indefinitely, but give us maximum acceleration only up to dephasing length or dephasing time. If phase mixing time is longer than dephasing time, phase mixing would not affect the acceleration process significantly. However, if the phase mixing time is shorter, maximum acceleration cannot be achieved as the wave gets damped before reaching the dephasing time because of phase mixing leading to breaking. Note here that numerical scaling in figure(4.5) gives a clue that we have to reduce the noise in the particle acceleration experiments in order to get maximum acceleration and the scaling presented in figure(4.6) gives an indication that if one cannot reduce the noise below a threshold, one must use smaller amplitude AP waves in order to avoid phase mixing effect and to gain maximum energy.

4.4 Match between theory and simulation

Along with the choice of initial conditions as made above, equations (4.13) and (4.14) together with equation (4.9) at $t = 0$ respectively give velocity and displacement profiles of sheets which are loaded in the code so as to excite a AP wave. We note here that with this choice of "a" ω (equation (4.11)) becomes independent of position and therefore no phase mixing occurs as shown in figure(4.1).

In figure(4.7) we plot frequency of the the system as a function of position for both pure AP wave and AP wave with perturbations. From this figure we clearly see that for pure AP wave frequency shows a flat dependence on position, i.e., each sheet oscillates with the same frequency and hence no phase mixing occurs. However, for nonzero 'δ', frequency of the system acquires a position dependence which gets stronger for larger value of 'δ'. Since frequency here becomes function of position , phase mixing happens [102, 103, 106, 108] which is responsible for the breaking of AP waves at arbitrary amplitude.

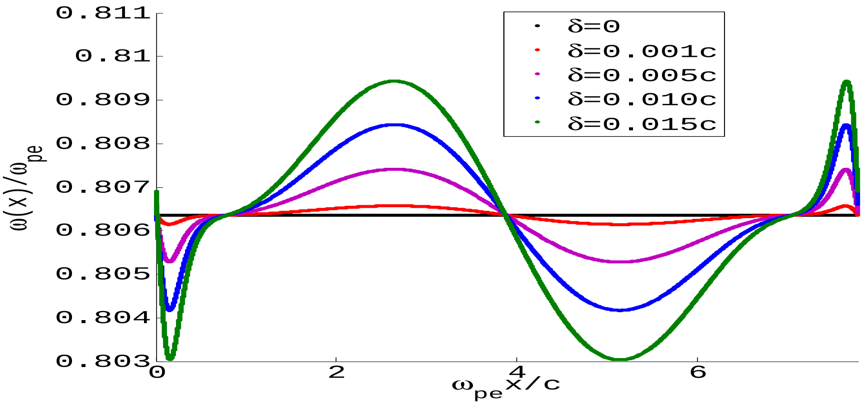

Figure 4.7: Frequency of the system as a function of position for fixed AP wave ($u_m = 0.81$) along with various perturbation amplitudes δ.

It is well known that plasma oscillations/waves phase mix away when the plasma frequency for some physical reason acquires a spatial dependence. In our case also frequency acquires a position dependence in the presence of perturbations. We therefore expect that scaling of phase mixing can be interpreted from Dawson's formula [102] for phase mixing in inhomogeneous plasma, which is

$$\omega_{pe}\tau_{mix} \sim \frac{1}{\frac{d\omega}{dx_{eq}}\xi}$$

From equation (4.11) we numerically evaluate $d\omega/dx_{eq}$ and use Dawson's formula [102] to get theoretical scaling of phase mixing time. In figures (4.5) and (4.6) solid lines represent the theoretical scaling of phase mixing time with "δ" and "u_m" which clearly show a good match between numerical experiments and theory.

4.5 Summary

In summary, we have first obtained the initial conditions to excite AP waves from the exact space time dependent solution of Infeld and Rowlands. Later, in order to validate our code we have used these initial conditions in the relativistic sheet code to show their propagation upto thousands of plasma periods in all physical variables. We have further added a small perturbation (sine wave) to the larger amplitude AP wave and found that AP wave show an explosive behavior (wave breaking) after finite time. In order to get a dependence of wave breaking time on the amplitude of the perturbation and amplitude of the AP wave, we have repeated the numerical experiment and found two results which are as follows. For a finite amplitude AP wave, larger the amplitude of the perturbation, smaller the wave breaking time is. Thus one has to reduce noise in the experiment in order to get maximum acceleration. Also for finite perturbation amplitude, smaller the amplitude of AP wave, larger the wave breaking time is. Thus one needs to work at smaller amplitude AP waves to gain maximum energy if the noise can not be reduced below a threshold. In order to gain an insight into the physics behind these results we have plotted plasma frequency with respect to the position and found that for pure AP wave, frequencies of the sheets shows a flat dependence on the position. On the other hand, if we add a small perturbation to the AP wave, frequency of the system acquires a spatial dependence which is responsible for phase mixing leading to wave breaking. We have also shown that scaling of phase mixing for both the results discussed above can be interpreted from Dawson's formula [102] . Thus we have shown that although breaking amplitude of AP waves is very high, they break at arbitrary amplitude via the process of phase mixing when perturbed slightly.

Therefore all those experiments/simulation which use AP wave breaking formula may require revisiting. For example, in a recent particle acceleration experiment [28] a maximum gain in the energy up to 200 MeV was observed. The authors used the the old formula for energy gain [2] (which is valid as long as $eE/(m\omega_{pe}c) \leq 1$) to interpret their observation. However, in their case $eE/(m\omega_{pe}c)$ was approximately 3.8 which is much greater than unity and therefore one has to use the energy gain expression for nonlinear waves [27]. If we do so, energy gain would have been approximately 975 MeV. This much energy can be obtained if the plasma wave accelerates particles upto the full dephasing length. However, from the experimental observation [28] it seems that wave is not able to travel up to the dephasing time. We believe that it may be the phase mixing effect due to noise in the system which is preventing electrons to gain energy greater than 200 MeV in the above mentioned experiment [28].

The studies presented upto this chapter assume that ions are static. In the next chapter we going to study the effect of ion motion on plasma oscillations.

Appendix : Relativistic wave frame solution

In this appendix we are going to present a new derivation of longitudinal AP waves. We assume that wave is quasi-static *i.e.* all quantities are functions of a the single variable $\psi = t - x/\beta$, here $\beta = \omega/k$ is the phase velocity the plane wave. This permits the substitutions $\partial/\partial x = -(1/\beta)d/d\psi$ and $\partial/\partial t = d/d\psi$ and therefore set of Eqs.(4.1)-(4.4) can be combined as

$$(1 - \frac{v}{\beta})\frac{d}{d\psi}(1 - \frac{v}{\beta})\frac{d}{d\psi}p + \omega_{pe}^2 \frac{p}{[1 + p^2/(m^2c^2)]^{1/2}} = 0 \tag{4.18}$$

with $p = \gamma m v$ and

$$n = \frac{n_0}{1 - v/\beta} \tag{4.19}$$

$$v = \frac{(p/m)}{[1 + p^2/(m^2c^2)]^{1/2}} \tag{4.20}$$

Now we use the following transformation as

$$(1 - v/\beta)\frac{d}{d\psi} = \frac{d}{d\phi} \tag{4.21}$$

and Eqn. (4.18) becomes

$$\frac{d^2p}{d\phi^2} + \omega_{pe}^2 \frac{p}{[1 + p^2/(m^2c^2)]^{1/2}} = 0 \tag{4.22}$$

Integrating once, we obtain

$$\frac{dp}{d\phi} = \pm\sqrt{2}\omega_{pe}c\big[A - [1 + p^2/(m^2c^2)]^{1/2}\big]^{1/2} = 0, \text{here } A = \text{cons.} \tag{4.23}$$

We now substitute

$$A - [1 + p^2/(m^2c^2)]^{1/2} = (A - 1)\sin^2\theta \tag{4.24}$$

Then the solution of Eq.(4.25) can be expressed in terms of Elliptic integrals *i.e.*

$$\omega_{pe}\phi = \sqrt{2(A+1)}E(\theta, r) - \sqrt{\frac{2}{A+1}}F(\theta, r) + B \tag{4.25}$$

Here $E(\theta, r)$, $F(\theta, r)$ are incomplete elliptic integrals of second and first kind respectively, B is the second integration constant and

$$r = \left[\frac{A-1}{A+1}\right]^{1/2} \tag{4.26}$$

Now integrating Eq.(4.21) we get

$$\psi = \phi - \frac{1}{\beta}\int v d\phi \tag{4.27}$$

Using Eqs.(7.20),(4.24) and (4.25), Eq.(4.27) becomes

$$\omega_{pe}\psi = \sqrt{2(A+1)}E(\theta, r) - \sqrt{\frac{2}{A+1}}F(\theta, r) - \frac{c}{\beta}\frac{2r}{r'}\sin\theta + B$$

Since the constant ‘B’ affects only phase of the wave, it can be chosen to be zero *i.e.*

$$\omega_{pe}(t - x/\beta) = \frac{2}{r'}E(\theta, r) - r'F(\theta, r) - \frac{c}{\beta}\frac{2r}{r'}\sin\theta \tag{4.28}$$

Here $r' = \sqrt{1 - r^2}$.

Thus Eq.(4.28) together with (4.24) gives the plane wave solution for relativistic Langmuir waves for an arbitrary phase velocity in cold plasma. Note here that Eq.(4.28) is exactly similar to the Eq.(4.17).These solutions are identical to the plane wave solution obtained by Akhiezer and Polovin [119].

Chapter 5

Nonlinear oscillations and waves in an arbitrary mass ratio cold plasma

It is the understanding till date that oscillations in an arbitrary mass ratio cold plasma phase mix away due to nonlinearly driven ponderomotive forces only. We propose here that the naturally excited zero frequency mode of the system may also be responsible for phase mixing. We also show here that the cold plasma BGK waves [Albritton et al.,Nucl. Fusion, 15, 1199 (1975)] phase mix away due to the zero frequency mode of the system if ions are allowed to move and scaling of phase mixing is found to be different from earlier work [Sengupta et al., Phys. Rev. Lett. 82, 1867 (1999)]. Phase mixing of these waves have been further verified in 1-D particle in cell simulation. Moreover, we demonstrate the existence of nonlinear solutions in an arbitrary mass ratio cold plasma which do not exhibit phase mixing due to absence of zero frequency mode and ponderomotive force. These solutions are nothing but nonlinear electron-ion travelling wave solutions

5.1 Introduction

As discussed in chapter 1, if the ion background is inhomogeneous but static, plasma frequency becomes function of position. As a result plasma oscillations phase mix away and break at arbitrarily small amplitude [102]. Kaw et al. [103] interpreted this phenomenon as mode coupling where energy goes from long wavelength mode to short wavelength mode. These authors used the sinusoidal background ion density profile and found the time scale of mode coupling as $\omega_{pe}t \sim \frac{2}{\epsilon\omega_{p0}}$, where "$\epsilon$" is the amplitude of the background inhomogeneity. Later Infeld et al. obtained an exact solution for electron plasma oscillations with sinusoidal but static ion background and described phase mixing as electron density burst [104]. Nappi et al. [105] have extended the Infeld's work and have shown that if ions are allowed to move, the inhomogeneous ion distribution gets modified significantly due to ponderomotive force before wave breaks. Later Sengupta et al. have shown that phase mixing of plasma oscillations can occur even if one starts with homogeneous but mobile ions [106]. The authors have shown that ion distribution becomes inhomogeneous in response to low frequency force (ponderomotive force) and hence oscillations phase mix away [106].

We first demonstrate in this chapter that the nonlinearly driven ponderomotive force is not the only candidate responsible for phase mixing of plasma oscillations, but the naturally excited zero frequency mode of the system (which appears in the first order solution) may also trigger phase mixing. We propose here that if one chooses an arbitrary initial condition to excite plasma oscillations, phase mixing may occur due to both zero frequency mode and ponderomotive forces. However, it is shown that in order to excite plasma oscillations we can choose the initial conditions such that the effect of zero frequency mode can be ignored and then, phase mixing occurs only due to ponderomotive forces.

We also study the behavior of cold electron plasma BGK waves [116, 120] with ion motion and find that although the breaking amplitude of these waves is very high $keE/(m\omega_{pe}^2) \sim 1$, they break at arbitrarily small amplitude via phase mixing. In this case zero frequency mode of the system is found to be the only possible candidate responsible for phase mixing as ponderomotive force for waves is zero.

As we have studied in the last chapter that the phenomena of phase mixing can also be seen in relativistic plasma oscillations [107, 108, 109], however there exist nonlinear traveling AP wave solutions [119] which do not exhibit phase mixing.

Thus we note here that behavior of oscillations [107] in the relativistic cold plasma is analogous to behavior of oscillation in nonrelativistic arbitrary mass ratio cold plasma [106]. Therefore we expect that there must be a corresponding solution in the arbitrary mass ratio cold plasma analogous to the AP wave solution which do not exhibit phase mixing. We demonstrate the existence of these solutions using a perturbation theoretic calculation.

The chapter is organized as follows. Section.(5.2) contains the basic equations governing the dynamics of two fluids and the first order solution. In section.(5.3), phase mixing of nonlinear standing oscillation has been presented. Section.(5.4) deals with the phase mixing of cold plasma BGK waves [116, 120] due to ion motion. In section.(5.5), nonlinear electron-ion traveling wave solutions, correct up to second order, have been constructed. Section.(5.6) contains summary of all the results.

5.2 Governing equations and perturbation analysis

The basic equations describing the motions of two species in cold plasma are the continuity equations, momentum equations and the Poisson equation, which in the normalized form can be expressed as

$$\frac{\partial n_e}{\partial t} + \frac{\partial (n_e v_e)}{\partial x} = 0 \tag{5.1}$$

$$\frac{\partial n_i}{\partial t} + \frac{\partial (n_i v_i)}{\partial x} = 0 \tag{5.2}$$

$$\frac{\partial v_e}{\partial t} + v_e \frac{\partial v_e}{\partial x} = -E \tag{5.3}$$

$$\frac{\partial v_i}{\partial t} + v_i \frac{\partial v_i}{\partial x} = \Delta E \tag{5.4}$$

$$\frac{\partial E}{\partial x} = n_i - n_e \tag{5.5}$$

Where $x \to kx$, $t \to \omega_{pe} t$, $n_e \to n_e/n_0$, $n_i \to n_i/n_0$, $v_e \to v_e/(\omega_{pe} k^{-1})$, $v_i \to v_i/(\omega_{pe} k^{-1})$, $E \to keE/m\omega_{pe}^2$, $\Delta = m_e/m_i$ and the symbols have their usual meaning.

In order to make the problem analytically simple, one can introduce new variable as $\delta n_d = \delta n_i - \delta n_e = n_i - n_e$, $\delta n_s = \delta n_i + \delta n_e = n_i + n_e - 2$, $v = v_i - v_e$, $V = v_i + v_e$ and the set of Eqs. (5.1)-(5.5) takes the form as

$$\frac{\partial \delta n_d}{\partial t} + \frac{\partial}{\partial x}\left[v + \frac{\delta n_d V + \delta n_s v}{2}\right] = 0 \tag{5.6}$$

$$\frac{\partial \delta n_s}{\partial t} + \frac{\partial}{\partial x}\left[V + \frac{\delta n_s V + \delta n_d v}{2}\right] = 0 \tag{5.7}$$

$$\frac{\partial v}{\partial t} + \frac{\partial}{\partial x}\left[\frac{vV}{2}\right] = (1+\Delta)E \tag{5.8}$$

$$\frac{\partial V}{\partial t} + \frac{\partial}{\partial x}\left[\frac{V^2+v^2}{4}\right] = -(1-\Delta)E \tag{5.9}$$

$$\frac{\partial E}{\partial x} = \delta n_d \tag{5.10}$$

In order to solve the above set of equations, a perturbation method is used. Therefore set of Eqs.(5.6)-(5.10) correct up to first order can be expressed as

$$\frac{\partial \delta n_d^{(1)}}{\partial t} + \frac{\partial v^{(1)}}{\partial x} = 0 \tag{5.11}$$

$$\frac{\partial \delta n_s^{(1)}}{\partial t} + \frac{\partial V^{(1)}}{\partial x} = 0 \tag{5.12}$$

$$\frac{\partial v^{(1)}}{\partial t} = (1+\Delta)E^{(1)} \tag{5.13}$$

$$\frac{\partial V^{(1)}}{\partial t} = -(1-\Delta)E^{(1)} \tag{5.14}$$

$$\frac{\partial E^{(1)}}{\partial x} = \delta n_d^{(1)} \tag{5.15}$$

Now the set of Eqs.(5.11)-(5.15) can be combined to give

$$\frac{\partial^2 \delta n_d^{(1)}}{\partial t^2} + \omega_p^2 \delta n_d^{(1)} = 0 \tag{5.16}$$

Here $\omega_p^2 = 1+\Delta$. Solution of Eq.(5.16) can be expressed as

$$\delta n_d^{(1)} = A(x)\cos\omega_p t + B(x)\sin\omega_p t \tag{5.17}$$

Here A and B are constants which are to be determined from the initial conditions.

Note here that if we linearize the set of equations (5.1)-(5.5) in order to get a dispersion relation, we get two natural modes of the system "ω_p" and "0". Here "ω_p" is responsible for the high frequency oscillations and "0" which is ion acoustic mode for the cold plasma model (zero temperature), excites DC and secular terms in the first order solution. These DC and secular terms may also be responsible for the phase mixing of plasma oscillations/waves.

If we choose an arbitrary initial condition, we may get a mixture of both the modes [106]. However, we can select the initial conditions such that only one of the two modes get excited. In the following section, we will choose the initial conditions such that the zero frequency mode does not get excited and we see pure oscillations in the first order solution.

5.3 Standing plasma oscillations

In this section, different set of initial conditions have been chosen, in order to excite nonlinear standing oscillations in the arbitrary mass ratio cold plasma, such that in the first order one can see pure oscillations.

5.3.1 sinusoidal velocity perturbations to both electron and ion fluids

Let us choose the initial conditions as follows.

$$n_e(x,0) = n_i(x,0) = 1,$$

$$v_e(x,0) = \omega_p \delta \cos x, v_i(x,0) = -\omega_p \delta \Delta \cos x \tag{5.18}$$

Now the first order solution can be obtained as

$$\delta n_d^{(1)} = -\delta(1+\Delta) \sin x \sin \omega_p t \tag{5.19}$$

$$v^{(1)} = -\delta \omega_p (1+\Delta) \cos x \cos \omega_p t \tag{5.20}$$

$$V^{(1)} = \delta \omega_p (1-\Delta) \cos x \cos \omega_p t \tag{5.21}$$

$$\delta n_s^{(1)} = \delta(1-\Delta) \sin x \sin \omega_p t \tag{5.22}$$

$$E^{(1)} = \delta(1+\Delta) \cos x \sin \omega_p t \tag{5.23}$$

The set of Eqs.(5.19)-(5.23) exhibit pure oscillatory solution in the first order. Now we write the second order solution as follows

$$\delta n_d^{(2)} = \frac{\delta^2}{2}(1-\Delta^2) \cos 2x (1-\cos 2\omega_p t) \tag{5.24}$$

$$V^{(2)} = \frac{\delta^2}{2}\omega_p \sin 2x\Big[\omega_p \Delta t + \frac{(1+\Delta^2-\Delta)}{2}\sin 2\omega_p t\Big] \tag{5.25}$$

$$\delta n_s^{(2)} = -\delta^2 \omega_p \cos 2x\Big[\omega_p \Delta \frac{t^2}{2} - \frac{(1+\Delta^2-\Delta)}{4\omega_p}\cos 2\omega_p t\Big] + C2 \tag{5.26}$$

$$E^{(2)} = \frac{\delta^2}{4}(1-\Delta^2)\sin 2x(1-\cos 2\omega_p t) \tag{5.27}$$

If we take average over fast time scales of Eqs.(5.23) and (5.27), there is non-zero DC electric field which makes the ponderomotive force non-zero. This ponderomotive force redistributes the ions in such a way that frequency becomes function of position which is the clear signature of phase mixing [102]. According to Zakharov [131], the slow variation (in the ion time scale) of the background density in the presence of a high frequency oscillation is governed by $\partial_{tt}\delta n_s - T\partial_{xx}\delta n_s = \partial_{xx}|E|^2$. Note here that, the term on RHS is ponderomotive force term. For cold plasma, second term on LHS can be ignored. Therefore Zakharov's theory says that if there is a non-zero ponderomotive force in the system, ion density must go as $\sim t^2$. Thus we see that Eq.(5.26) is consistent with the Zakharov theory.

5.3.2 sinusoidal density perturbations to both electron and ion fluids

Here the initial conditions are chosen as follows.

$$n_e(x,0) = 1 + \delta\cos x, n_i(x,0) = 1 - \delta\Delta\cos x,$$
$$v_e(x,0) = v_i(x,0) = 0. \tag{5.28}$$

Therefore the solution of set of Eqs.(5.11)-(5.15) can be written as

$$\delta n_d^{(1)} = -\delta(1+\Delta)\cos x \cos\omega_p t \tag{5.29}$$

$$v^{(1)} = -\delta\omega_p(1+\Delta)\sin x \sin\omega_p t \tag{5.30}$$

$$V^{(1)} = \delta\omega_p(1-\Delta)\sin x \sin\omega_p t \tag{5.31}$$

$$\delta n_s^{(1)} = \delta(1-\Delta)\cos x\cos\omega_p t \tag{5.32}$$

$$E^{(1)} = -\delta(1+\Delta)\sin x\cos\omega_p t \tag{5.33}$$

Note here that the set of Eqs.(5.29)-(5.33) shows pure oscillations in the first order, i.e., at the linear level there is no phase mixing. Now let us write down the second order solution which is

$$\delta n_d^{(2)} = \frac{\delta^2}{2}(1-\Delta^2)\cos 2x\Big[2\cos\omega_p t - (1+\cos 2\omega_p t)\Big] \tag{5.34}$$

$$V^{(2)} = -\frac{\delta^2}{2}\omega_p \sin 2x\Big[\omega_p \Delta t + (1-\Delta)^2\sin\omega_p t - \frac{(1+\Delta^2-\Delta)}{2}\sin 2\omega_p t\Big] \tag{5.35}$$

$$\delta n_s^{(2)} = \delta^2\omega_p \cos 2x\Big[\omega_p\Delta\frac{t^2}{2} - \frac{(1-\Delta)^2}{\omega_p}\cos\omega_p t + \frac{(3+3\Delta^2-\Delta)}{4\omega_p}\cos 2\omega_p t\Big] + C2 \tag{5.36}$$

$$E^{(2)} = \frac{\delta^2}{4}(1-\Delta^2)\sin 2x\Big[2\cos\omega_p t - (1+\cos 2\omega_p t)\Big] \tag{5.37}$$

We note here that density in this case also goes as $\sim t^2$ which is qualitatively same as found in ref.[106] and is consistent with the Zakharov theory [131].

The studies, presented in this section, are different from the earlier work [106], because phase mixing is coming here nonlinearly due to ponderomotive forces only. In the next section, the behavior of cold plasma BGK waves [120] in the presence of ion motion has been presented.

5.4 Phase mixing of traveling waves

Albritton modes are nonlinear traveling waves in cold homogeneous plasma where ions are assumed to be infinitely massive [120]. It is the question of interest that what happens to these modes, if ions are allowed to move. In order to study this behavior using perturbative approach, let us choose linearized Albritton type initial conditions, which are

$$n_e^{(1)} = 1 + \delta \cos x, v_e^{(1)} = \delta \cos x,$$
$$n_i = 1, v_i = 0, \tag{5.38}$$

The first order solution, for above set of initial conditions, can be obtained as

$$\delta n_s^{(1)} = \frac{\delta}{\omega_p}\frac{(1-\Delta)}{(1+\Delta)}\Big[\omega_p \cos x \cos \omega_p t + \sin x \sin \omega_p t\Big] + \delta\frac{2\Delta}{1+\Delta}\Big[t \sin x + \cos x\Big] \tag{5.39}$$

$$v^{(1)} = -\delta\Big[\cos x \cos \omega_p t + \omega_p \sin x \sin \omega_p t\Big] \tag{5.40}$$

$$V^{(1)} = \delta\frac{(1-\Delta)}{(1+\Delta)}\Big[\cos x \cos \omega_p t + \omega_p \sin x \sin \omega_p t\Big] + \delta\frac{2\Delta}{1+\Delta}\cos x \tag{5.41}$$

$$E^{(1)} = -\frac{\delta}{\omega_p}\Big[\omega_p \sin x \cos \omega_p t - \cos x \sin \omega_p t\Big] \tag{5.42}$$

One can note form Eq.(5.39) that there are DC and secular terms present in the first order solution. As has been discussed in section.(6.2) that, the DC and secular terms come in response to the zero frequency mode. Therefore it can be noted that if ions are allowed to move, cold plasma BGK waves [120] will phase mix away and the scaling of phase mixing will be as $t_{mix} \sim (1+\Delta)/(2\delta\Delta)$.

In order to verify the analytical treatment, 1D PIC simulation [128] has been carried out for exact Albritton type initial conditions [120]. Here, the simulation parameters are chosen to be as follows.

Total number of particles = 40960, total number of grid points = 4096, time step = $\pi/50$, temperature = 0, system length = 2π.

Normalizations are as follows. $x \rightarrow k^{-1}$, $t \rightarrow \omega_{pe}^{-1}$, $n_e \rightarrow n_0$, $v_e \rightarrow \frac{\omega_{pe}}{k}$, $E \rightarrow \frac{m\omega_{pe}^2}{ke}$, where all the symbols have their usual meanings.

Analytical expressions, for various physical quantities, have been plotted against the results from the simulation. It is to be noted the in all figures, lines represent the numerical results and points ('*') denote the analytical profile. In the Figures.(5.1) and (5.2) numerical and analytical profiles of δn_d and δn_s have been plotted respectively at $\delta = 0.001$ and $\Delta = 1.0$ for one plasma period.

Figures.(5.3) and (5.4) shows the time evolution of δn_d and δn_s respectively at

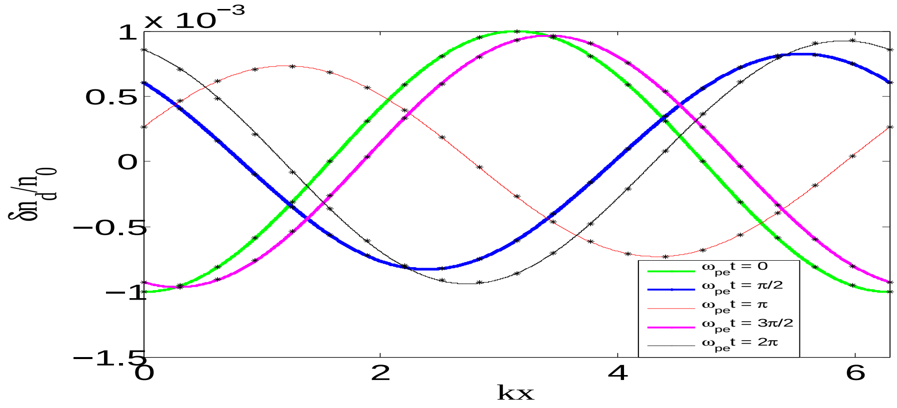

Figure 5.1: Numerical (solid lines) vs analytical ('*') profiles of δn_d at $\delta = 0.001$ and $\Delta = 1.0$ for one plasma period.

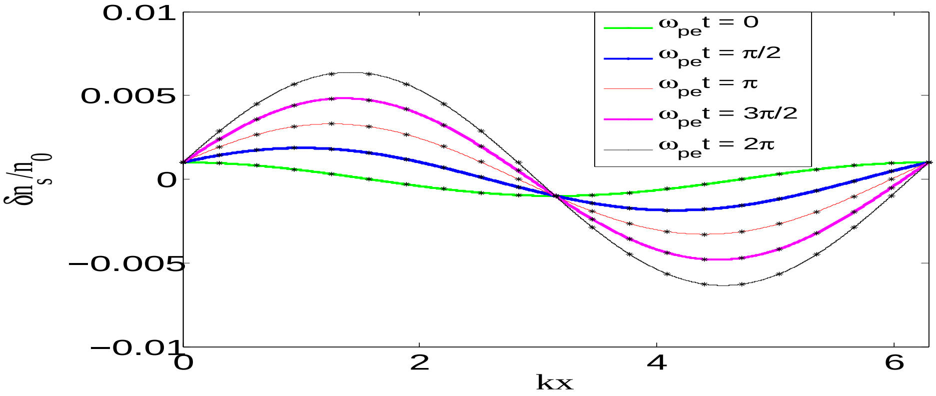

Figure 5.2: Numerical (solid lines) vs analytical ('*') profiles of δn_s at $\delta = 0.001$ and $\Delta = 1.0$ for one plasma period.

$kx = 1.257$, $\delta = 0.001$, $\Delta = 1.0$ up to two plasma periods.

From all the figures one can see a good match between numerical results and theory.

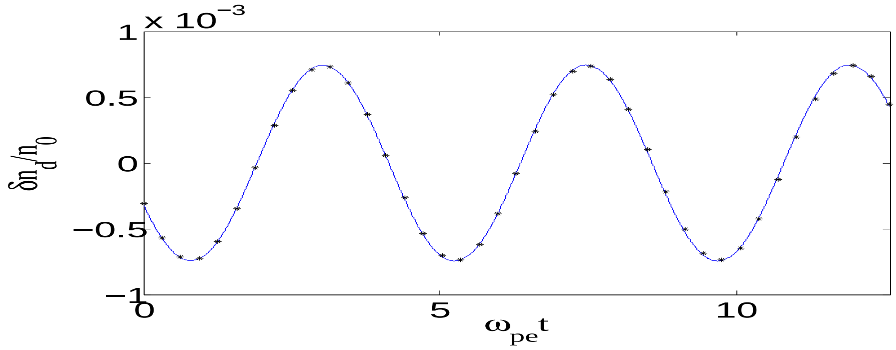

Figure 5.3: Numerical (solid lines) vs analytical ('*') profiles of δn_d at $kx = 1.257$, $\delta = 0.001$ and $\Delta = 1.0$ up to two plasma periods.

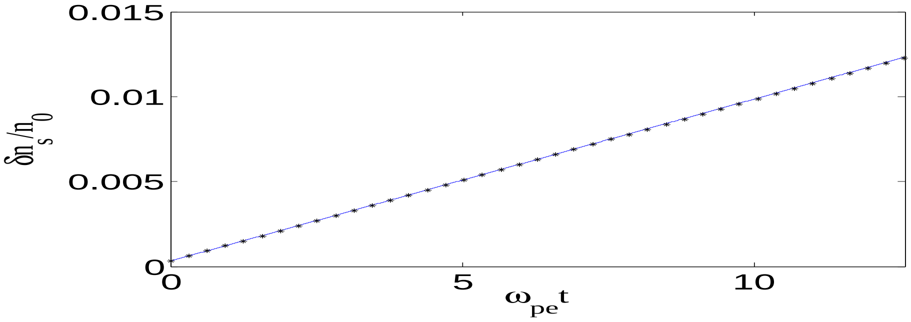

Figure 5.4: Numerical (solid lines) vs analytical ('*') profiles of δn_s at $kx = 1.257$, $\delta = 0.001$ and $\Delta = 1.0$ up to two plasma periods.

Till now we have seen that if one excites plasma oscillations, either by a density perturbations or by a velocity perturbations or due to both, they will always phase mix and break at arbitrarily small amplitude. However, in the next section we demonstrate the existence of solutions in an arbitrary mass ratio cold plasma which do not exhibit phase mixing.

5.5 Electron-ion traveling wave solution

In order to get wave like solution, let us choose the first order perturbations such that zero frequency mode does not get excited. These initial conditions are as follows.

$$\begin{aligned} n_e^{(1)} &= 1+\delta\cos x, n_i^{(1)} = 1-\delta\Delta\cos x, \\ v_e^{(1)} &= \omega_p\delta\cos x, v_i^{(1)} = -\omega_p\Delta\delta\cos x. \end{aligned} \tag{5.43}$$

For these initial conditions the solution of set of Eqs.(5.11)-(5.15) can be written as

$$\delta n_d^{(1)} = -\delta(1+\Delta)\cos(x-\omega_p t) \tag{5.44}$$

$$v^{(1)} = -\delta\omega_p(1+\Delta)\cos(x-\omega_p t) \tag{5.45}$$

$$V^{(1)} = \delta\omega_p(1-\Delta)\cos(x-\omega_p t) \tag{5.46}$$

$$\delta n_s^{(1)} = \delta(1-\Delta)\cos(x-\omega_p t) \tag{5.47}$$

$$E^{(1)} = -\delta(1+\Delta)\sin(x-\omega_p t) \tag{5.48}$$

The set of Eqs.(5.44)-(5.48) clearly exhibits a pure traveling solution in the first order. Now the second order equation for δn_d can be written as

$$\begin{aligned} \frac{\partial^2\delta n_d^{(2)}}{\partial t^2} + \omega_p^2\delta n_d^{(2)} &= \frac{\partial^2}{\partial x^2}\left[\frac{v^{(1)}V^{(1)}}{2}\right] \\ &- \frac{\partial^2}{\partial x\partial t}\left[\frac{\delta n_d^{(1)}V^{(1)} + \delta n_s^{(1)}v^{(1)}}{2}\right] \end{aligned} \tag{5.49}$$

Using Eqs.(5.44)-(5.48) in Eq.(5.49) one can get

$$\frac{\partial^2\delta n_d^{(2)}}{\partial t^2} + \omega_p^2\delta n_d^{(2)} = 3\delta^2\omega_p^2(1-\Delta^2)\cos(2x-2\omega_p t) \tag{5.50}$$

Now the solution of Eq.(5.50) can be expressed as

$$\begin{aligned}\delta n_d^{(2)} &= C(x)\cos\omega_p t + D(x)\sin\omega_p t \\ &\quad -\delta^2(1-\Delta^2)\cos(2x-2\omega_p t)\end{aligned} \tag{5.51}$$

Let us now choose the second order perturbations in $\delta n_d^{(2)}$ and $V^{(2)}$ such that C(x) = D(x) = 0 i.e. Eq.(5.51) becomes

$$\delta n_d^{(2)} = -\delta^2(1-\Delta^2)\cos(2x-2\omega_p t) \tag{5.52}$$

Now from Eq.(5.15) second order solution for the electric field can be written as

$$E^{(2)} = -\frac{\delta^2}{2}(1-\Delta^2)\sin(2x-2\omega_p t) \tag{5.53}$$

Similarly one can write second order solution for V, v and δn_s which is

$$V^{(2)} = \frac{\delta^2}{2}(1+\Delta^2-\Delta)\cos(2x-2\omega_p t) \tag{5.54}$$

$$v^{(2)} = -\frac{\delta^2}{2}\omega_p(1-\Delta^2)\cos(2x-2\omega_p t) \tag{5.55}$$

$$\delta n_s^{(2)} = \frac{\delta^2}{2}(2+2\Delta^2-\Delta)\cos(2x-2\omega_p t) \tag{5.56}$$

Note here that second order solution is pure traveling one without any DC or secular term. Now if we take average over fast time scales of Eqs.(5.48) and (5.53), slow component of electric field is found to be zero which makes ponderomotive force zero. Because of absence of ponderomotive force, redistribution of ions does not take place and therefore, both electrons and ions keep oscillating coherently at the plasma frequency for indefinite time.

Thus, the set of Eqs. (5.44)-(5.48) together with Eqs.(5.52)-(5.56) gives the nonlinear electron-ion traveling wave solutions up to second order. These solutions do not show phase mixing as ponderomotive force for waves is zero and zero frequency mode is absent here. Note here that an exact solution for nonlinear electron-ion traveling waves can be obtained from the set of Eqs.(5.1)-(5.5), assuming each quantity to be a function of single variable i.e., "$x - v_{ph}t$". Here $v_{ph} = \omega_p$ is the phase velocity of these waves. One can also note here that, like

Albritton waves [120] and AP waves [119], these waves also need a very special set of initial conditions,to set them up. Therefore we expect that these waves may also phase mix, if perturbed slightly.

5.6 Summary

In this chapter, we have shown that it is not only the nonlinearly driven ponderomotive force but the naturally excited zero frequency mode of the system may also be responsible for phase mixing of oscillations in an arbitrary mass ratio cold plasma. We have also demonstrated how to choose initial conditions, in order to excite plasma oscillations, such that phase mixing can be avoided in the linear solution. We have further studied the behavior of cold plasma BGK waves [120] with ion motion. It is found that although the breaking amplitude of these waves is very high, they break at arbitrarily small amplitude via phase mixing which is triggered only by zero frequency mode of the system as ponderomotive force for waves is zero. This phase mixing effect has been further verified in PIC simulation and results are found to show a good match with the theory.

Moreover, it is shown that there exist nonlinear electron-ion traveling wave solutions which do not exhibit phase mixing due to absence of both ponderomotive forces and zero frequency mode.

The studies presented upto this chapter do not include the physics of plasma oscillations beyond wave breaking. In the next chapter, we study the long time evolution of electron plasma oscillations in the wave breaking regime.

Chapter 6

Breaking of nonlinear oscillations in a cold plasma

In this chapter we carry out 1-D particle in cell simulation of large amplitude plasma oscillations to explore the physics beyond wave breaking in a cold homogeneous plasma.It is shown that after the wave breaking all energy of the plasma oscillation does not end up as the random kinetic energy of particles but some fraction which is decided by Coffey's wave breaking limit in warm plasma, always remains with two oppositely propagating coherent BGK like modes with supporting trapped particle distributions. The randomized energy distribution of untrapped particles is found to be characteristically non-Maxwellian with a preponderance of energetic particles.

6.1 Introduction

As we have discussed earlier that beyond a critical amplitude there will be fine scale mixing of various parts of the oscillations, as a result of which they will destroy themselves through the development of multistream flow [102].

Wang et al. [122] extended the study of nonlinear plasma oscillations beyond breaking by solving the fluid equations numerically using the Lagrange description for the electrons because the Eulerian description can only describe the average properties of the fluid, while the Lagrange description can describe the fine structure such as multistream flow and wave breaking etc. The authors have seen the multistream flow and generation of fast electrons when the initial amplitude of the perturbation becomes greater than the wave breaking amplitude. It is to be emphasized that although the authors did not study long time evolution of plasma oscillations in the breaking regime, they speculated that after the wave breaking coherent oscillation energy transforms into disordered electron kinetic energy.

Thus it is generally believed that after the wave breaking, plasma gets heated and all energy of the wave goes to the randomized kinetic energy of particles [102, 122]. The simulations presented in this paper show in contrast that this is not true as after the breaking of plasma oscillations, a fraction of the energy always remains with a pair of oppositely propagating coherent waves which are in the nature of nonlinear BGK modes with supporting trapped and untrapped particle distributions. The magnitude of the energy surviving in the coherent BGK modes gets smaller as the electric field parameter is increased beyond the critical value and becomes very small when the parameter approaches unity.

It is to be emphasized that to understand these results, we need to get familiar with the wave breaking criterion in warm plasmas [121, 135]. This is because as soon as wave breaking starts and part of the coherent wave energy goes into randomized kinetic energy of particles, the plasma begins to exhibit characteristic features of a warm plasma. Coffey analytically derived an expression for maximum (breaking) amplitude of the oscillations in warm plasma using a water-bag distribution for the electrons and showed that as the ratio of the electron thermal velocity to the wave phase velocity increases, the maximum amplitude for wave breaking decreases monotonically [121]. This breaking amplitude comes from the trapping condition also i.e., when the electrons from the boundary of the water bag distribution get trapped in the potential well, the wave breaks [136]. The waterbag distribution has a substantial number of particles at the boundary (the number of particles interacting with the wave does not go up gradually as in a Maxwellian) and once trapping condition is satisfied, the wave collapses and breaks immediately.

Thus the present understanding is that the maximum amplitude of a coherent wave which does not break in a warm plasma is decided by the Coffey limit [121]. In our case, we start with the cold plasma model but after the wave breaking commences, the plasma becomes warm as some fraction of energy gets converted to random energy of particles. We therefore expect that the final amplitude of the surviving wave should be such that it matches with the Coffey criterion . It will be shown that there is indeed a good qualitative match between the two.

In section.(6.2), we report our results from 1-D PIC simulations on the breaking of nonlinear plasma oscillations which may be initiated either by a density perturbation or by a velocity perturbation. Section.(6.3) contains the interpretation of the numerical results and demonstrates a good qualitative match with the theoretical prediction. Finally sections.(6.4), describes the summary of our results.

6.2 Results from the simulation

Here we carry out 1-D PIC simulation with periodic boundary conditions, in order to study the evolution of large amplitude plasma oscillations initiated by sinusoidal density profile beyond wave breaking amplitude. Our simulation parameters are as follows: total number of particles (N) $\sim 3\times10^5$, number of grid points (NG) $\sim 5\times10^2$, time step $\Delta t \sim \pi/50$ and system length (L) $\sim 2\pi$. The initial electron density and velocity profiles are chosen to be as follows. $\mathrm{n}_e(x,0) = 1+\Delta\cos kx, v_e(x,0) = 0$; Ions are assumed to be infinitely massive which are just providing the neutralizing background to the electrons. Normalization is as follows. $x \to kx$, $t \to \omega_{pe}t$, $n_e \to n_e/n_0$, $v_e \to v_e/(\omega_{pe}k^{-1})$ and $E \to keE/(m\omega_{pe}^2)$, where ω_{pe} is the plasma frequency and "k" is the wave number of the longest (fundamental) mode. It is well known that a sinusoidal initial density profile does not break as long as $\Delta < 0.5$ [116], therefore we perform our first numerical experiment at $\Delta = 0.6$, $\mathrm{L} = 2\pi$ and $k = 1$.

Fig.(6.1) shows snap shots of the phase space at $\omega_{pe}t = \pi/2$, π, $3\pi/2$ and $5\pi/2$. It is clear that at $\omega_{pe}t = \pi/2$, the v-x plot has a smooth profile since the particles have not experienced the trajectory crossing as yet.

When $\omega_{pe}t$ becomes greater than $\pi/2$ trajectory crossing occurs at $kx = \pi$ and we see a density burst (wave breaking) [116]. Multistream motion results [102, 122] after wave breaking has occurred as shown in the snap shots at $\omega_{pe}t = \pi$, $3\pi/2$ and $5\pi/2$.

With the progress of time more and more streams are developing as shown in Figs.(6.2) and (6.3). Thus we can say that the plasma is being heated by wave breaking. It is observed that the phase space stops evolving any further after approximately 25 plasma periods as shown in Fig.(6.4) and in the phase space we

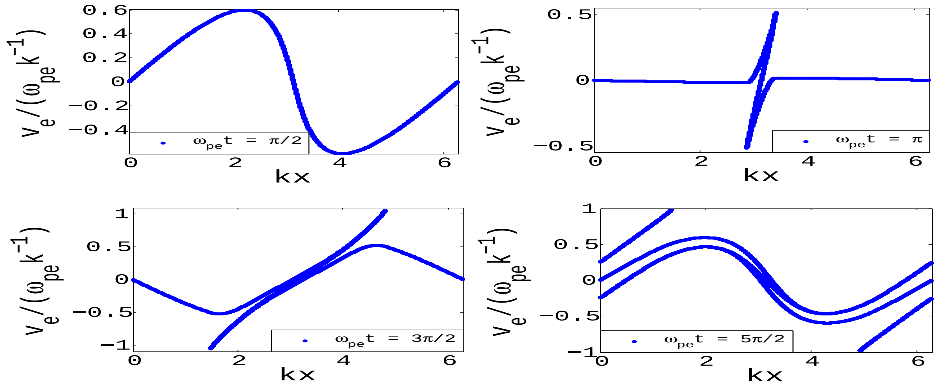

Figure 6.1: Snap shots of phase space at Δ = 0.6, L = 2π and k = 1 at $\omega_{pe}t$ = $\pi/2, \pi, 3\pi/2$ and $5\pi/2$

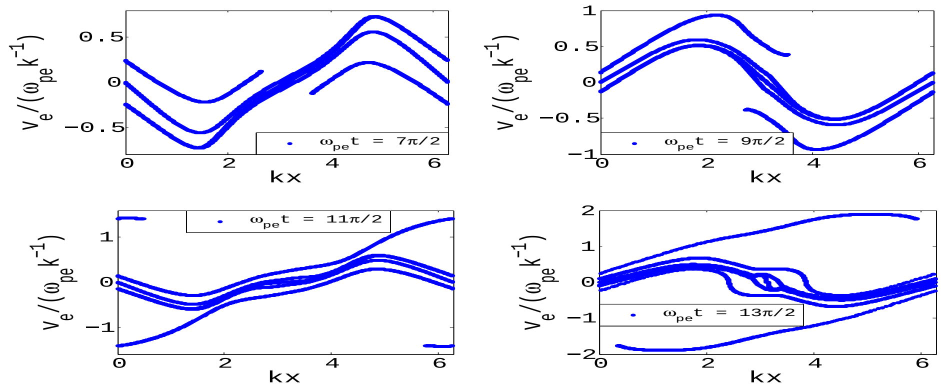

Figure 6.2: Snap shots of phase space at Δ = 0.6, L = 2π and k = 1 at $\omega_{pe}t$ = $7\pi/2, 9\pi/2, 11\pi/2$ and $13\pi/2$

see two holes propagating in opposite direction. Also in Fig.(6.5) we observe the evolution of electrostatic energy (ESE) up to 200 plasma periods and find that ESE decreases initially (approximately up to 25 plasma periods) and later saturates at

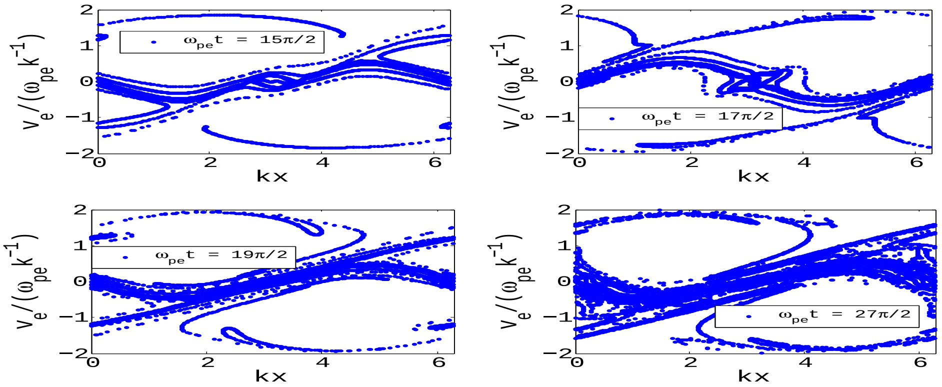

Figure 6.3: Snap shots of phase space at $\Delta = 0.6$, L $= 2\pi$ and k $= 1$ at $\omega_{pe}t = 15\pi/2, 17\pi/2, 19\pi/2$ and $27\pi/2$

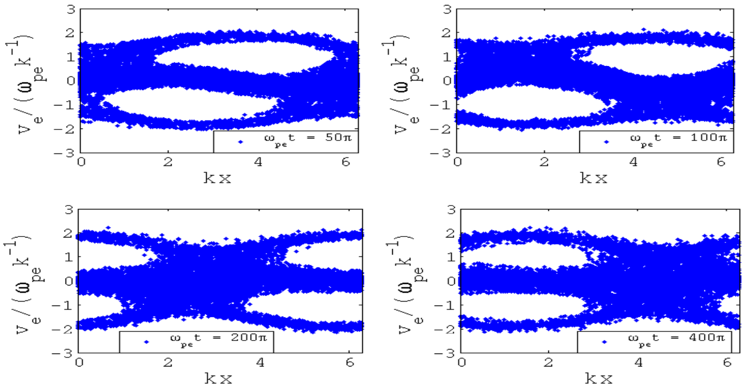

Figure 6.4: Snap shots of phase space at $\Delta = 0.6$, L $= 2\pi$ and k $= 1$ at $\omega_{pe}t = 50\pi, 100\pi, 200\pi$ and 400π

a finite amplitude. This indicates that all energy of the wave does not vanish after wave breaking but a fraction always remains with the wave.

Figs.(6.6)-(6.9) contain the evolution of distribution function at various time

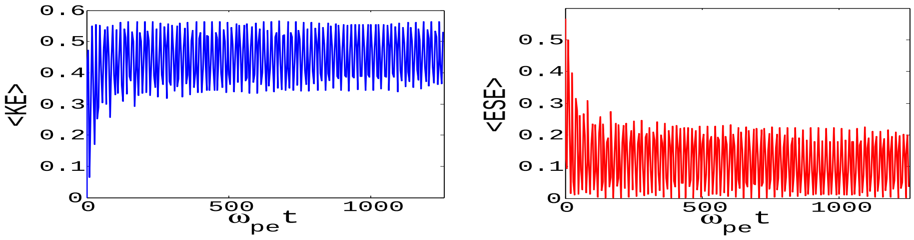

Figure 6.5: Average kinetic energy (KE) and ESE at $\Delta = 0.6$, L $= 2\pi$ and k $= 1$ up to 200 plasma periods

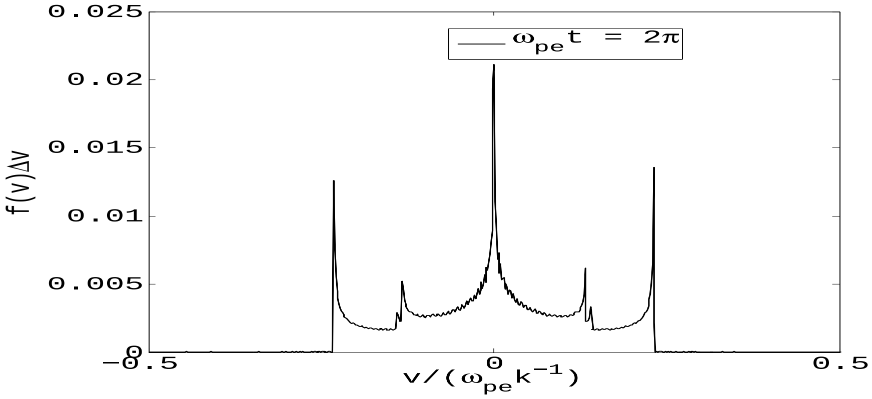

Figure 6.6: Distribution function of electrons at $\omega_{pe}t = 2\pi$

steps which clearly show how more and more streams keep developing as time progresses and finally the distribution function becomes continuous and the system acquires a finite temperature. The distribution function at $\omega_{pe}t \sim 400\pi$ is shown in Fig.(6.10). Note here that the final distribution is non-Maxwellian as it is found to fit with two Maxwellians. However, for the use of an effective parameter measuring the width of the waterbag in the waterbag model of Coffey, we numerically calculate

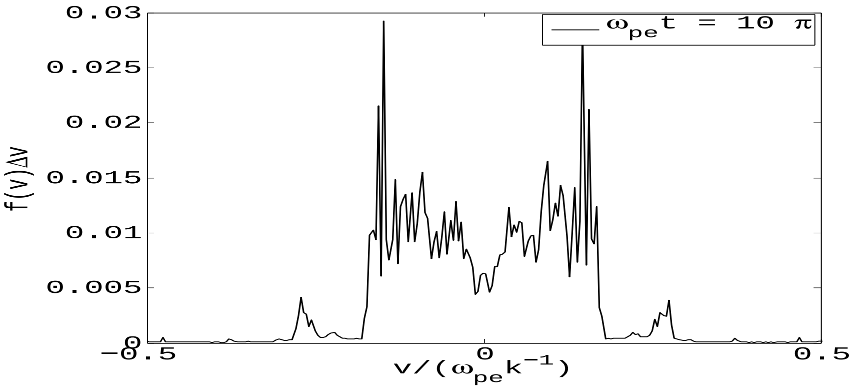

Figure 6.7: Distribution function of electrons at $\omega_{pe}t = 10\pi$

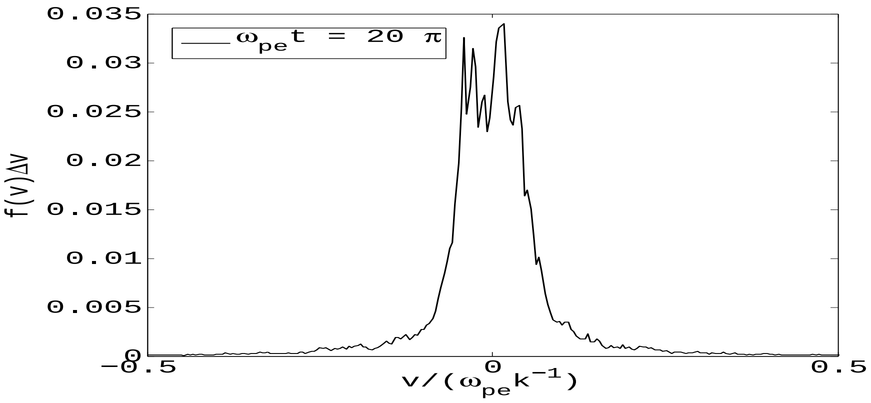

Figure 6.8: Distribution function of electrons at $\omega_{pe}t = 20\pi$

the second moment of the final distribution function and define an effective thermal velocity v_{th} of the particles , which is found to be ~ 0.26.

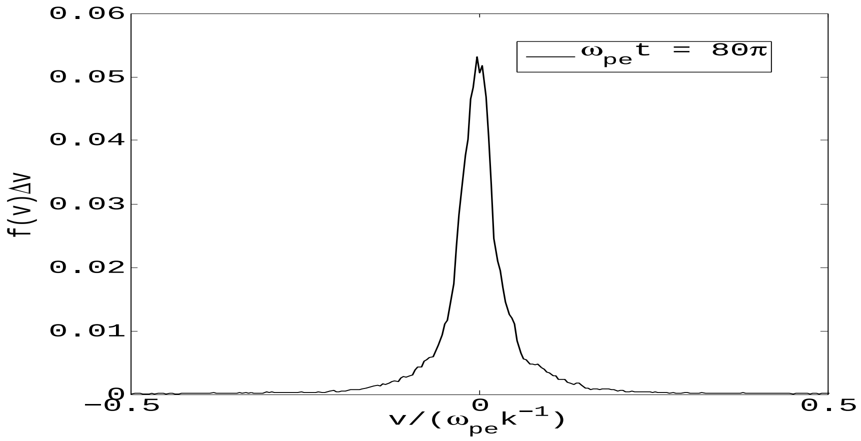

Figure 6.9: Distribution function of electrons at $\omega_{pe}t = 80\pi$

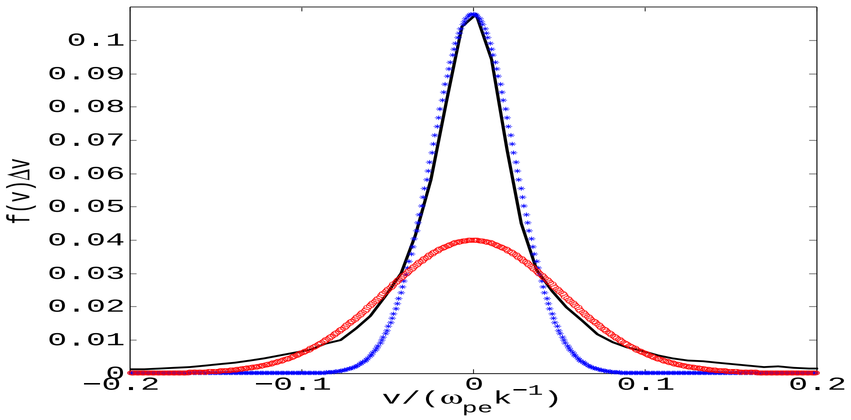

Figure 6.10: Distribution of electrons at $\omega_{pe}t = 400\pi$ shown by black solid line fitted with Maxwellians shown by points

6.3 Interpretation of the results

As long as amplitude of the initial density perturbation is less than the critical value for breaking, nonlinearly generated high "k" modes do not interact resonantly with the particles in the distribution for two reasons. One is that the amplitude of the high "k" modes whose phase velocities lie in the distribution have negligible energy. Second one is that the high "k" modes which have finite energy but being their phase velocity far from the distribution, cannot interact with the particles. However, beyond the critical amplitude wave breaking occurs which leads to the production of very short wavelengths (very high "k" modes). These very high "k" modes can more easily interact with the particles because they move with lower velocities and need lower amplitudes to nonlinearly resonate with the cold particles. When some very high "k" mode, having significant amount of energy, interacts resonantly with particles in the distribution, it loses energy in accelerating them up to a little higher velocity. When these fast electrons come in resonance with comparatively low "k" modes with little larger amplitudes, they get accelerated to slightly higher velocities. As soon as these energetic electrons interact resonantly with the fundamental mode with phase velocity ω_{pe}/k, they get accelerated up to twice the the phase velocity because amplitude of the fundamental mode is the largest. The electrons which acquire velocity twice of phase velocity, may be called freely moving electrons as they are not trapped in the wave and do not give their energy back to the wave. Therefore, amplitude of the wave keeps diminishing as density of these freely moving electrons increases. At the same time a few electrons having wave frame kinetic energy less than potential maxima, get trapped in the wave which can then exchange energy with the wave during trapped oscillations. Since wave is losing energy in accelerating particle i.e., amplitude of the wave is decreasing, it is no longer able to accelerate slow electrons to higher velocities. Meanwhile, with the progress of time, the trapped particle distribution is becoming well phase mixed through nonlinear Landau effects [112] such that an asymptotic state is finally reached where the distribution function becomes stationary in its own frame and the ESE neither grows nor damps. This further becomes clear from the Fig.(6.4), which contains the snap shots of phase space at $\omega_{pe}t = 50\pi$, 100π, 200π and 400π and clearly shows that all the snap shots are exactly similar. Fig.(6.5) contains the space average of kinetic energy (KE) and ESE over 200 plasma periods which shows that up to $\omega_{pe}t \sim 150$, wave keeps on losing its energy and as soon as the asymptotic state is reached, no further dissipation in the ESE is seen. This is consistent with phase space snap shots in Fig.(6.4). The asymptotic states we get after the wave breaking may be interpreted as a superposition of two oppositely propagating BGK type waves. Such superposed solutions are not exact solutions of BGK's original set of equations [113]. However, such states have also been reported by several authors in warm plasma well below the breaking amplitude using Vlasov simulation [137, 138, 139, 140]. It is to be noted that these states can be considered as approximate superpositions of independent oppositely propagating BGK modes, as long as their relative phase velocity is sufficiently large, so that particles trapped in one wave feel only high frequency perturbation from the other [137, 138, 139, 140].

Since we know that the amplitude of a BGK wave depends on the plateau width over which electrons are trapped in the wave troughs as $(\Delta v_{trap})^2 \sim E/k$ [141]. From Fig.(6.4 we can see that $\Delta v_{trap} \sim 1.22$, while its theoretical values is $\Delta v_{trap} = 2\sqrt{E^{sat}/k} \sim 1.216$, here $E^{sat} = 0.37$ which is the saturation amplitude of the electric field. Thus we find that these BGK waves are in agreement with theoretical prediction.

Thus we see that wave saturates at finite amplitude after the wave breaking, now the question is that "what decides the final amplitude ?". Answer to this question can be addressed as follows. The wave amplitude drops as part of the coherent ESE is converted to random KE of untrapped particles and if it drops below the threshold for wave breaking in warm plasma [121], it stops breaking and converting any more coherent wave energy into heat. To verify this interpretation we have repeated the numerical experiment for different values of Δ and in Fig.(6.11), we have compared maximum amplitude of the saturated electric field (shown by points '*') with Coffey's results (shown by solid line '-') which clearly show a qualitative match between theory and simulation.

Thus we have shown that after the wave breaking, plasma becomes warm but all initial energy does not go to particles and a fraction, depending on initial amplitude, always remains with the wave which support a trapped particle distribution in the form of averaged BGK waves.

6.4 Summary

In summary, we have studied in this chapter, a long time behavior of plasma oscillation in the wave breaking regime using 1D PIC simulation and demonstrated

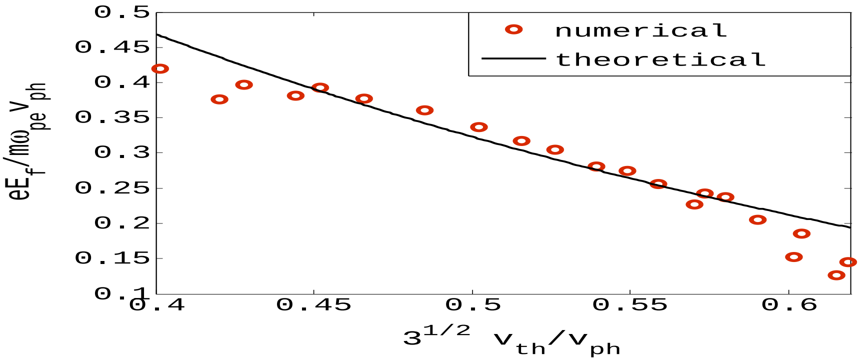

Figure 6.11: Final amplitude of the electric field at the end of the run vs thermal velocity ('*') and its comparison with Coffey's result ('-' solid line)

that all the coherent ESE does not convert to random energy of particles but a fraction which is decided by the Coffey criterion, always remains with the wave which support a trapped particle distribution in the form of BGK waves. The randomized energy distribution of untrapped particles is found to be characteristically non-Maxwellian with a preponderance of energetic particles.

In the next chapter, we are going to study the development and collapse of double layers due to streaming of electrons over ions by using method of Lagrange variables.

Chapter 7

Development and breaking of double layers using method of Lagrange variables

The nonlinear development and collapse (breaking) of double layers in the long scale length limit is well described by equations for the cold ion fluid with quasineutrality. It is shown that electron dynamics is responsible for giving an *equation of state* with negative ratio of specific heats to this fluid. Introducing a transformation for the density variable, the governing equation for the transformed quantity in terms of Lagrange variables turns out exactly to be a linear partial differential equation. This equation has been analyzed in various limits of interest. Nonlinear development of double layers with a sinusoidal initial disturbance and collapse of double layers with an initial perturbation in the form of a density void are analytically investigated.

7.1 Introduction

In all the chapters which have been discussed so far, behavior of nonlinear oscillations/waves and their wave breaking criterion have been studied in cold plasma in various physical limits. We know that in the field of plasma waves, particles can be accelerated to very high energy in a distance much shorter than a conventional accelerator and the breaking of plasma waves lead to conversion of collective energy into random energy of the particles. There is also another kind of field due to double layers which may exist in the plasma. These double layers may also be used in particle acceleration and their collapse is analogous to the wave breaking where collective energy gets converted into random kinetic energy of the particles. Formation and collapse of double layers may be triggered by the most elementary cold plasma electrostatic instability involving streaming of electron with respect to ions.

Electrons streaming rapidly past the ions excite electrostatic fluctuations which can either lead to anomalous resistivity of plasma by random scattering of electrons or double layer formation by reflection of streaming electrons. Formation and breaking of double layers is of importance in many laboratory plasma experiments with intense parallel electric fields, such as for example in turbulent Tokamaks and in astrophysical situations with relativistic jets.

The physics of development of double layers in the long scale length limit, when the perturbations are quasineutral, is well described by nonlinear cold ion fluid equations along with electron dynamics giving an equation of state with negative ratio of specific heat to this fluid. In the linear limit, it exhibits an instability similar to that found in a plasma / fluid with negative pressure perturbation with growth rate which scales as $\sim \sqrt{(}m/M)$.

In this chapter, we present a full nonlinear treatment describing the development and collapse of double layers in the long scale length limit, by transforming the nonlinear cold ion fluid equations to a linear partial differential equation using the method of Lagrange variables. Solution of the resulting partial differential equation shows a similar scaling of growth rate with mass ratio as seen in the linear case. Using harmonic and void like initial conditions, we analytically describe the early results [123].

7.2 Governing Equations and the Linear limit

In the low frequency, long scale length limit ($\omega \ll kv_e$), we neglect the time derivative in the cold electron fluid equations. In this limit, the electron continuity equation gives $n_e v_e = I$ (a constant) and the electron momentum equation reduces to

$$\frac{\partial}{\partial x}\left(\frac{I^2}{n_e^2}\right) = \frac{\partial}{\partial x}\left(\frac{2e\phi}{m}\right) \tag{7.1}$$

where electron fluid velocity is substituted in terms of constant electron current $I = n_0 v_{e0}$. The ion fluid equations in the cold limit are

$$\frac{\partial n}{\partial t} + \frac{\partial nv}{\partial x} = 0 \tag{7.2}$$

$$\frac{\partial v}{\partial t} + v\frac{\partial v}{\partial x} = -\frac{e}{M}\frac{\partial \phi}{\partial x}$$
$$= -\frac{m}{2M}\frac{\partial}{\partial x}\left(\frac{I^2}{n^2}\right) = -\frac{m}{M}I^2\left(\frac{1}{n}\right)\frac{\partial}{\partial x}\left(\frac{1}{n}\right) \tag{7.3}$$

where electron momentum equation (7.1) and constant current I is used to eliminate ϕ on the r.h.s of ion momentum equation (7.3) and quasineutrality is used to replace n_e by n. It is clear from above that for a given $(m/2M)I^2$, the problem is closed within the ion fluid itself and reduces to that of a nonlinear ion fluid with a novel equation of state. It is effectively an equation of state with $\Gamma = -1$, *viz.* a negative ratio of specific heats (The effective pressure goes as $p \sim 1/n$).

Linearising equations (7.2) and (7.3), the equation describing the evolution of density perturbation δn can be written as

$$\frac{\partial^2}{\partial t^2}\delta n + \alpha^2\frac{\partial^2}{\partial x^2}\delta n \approx 0 \tag{7.4}$$

where $\alpha^2 = (mI^2/Mn_0^2)$. This immediately gives an exponential growth of the density perturbation at a growth rate $\gamma \sim k\sqrt{m/M}I/n_0 \sim v_{e0}\sqrt{m/M}$. It is shown in the later sections that, similar exponential growth is also seen in the fully nonlinear case.

In order to physically understand the cause of this instability, we compare a sound wave with negative pressure perturbation, with the usual ion-acoustic wave. For a standard ion fluid with warm electrons, the ion acoustic dispersion relation is

$$1 - \frac{\omega_{pi}^2}{\omega^2} + \frac{\omega_{pe}^2}{k^2 v_{th}^2} = 0 \tag{7.5}$$

where $v_{th}^2 = T_e/m$. For quasineutral perturbations, "1" is negligible and the ion and electron density responses are equal in magnitude with $\omega^2 = k^2(T_e/M) > 0$. This is because ion density perturbation is related to potential as $(\delta n/n_0) \sim (e\phi/mv_{th}^2)$. Thus the cold ions are shielded by the warm electrons with electrons congregating around the ion peaks providing a shielding which produces the dispersion free ion acoustic wave. For the present novel ion fluid with streaming electrons, the complete dispersion relation is [147]

$$1 - \frac{\omega_{pe}^2}{(\omega - kv_{e0})^2} - \frac{\omega_{pi}^2}{\omega^2} = 0 \tag{7.6}$$

Again, evoking quasineutrality "1" may be neglected. Further taking $\omega \ll kv_{e0}$, we get

$$\frac{\omega_{pe}^2}{k^2 v_{e0}^2} + \frac{\omega_{pi}^2}{\omega^2} = 0 \tag{7.7}$$

Now the electron and ion charge density responses can balance only if $\omega^2 < 0$ *i.e.* there is an instability. Physically, if ion motions produce a positive potential somewhere, electron stream gets accelerated and to maintain constant current produces a reduction of electron density thus locally enhancing the original potential perturbation. This positive feedback of streaming electrons is responsible for the instability $\gamma^2 = k^2 v_{e0}^2(m/M)$ and is the source of the negative specific heat ratio of the nonlinear ion fluid in the quasineutral limit. This is evident from the linearised perturbation equation $(\delta n_e/n_0) \sim -(e\phi/mv_{e0}^2)$ (note the negative sign).

The closed set of equations (7.2) and (7.3) contain (1) convective nonlinearity and (2) $\sim 1/n^2$ pressure nonlinearity. These look very similar to sound wave equations with a negative pressure perturbation and can be solved exactly by transforming to Lagrange variables, which we present in the next section.

7.3 Governing Equation in Lagrange Variables

Transformation of Euler coordinates (x, t) to Lagrange coordinates (x_0, τ) is defined as [116]

$$x = x_0 + \int_0^\tau v(x_0, \tau^{'})d\tau^{'} \tag{7.8}$$

$$t = \tau \tag{7.9}$$

which immediately gives

$$
\begin{aligned}
\frac{\partial}{\partial x_0} &= \left[1+\int_0^{\tau}\frac{\partial v(x_0,\tau^{'})}{\partial x_0}d\tau^{'}\right]\frac{\partial}{\partial x} && (7.10)\\
\frac{\partial}{\partial \tau} &= \frac{\partial}{\partial t}+v\frac{\partial}{\partial x} && (7.11)
\end{aligned}
$$

Using equations (7.10) and (7.11), the ion continuity equation gives the ion density as

$$n(x_0,\tau)=n(x_0,0)\left[1+\int_0^{\tau}\frac{\partial v(x_0,\tau^{'})}{\partial x_0}d\tau^{'}\right]^{-1} \qquad (7.12)$$

where $n(x_0,0)$ is the initial density profile. The momentum equation in Lagrange coordinates now stands as

$$
\begin{aligned}
\frac{\partial v}{\partial \tau} &= -\tfrac{m}{M}\tfrac{I^2}{2}\left[1+\int_0^{\tau}\tfrac{\partial v(x_0,\tau^{'})}{\partial x_0}d\tau^{'}\right]^{-1}\tfrac{\partial}{\partial x_0}\tfrac{1}{n^2}\\
&= -\tfrac{m}{M}I^2\left[1+\int_0^{\tau}\tfrac{\partial v(x_0,\tau^{'})}{\partial x_0}d\tau^{'}\right]^{-1}\tfrac{1}{n}\tfrac{\partial}{\partial x_0}\tfrac{1}{n}\\
&= -\tfrac{m}{M}I^2\tfrac{1}{n(x_0,0)}\tfrac{\partial}{\partial x_0}\tfrac{1}{n(x_0,\tau)} \qquad (7.13)
\end{aligned}
$$

where we have used equation (7.12) in the last step. Differentiating the above equation further w.r.t x_0, we get

$$\frac{\partial}{\partial \tau}\frac{\partial v}{\partial x_0}=-\frac{m}{M}I^2\frac{\partial}{\partial x_0}\frac{1}{n(x_0,0)}\frac{\partial}{\partial x_0}\frac{1}{n(x_0,\tau)} \qquad (7.14)$$

Defining inverse of density as a new variable $\psi(x_0,\tau)=n_0/n(x_0,\tau)$ and using a second coordinate transformation [148] which depends on initial density profile as

$$\frac{\partial}{\partial z}=\frac{n_0}{n(x_0,0)}\frac{\partial}{\partial x_0} \qquad (7.15)$$

the ion momentum equation (7.14), finally becomes a linear elliptic PDE in (z,τ)

$$\frac{\partial^2\psi}{\partial \tau^2}+\alpha^2\frac{\partial^2\psi}{\partial z^2}=0 \qquad (7.16)$$

where

$$\frac{\partial\psi}{\partial \tau}=\frac{n_0}{n(x_0,0)}\frac{\partial v}{\partial x_0}=\frac{\partial v}{\partial z} \qquad (7.17)$$

Here "z" is a new Lagrange coordinate. The linearity of equation (7.16) shows that the nonlinear problem with arbitrary initial conditions can be solved in principle.

In the next section, we give the general solution of equation (7.16), and explore the nonlinear development and collapse of double layers with sinusoidal and void like initial perturbations respectively.

7.4 Exact Nonlinear Solution

The exact solution of equation (7.16) is given by

$$\psi(z, \tau) = F(z + i\alpha\tau) + G(z - i\alpha\tau) \tag{7.18}$$

where F and G are arbitrary functions of the complex characteristics $z \pm i\alpha\tau$ and are determined from the initial conditions. Once the the expression for $\psi(z, \tau)$ is known, the ion density, ion fluid velocity and the inversion from Lagrange coordinates (z, τ) to Euler coordinates (x, t) are respectively given by the following relations

$$n(z, \tau) = \frac{n_0}{\psi(z, t)} \tag{7.19}$$

$$\frac{\partial \psi}{\partial \tau} = \frac{\partial v}{\partial z} \tag{7.20}$$

$$\begin{aligned} \frac{\partial x}{\partial z} &= \frac{n_0}{n(x_0, 0)} \frac{\partial x}{\partial x_0} \\ &= \frac{n_0}{n(x_0, \tau)} = \psi(z, \tau) \end{aligned} \tag{7.21}$$

In the next two subsections, we respectively present exact solutions with harmonic initial conditions and void like initial conditions.

7.4.1 Harmonic initial conditions

Here we choose initial conditions for ion density and ion fluid velocity as

$$n(x, 0) \quad = n_0 \left(1 + \tfrac{v_0}{\alpha} \sin(kx)\right) \tag{7.22}$$

$$v(x, 0) \qquad = v_0 \cos(kx) \qquad \frac{v_0}{\alpha} \ll 1 \tag{7.23}$$

Using the above initial conditions, $\psi(z,0)$ and $\dot{\psi}(z,0)$ linearised in perturbation amplitude "v_0/α" are given by

$$\psi(z,0) \approx 1 - \tfrac{v_0}{\alpha}\sin(kz) \tag{7.24}$$

$$\dot{\psi}(z,0) \approx -kv_0\sin(kz) \tag{7.25}$$

Using equations (7.24) and (7.25) in equation (7.18) we get

$$F(z) = \tfrac{1}{2} - i\tfrac{v_0}{2\alpha}e^{-ikz} \tag{7.26}$$

$$G(z) = \tfrac{1}{2} + i\tfrac{v_0}{2\alpha}e^{ikz} \tag{7.27}$$

Using the above form of F and G, the ion density, ion fluid velocity and the transformation from the Lagrange coordinates (z,τ) to Euler coordinates (x,t) are given by

$$n(z,\tau) = n_0\left[1 - \tfrac{v_0}{\alpha}\sin(kz)e^{k\alpha\tau}\right]^{-1} \tag{7.28}$$

$$v(z,\tau) = v_0\cos(kz)e^{k\alpha\tau} \tag{7.29}$$

$$kx = kz + \tfrac{v_0}{\alpha}e^{k\alpha\tau}\cos(kz) \tag{7.30}$$

Using equation (7.30), the ion velocity, density and potential can finally be written in terms of Euler coordinates as

$$v(x,t) = v_0 e^{k\alpha t}\cos\left[kx - \tfrac{v(x,t)}{\alpha}\right] \tag{7.31}$$

$$n(x,t) = n_0\left[1 - \tfrac{v_0}{\alpha}\sin(kx - \tfrac{v(x,t)}{\alpha})e^{k\alpha t}\right]^{-1} \tag{7.32}$$

$$\frac{e\phi(x,t)}{M} = \tfrac{1}{2}\left(v_0 e^{k\alpha t}\sin\left(kx - \tfrac{v(x,t)}{\alpha}\right) - \alpha\right)^2 - \tfrac{\alpha^2}{2} \tag{7.33}$$

where the expression for potential is obtained using equation (7.1) and quasineutrality condition. Figs. (7.1),(7.2) and (7.3) respectively show the evolution of ion fluid velocity, potential and ion number density for $v_0/\alpha = 0.1$. The potential exhibits the formation of a double layer type structure.

The evolution of sinusoidal density perturbation clearly follows the physics discussed in section.(7.2). Physically, the regions where potential is negative to begin with, decelerates the electrons. In order to keep the electron current constant,

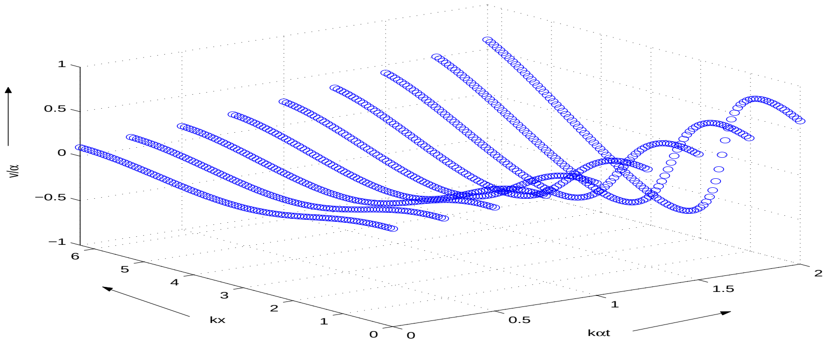

Figure 7.1: Evolution of ion velocity for $v_0/\alpha = 0.1$

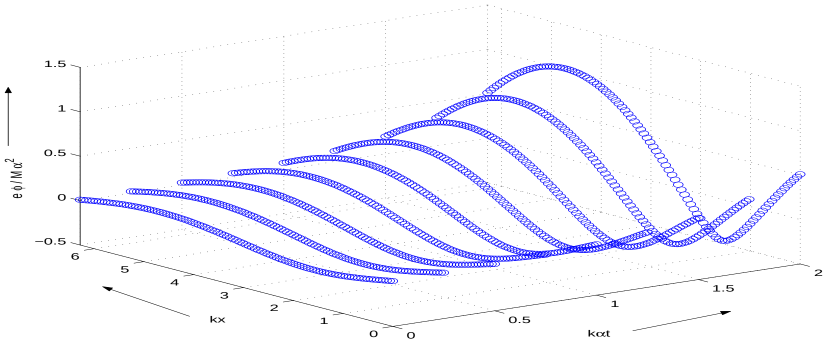

Figure 7.2: Evolution of potential for $v_0/\alpha = 0.1$. Note that at $e\phi/M\alpha^2 = 0.5$, the electrostatic potential energy becomes equal to the initial kinetic energy and reflection of electron beam occurs from this point. Assumption of constant electron current gets violated at this point

the electron number density increases in these regions making the potential further negative.Now, due to this continuous positive feedback eventually the potential

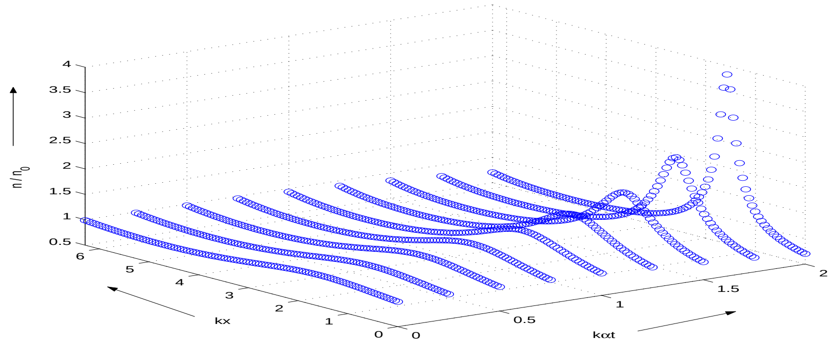

Figure 7.3: Evolution of ion density for $v_0/\alpha = 0.1$

becomes so large (negative) that the electrostatic potential energy becomes equal to the initial kinetic energy. As a result the potential starts reflecting the electron current and the double layer is formed. At this point, the number density shows a peak Fig.(7.3) and the electron current is no longer constant; so the solution does not hold beyond this point.

7.4.2 “Void” like initial conditions

Here we choose initial conditions for ion density and ion fluid velocity as

$$n(x,0) = n_0 \left(1 - \tfrac{\epsilon}{2} sech\left(\tfrac{x}{L}\right)\right) \tag{7.34}$$

$$v(x,0) = 0.0 \qquad \frac{\epsilon}{2} \ll 1 \tag{7.35}$$

In contrast to the previous case, here the initial density perturbation is negative everywhere and the associated potential perturbation is positive everywhere. As a result it cannot reflect the electron current. Following as above, the initial conditions on ψ and $\dot{\psi}$ linearised in perturbation amplitude is given by

$$\psi(z,0) \approx 1 + \tfrac{\epsilon}{2} sech\left(\tfrac{z}{L}\right) \tag{7.36}$$

$$\dot{\psi}(z,0) \approx 0.0 \tag{7.37}$$

Substituting this in the general solution (7.18), gives the general form of the arbitrary functions F and G as

$$F(z) = G(z) = \frac{1}{2}\left(1 + \frac{\epsilon}{2} sech\left(\frac{z}{L}\right)\right) \tag{7.38}$$

Using the above form of F and G, the final expressions for ion density, ion fluid velocity and the transformation from Lagrange coordinates (z, τ) to Euler coordinates (x, t) is given by

$$\begin{aligned} n(z,\tau) \quad &= n_0 \left[1 + \tfrac{\epsilon}{2}\cosh\left(\tfrac{z}{L}\right)\cos\left(\tfrac{\alpha\tau}{L}\right)\left\{f\left(\tfrac{z}{L}, \tfrac{\alpha\tau}{L}\right)\right\}^{-1}\right]^{-1} && (7.39) \\ v(z,\tau) \quad &= \tfrac{\epsilon\alpha}{2}\sinh\left(\tfrac{z}{L}\right)\sin\left(\tfrac{\alpha\tau}{L}\right)\left\{f\left(\tfrac{z}{L}, \tfrac{\alpha\tau}{L}\right)\right\}^{-1} && (7.40) \\ x \quad &= z + \tfrac{\epsilon L}{4}\tan^{-1}\left(\tfrac{2\sinh(z/L)\cos(\alpha t/L)}{\cos^2(\alpha t/L) - \sinh^2(z/L)}\right) && (7.41) \end{aligned}$$

where

$$f\left(\frac{z}{L}, \frac{\alpha\tau}{L}\right) = \cosh^2\left(\frac{z}{L}\right)\cos^2\left(\frac{\alpha\tau}{L}\right) + \sinh^2\left(\frac{z}{L}\right)\sin^2\left(\frac{\alpha\tau}{L}\right) \tag{7.42}$$

Figs. (7.4), (7.5) and (7.6) respectively show the evolution of ion fluid velocity, potential and ion number density for $\epsilon = 0.3$. As before, the potential is obtained

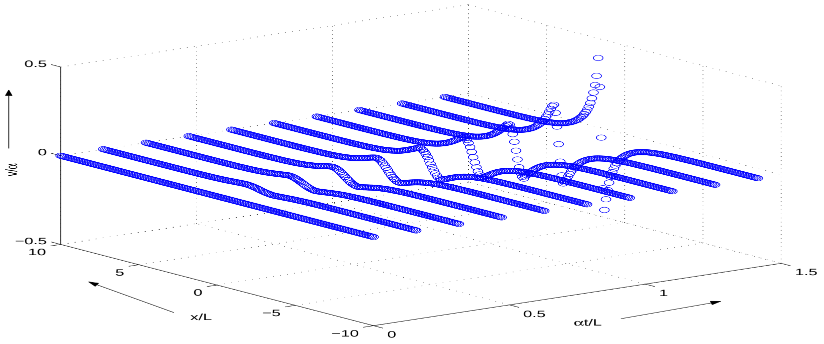

Figure 7.4: Evolution of ion velocity for $v_0/\alpha = 0.1$

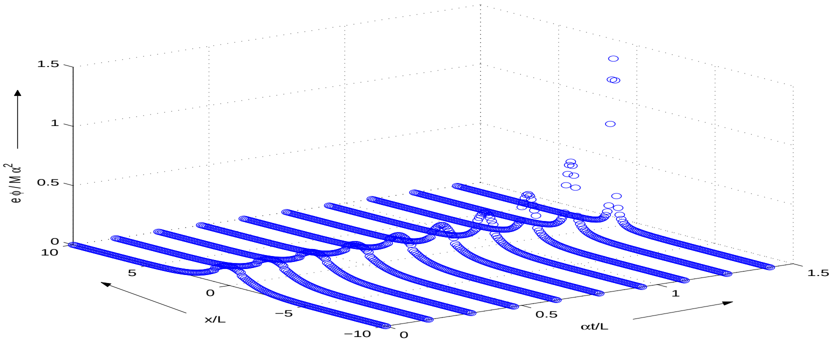

Figure 7.5: Evolution of potential for $\epsilon = 0.3$; Note that at $x/L = 0$ and $\alpha t/L = \pi/2$, the potential goes to ∞

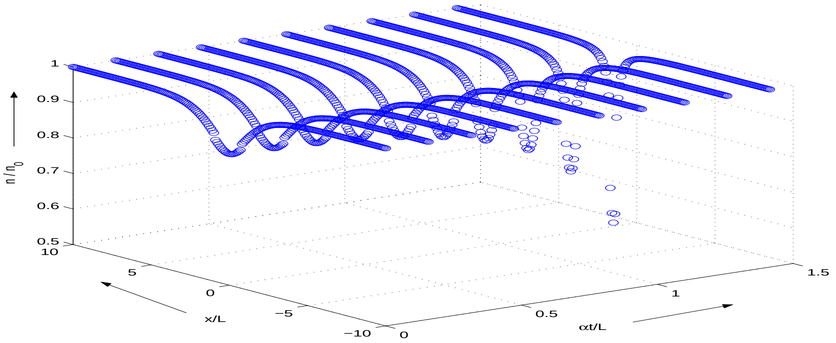

Figure 7.6: Evolution of density for $\epsilon = 0.3$; Note that at $x/L = 0$ and $\alpha t/L = \pi/2$, the number density vanishes

using equation (7.1) and the quasineutrality condition. The above expressions (and also figures) show that at $x/L = 0$ and at $\alpha t/L = \pi/2$, the potential goes to infinity and the number density vanishes. This phenomena is known as collapse of double layers. Such explosive potentials have been seen in experiments [124]. Since the collapse of double layers leads to the conversion of collective energy into random kinetic energy of the particle, we call it breaking of double layers as it is very much similar to wave breaking. Here again, we see the evolution of potential and density following the same physics as discussed in section.(7.2).

7.5 Summary

We have reduced the problem of nonlinear development and collapse of double layers to a linear partial differential equation in Lagrange coordinates. The linear PDE is solved for two sets of initial conditions *viz.* (i) harmonic in density and velocity which leads to formation of a double layer and (ii) “Void” like initial conditions which leads to explosive potentials. Our results for these initial conditions are in general agreement with those obtained in reference [123] using other methods.

Chapter 8

Conclusion

The present thesis mainly investigates some novel aspects of nonlinear plasma oscillations and wave breaking which have not been considered as yet.

In the second chapter of this thesis, we report on space time evolution of nonlinear oscillations in the lab frame, initiated by an arbitrary density perturbation which can be expressed as Fourier series in 'x'. Before our solution, we were only aware of space time evolution of a pure sinusoidal density perturbation in the lab frame which is nothing but a very special case of our general solution. We have obtained this general solution as in realistic laser/beam plasma interaction experiments or simulations, instead of a single mode a bunch of modes get excited. We believe that space time evolution of these bunch of modes may be explained from our general solution. We have also shown the usefulness of our solution by giving examples of the space-time evolution of square wave, triangular wave and Dawson like initial density profiles. Moreover, we have obtained the breaking criteria for all the above mentioned profiles using the inequality as given in ref.[116]. It is found that square and triangular wave profiles break when their height becomes greater than or equal to 0.5. Our general solution provides the evolution of any arbitrary density profile only below the wave breaking amplitude as beyond the breaking amplitude transformation from Lagrange to Euler coordinates is no longer unique. We also studied the evolution and breaking of two mode case which is again a special case of our general solution. We found that addition of a second harmonic increases the breaking amplitude of the fundamental mode. Note here that a pure sine wave breaks when the amplitude of the normalized density perturbation becomes greater than or equal to 0.5. However, we found that if we add a very small perturbation to the second harmonic, oscillations do not break even when amplitude of the fundamental mode is greater than 0.5. Physically this happens because the second mode interfere with the fundamental mode in such a way that the inequality [116] does not satisfied anywhere. The breaking of two mode case has been further verified in 1-D particle in cell simulation. This result may have relevance in wake field acceleration experiments. Furthermore, we have studied the evolution and breaking of a more general two mode case where second mode need not be an integral multiple of the fundamental mode. From this solution we recover the case of Davidson et al. and commensurate mode case for different set of initial conditions.

In the chapter 3, we have studied the behavior of nonlinear oscillations in a cold viscous/hyperviscous and resistive plasma. Note here that the behavior of nonlinear oscillations in a cold viscous and resistive plasma has also been studied by Infeld et al. [118] for an unrealistic model of viscosity; they chose a viscosity coefficient which depends inversely on the density in order to obtain some simplification in the analytic treatment of this problem. They observed two new nonlinear effects : one is that oscillations do not break even beyond the critical amplitude and second one is that for larger value of viscosity coefficient density peak splits into two. It is to be noted here that in reality viscosity has a relatively weak dependence on density through Coulomb logarithm. Therefore we have first studied the evolution of these oscillations for more realistic case where viscosity coefficient is chosen to be independent of density. Later we have studied these oscillations for an alternative dissipative model by replacing viscosity by hyperviscosity. In both the cases, results are found to be qualitatively similar to Infeld et al. [118]. Physically, these nonlinear effects appears due to wave number dependent frequency and damping corrections that lead to interference effects between the various modes. We also found that resistivity alone do not show the splitting effect as the frequency shift introduced by resistivity is wave number independent. Moreover, we have given an analytical expression describing a relation between breaking amplitude and viscosity/hyperviscosity coefficient which clearly show that dissipative effects do not remove the wave breaking completely but enhance the critical amplitude.

In the chapter 4, we have included the relativistic effects in the cold plasma model in order to study the evolution and breaking properties of very large amplitude plasma waves. As we have discussed in the previous chapters that the longitudinal relativistic plasma (AP) waves can be excited in the wake of the ultra-intense ultra-short laser pulse when it goes through underdense plasma [1]. It is the understanding till date that breaking amplitude of longitudinal relativistic plasma wave (AP wave) approaches to infinity as its phase velocity approaches to speed of light. Since these waves can have very large amplitude with out breaking, they accelerate particles to very high energy in a distance much shorter than a conventional linear accelerator. Wave breaking formula for these waves is being used in recent particle acceleration experiments/simulations in order to interpret the observations [28, 30]. However, Infeld and Rowlands [107] have shown that all initial conditions, except the one which are needed to excite AP waves, lead to density burst (wave breaking) at an arbitrarily small amplitude. Thus in order to understand the connection between the theories of Akhiezer & Polovin [119] and Infeld & Rowlands [107], we have first obtained the initial conditions which excite AP waves when substituted in the solution of Infeld & Rowlands [107]. We have then loaded these initial conditions in a relativistic code based on Dawson sheet model to study the the sensitivity of these waves with respect to some perturbations. We have done this because in a realistic wakefield acceleration experiment, there is always some noise (due to group velocity dispersion of the pulse, thermal effects etc. [132, 133, 134, 126]) along with the AP waves in the wake. We have observed the smooth propagating nature of AP wave in all physical variables up to thousands of plasma periods for pure AP type initial conditions. This was done to show that there is no numerical dissipation visible in our code at least up to thousands of plasma periods. We have then added a small sinusoidal perturbation to the large amplitude AP wave and found that AP wave breaks after a few plasma periods. We have noted here that amplitude of the AP wave was found to be well below the critical amplitude [119] even at the time of breaking.

Now in order to get the scalings which describe the dependence of wave breaking time on the perturbation amplitude and AP wave amplitude respectively, we have further repeated the numerical experiment, first keeping the amplitude of the AP wave as fixed and varying amplitude of the perturbation, later keeping the perturbation amplitude as fixed and varying AP wave amplitude. We found that larger the amplitude of the perturbation or AP wave is, shorter the wave breaking time will be. Thus one has to reduce the noise or work at lower amplitude AP wave in order to get maximum acceleration. Now, to understand the physics behind this phenomena, we have plotted frequency of sheets as a function of position with and without perturbation. We found that frequency of the system shows a flat dependence for pure AP wave case and acquires a spatial dependence for nonzero perturbation which gets stronger for larger perturbation amplitude. This is a clear signature of phase mixing. It is also shown that the scalings we discussed here, can be interpreted from the Dawson's formula for phase mixing in inhomogeneous plasma [102]. We have thus shown that, although the ideal breaking amplitude of longitudinal AP waves is very high, they break at arbitrarily low amplitude via phase mixing when perturbed slightly. Thus all those experiments/simulations which use AP wave breaking formula may require revisiting. For example, Malka et al. [28] have observed the generation of 200 MeV electrons in their wake field acceleration experiment. Note here that the authors have used the formula [2] which valid as long as $eE/(m\omega_{pe}c) \leq 1$ in order to interpret their observation. However, in their experiment $eE/(m\omega_{pe}c)$ was approximately 3.8 which is much greater than unity and hence, one needed to use the energy gain formula for nonlinear waves [27]. If we do so, the energy gain would have been approximately 975 MeV. We believe that it is the phase mixing effect which damps the plasma wave well before the full dephasing length and is thus preventing electrons from gaining the full energy.

In chapter 5, we have looked at the phenomena that occur on the long time scale where the effect of ion motion can not be ignored anymore. It is the understanding till date that if we allow ions to move, plasma oscillations phase mix and break at arbitrarily small amplitude due to nonlinearly driven ponderomotive forces only. However, we have shown that it is not only the nonlinearly driven ponderomotive force but also the naturally excited zero frequency mode (which is nothing but the ion acoustic mode in a zero temperature cold plasma) which could be responsible for phase mixing. Actually, if we choose an arbitrary initial condition, solution will be a mixture of high frequency oscillations due to "ω_p" and, DC and secular terms due to ion acoustic mode "0". However, we can adjust the initial conditions in such a way that only one of the two modes get excited. In this chapter we have first shown how to choose initial conditions such that the zero frequency mode does not get excited and we see pure oscillation in the first order and then phase mixing occurs due to nonlinearly driven ponderomotive forces only. We have also shown that although the breaking amplitude of cold plasma BGK waves is high $keE/(m\omega_{pe}^2) \sim 1$, they break at arbitrarily small amplitude via phase mixing if ions are allowed to move. This result has been further verified in PIC simulation. Here zero frequency mode of the system is found to be the only candidate responsible for phase mixing because ponderomotive force for waves is zero. Moreover, we have reported nonlinear traveling wave solutions in an arbitrary mass ratio cold plasma which is correct up to second order. These waves do not exhibit phase mixing as for waves ponderomotive force is zero and zero frequency mode is absent here.

In chapter 6, we have studied the physics of plasma oscillations beyond wave breaking. It is the understanding till date that after the wave breaking plasma becomes warm and all energy of the wave goes to the random kinetic energy of the particles [102, 122]. We have studied, a long time evolution of plasma oscillation in the wave breaking regime using 1D PIC simulation and demonstrated that all the coherent ESE does not convert to random energy of particles but a fraction which is decided by the Coffey criterion [121], always remains with the wave which support a trapped particle distribution in the form of oppositely propagating BGK waves. These BGK waves have also been seen in warm plasma [137, 138, 139, 140] using Vlasov simulation well below the breaking amplitude. The randomized energy distribution of the particles is found to be characteristically non-Maxwellian with a preponderance of energetic particles.

In chapter 7, we have studied a full nonlinear treatment of the formation and collapse of double layers in the long scale length limit, using the method of Lagrange variables, and analytically described the early work, using harmonic and void like initial conditions.

Future scope

We know that a sine wave, square wave and triangular wave density profiles do not break as long as $keE/(m\omega_{pe}^2) \geq 0.5$. On the other hand, Dawson like initial density profile breaks only when $keE/(m\omega_{pe}^2)$ becomes greater than or equal to unity. Therefore, one needs to understand what is so special about this profile that it does not break even though $keE/(m\omega_{pe}^2)$ is greater than 0.5. We tried to understand this via a two modes case which does not show breaking even when

$keE/(m\omega_{pe}^2) \geq 0.5$. However, in order to make a more clear connection among the works carried out by Davidson et al., by us and by Dawson, a better understanding needs to be developed. Although, we have verified the evolution and breaking criteria of single mode case, two mode case and Dawson's case in PIC simulation, the evolution and breaking of square wave and triangular wave cases still need to be examined numerically in PIC or sheet simulation.

By taking an example of sinusoidal initial density perturbation, we have shown that after the wave breaking plasma becomes warm but some fraction of initial energy always remains with the remnant wave and the final distribution is found to be non-Maxwellian. This behavior may also be studied for the above mentioned profiles after verifying their evolution and breaking criteria. We know that the cold plasma BGK waves [120] breaks when $keE/(m\omega_{pe}^2)$ becomes greater than or equal to unity. Physics of these waves beyond wave breaking needs to be explored as it may have direct relevance in particle acceleration experiments. It is also interesting to know the type of distribution functions that will be formed after the breaking of these waves.

First thing one should note here that we have argued in the study beyond cold wave breaking that during the evolution of the distribution in the breaking regime when amplitude of the wave becomes smaller than the breaking amplitude in warm plasma by Coffey, wave stops breaking and converting coherent energy into heat. However, Coffey has derived the maximum amplitude in warm plasma for a water bag distribution function and in our case we found the distribution function bi-Maxwellian. Thus the wave breaking criteria in warm plasma needs revisiting for an arbitrary distribution function.

Second thing is that we have given a qualitative interpretation for the process of acceleration from multistream motion to coherent states. However, for a better understanding a quantitative analysis, which explains the stochastic acceleration of particles, is still needed.

We have studied the physics of nonrelativistic plasma oscillations in the presence of viscosity and resistivity and have derived an analytical formula for Dawson like initial density profile which describes how the critical amplitude depends on viscosity and resistivity coefficient. This formula needs to be verified numerically and one may ask whether this formula is valid for the realistic case also where viscosity coefficient is chosen to be independent of density. Besides, a general formula for an arbitrary initial condition is still required. Moreover one may explore the effects of viscosity and resistivity on relativistic plasma oscillations. For example, one may ask whether the splitting effects, in the density profile, persist for the relativistic case also. We know that relativistic plasma oscillations always phase mix away. Therefore, the effects of dissipative terms on the phase mixing time may also have some relevance in the particle acceleration experiments.

We have obtained the electron-ion traveling wave solutions correct up to second order in an arbitrary mass ratio cold plasma. An exact solution may be more interesting and then one may study the sensitivity of these waves with respect to some perturbations as these waves also (like AP waves) seem to phase mixed if perturbed slightly. Moreover, for a better understanding, phase mixing of plasma oscillations and waves in an arbitrary mass ratio cold plasma need to be examined experimentally.

We have shown that ideal breaking criteria of relativistic traveling waves in cold plasma does not hold in the presence of perturbations (due to noise). If we perturb these waves slightly they break at arbitrary amplitude after a finite time which is decided by both amplitude of the wave and the perturbation. We have proposed that if the wave breaking time is longer than the dephasing time it will not affect the acceleration process. However, if it is shorter one can never achieve the full expected energy. Therefore in order to support our theory one needs to do a qualitative analysis numerically as well as experimentally. For the relativistic studies, we have kept the ions fixed as we have looked only at short time scales phenomena. Hence one may include the effect of ion motion on the relativistic plasma oscillations and waves for the long time scale studies.

We have studied the behavior of relativistic plasma waves only up to the phase mixing time. Therefore, the behavior of these relativistic plasma waves beyond wave breaking (phase mixing time) needs to be understood. Do they also lead to coherent structures after long time evolution ? What kinds of distributions are formed after their breaking ? These questions are still unanswered .

We have studied the evolution and collapse of double layers using method of Lagrange variables. When double layer collapse i.e.; near the singularity, the electron and ion density tends to zero, which makes the electron relativistic. Therefore it will be of interest to explore the consequences of relativistic electron nonlinearities.

Bibliography

[1] P. Gibbon, Short Pulse Laser Interactions with Matter: An Introduction (Imperial College Press, London, 2005).

[2] T. Tajima, J. M. Dawson, Phys. Rev. Lett. 43, 267 (1979).

[3] T. Katsouleas and J. M. Dawson, Phys. Rev. Lett. 51, 392 (1983).

[4] Pisin Chen, J. M. Dawson, Robert W. Huff, and T. Katsouleas, Phys. Rev. Lett. 54, 693 (1985).

[5] P. Sprangle, E. Esarey, and A. Ting, Phys. Rev. Lett. 64, 2011 (1990).

[6] A. Ting, E. Esarey, P. Sprangle, Physics of Fluids B Plasma Physics 2, 1390 (1990).

[7] Y. Nishida, T. Okazaki, N. Yugami, and T. Nagasawa, Phys. Rev. Lett. 66, 2328 (1991)

[8] Jonathan Krall, Glenn Joyce, and Eric Esarey, Phys. Rev. A 44, 6854 (1991).

[9] P. Sprangle, E. Esarey, J. Krall, and G. Joyce, Phys. Rev. Lett. 69, 2200 (1992).

[10] Y. Kitagawa, T. Matsumoto, T. Minamihata, K. Sawai, K. Matsuo, K. Mima, K. Nishihara, H. Azechi, K. A. Tanaka, H. Takabe, and S. Nakai, Phys. Rev. Lett. 68, 48 (1992)

[11] S. V. Bulanov, I. N. Inovenkov, V. I. Kirsanov, N. M. Naumova, A. S. Sakharov, Phys. Fluids B Plasma Physics 4, 1935 (1992).

[12] G. Mourou, D. Umstadter, Phys. Fluids B Plasma Physics 4, 2315 (1992).

[13] A. Modena et al. Nature 377, 606 (1995).

[14] D. Umstadter, J. K. Kim, and E. Dodd, Phys. Rev. Lett. 76, 2073 (1996).

[15] R. J. Kingham and A. R. Bell, Phys. Rev. Lett. 79, 4810 (1997).

[16] E. Esarey, R. F. Hubbard, W. P. Leemans, A. Ting, and P. Sprangle, Phys. Rev. Lett. 79, 2682 (1997).

[17] Bernhard Rau, T. Tajima, and H. Hojo, Phys. Rev. Lett. 78, 3310 (1997).

[18] F. Amiranoff, S. Baton, D. Bernard, B. Cros, D. Descamps, F. Dorchies, F. Jacquet, V. Malka, J. R. MarquÃÍs, G. Matthieussent, P. MinÃľ, A. Modena, P. Mora, J. Morillo, and Z. Najmudin Phys. Rev. Lett. 81, 995 (1998).

[19] Pisin Chen, Toshiki Tajima, and Yoshiyuki Takahashi, Phys. Rev. Lett. 89, 161101 (2002).

[20] Z.-M. Sheng, K. Mima, Y. Sentoku, M. S. JovanoviÄĞ, T. Taguchi, J. Zhang, and J. Meyer-ter-Vehn Phys. Rev. Lett. 88, 055004 (2002).

[21] B. E. Blue, C. E. Clayton, C. L. OâĂŹConnell, F.-J. Decker, M. J. Hogan, C. Huang, R. Iverson, C. Joshi, T. C. Katsouleas, W. Lu, K. A. Marsh, W. B. Mori, P. Muggli, R. Siemann, and D. Walz, Phys. Rev. Lett. 90, 214801 (2003).

[22] A. J. Reitsma, R. A. Cairns, R. Bingham, and D. A. Jaroszynski, Phys. Rev. Lett. 94, 085004 (2005).

[23] M. Tzoufras, W. Lu, F. S. Tsung, C. Huang, W. B. Mori, T. Katsouleas, J. Vieira, R. A. Fonseca, and L. O. Silva, Phys. Rev. Lett. 101, 145002 (2008).

[24] D. Kaganovich, D. F. Gordon, and A. Ting, Phys. Rev. Lett. 100, 215002 (2008).

[25] C. Rechatin, X. Davoine, A. Lifschitz, A. Ben Ismail, J. Lim, E. Lefebvre, J. Faure, and V. Malka Phys. Rev. Lett. 103, 194804 (2009).

[26] M. J. H. Luttikhof, A. G. Khachatryan, F. A. van Goor, and K.-J. Boller Phys. Rev. Lett. 105, 124801 (2010).

[27] E. Esarey and M. pilloff, Phys. plasmas 2, 1432 (1995).

[28] V. Malka, S. Fritzler, E. Lefebvre, M.-M. Aleonard, F. Burgy, J.-P. Chambaret, J.-F. Chemin, K. Krushelnick, G. Malka, S. P. D. Mangles, Z. Najmudin, M. Pittman, J.-P. Rousseau, J.-N. Scheurer, B. Walton, and A. E. Dangor, Science 298, 1596 (2002).

[29] A. Modena et al. Nature 377, 606 (1995).

[30] J. Faure, C. Rechatin, A. Norlin, A. Lifschitz, Y. Glinec, and V. Malka, Nature (London) 444, 737 (2006).

[31] C. Rechatin et al., Phys. Rev. Lett. 102, 164801 (2009).

[32] Prabal Singh Verma, J. K. Soni, S. Sengupta, P. K. Kaw Phys. Plasmas 17, 044503 (2010).

[33] Chandan Maity, Nikhil Chakrabarti, Sudip Sengupta, Phys. Plasmas 17, 082306 (2010).

[34] Prabal Singh Verma, Sudip Sengupta, Predhiman K. Kaw, Phys. Plasmas 18, 012301 (2011).

[35] M. Tabak, J. Hammer, M. E. Glinsky, W. L. Kruer, S. C. Wilks, J. Woodworth, E. M. Campbell, M. D. Perryand R. J. Mason, Phys. Plasmas 1, 1625 (1994).

[36] S. GuÃľrin, P. Mora, J. C. Adam, A. HÃľron, and G. Laval,Phys. Plasmas 3, 2693 (1996).

[37] A. R. Piriz et al., Phys. Plasmas 5, 2721 (1998).

[38] A. R. Piriz et al., Phys. Plasmas 5, 4373 (1998).

[39] K. A. Tanaka et al., Phys. Plasmas 7, 2014 (2000).

[40] M. Honda et al., Phys. Rev. Lett. 85, 2128 (2000).

[41] M. Roth et al., Phys. Rev. Lett. 86, 436 (2001).

[42] S. Hain et al., Phys. Rev. Lett. 86, 1015 (2001).

[43] M. Temporal et al., Phys. Plasmas 9, 3098 (2002).

[44] Stephen A. Slutz et al., Phys. Plasmas 10, 234 (2003).

[45] K. A. Tanaka et al., Phys. Plasmas 10, 1925 (2003).

[46] P. A. Norreys et al., Phys. Plasmas 11, 2746 (2004).

[47] R. B. Stephens et al., Phys. Rev. E 69, 066414 (2004).

[48] J. R. Davies, Phys. Rev. E 69, 065402 (R) (2004).

[49] C. Ren et al., Phys. Rev. Lett. 93, 185004 (2004.

[50] M. Tabak et al., Phys. Plasmas 12, 057305 (2005).

[51] R. B. Stephens et al., Phys. Plasmas 12, 056312 (2005.

[52] S. A. Slutz et al., Phys. Plasmas 12, 062702 (2005).

[53] A. Bret et al., Phys. Plasmas 12, 102702 (2005).

[54] T. Yokota et al., Phys. Plasmas 13, 022702 (2006).

[55] C. Ren et al., Phys. Plasmas 13, 056308 (2006).

[56] A. L. Lei, K. A. Tanaka, R. Kodama, G. R. Kumar, K. Nagai, T. Norimatsu, T. Yabuuchi, and K. Mima, Phys. Rev. Lett. 96, 255006 (2006).

[57] R. Betti et al., Phys. Plasmas 13, 100703 (2006).

[58] A. L. Lei et al., Phys. Rev. E 76, 066403 (2007).

[59] M. H. Key et al., Phys. Plasmas 15, 022701 (2008).

[60] M. Temporal et al., Phys. Plasmas 15, 052702 (2008).

[61] L. A. Cottrill et al., Phys. Plasmas 15, 082108 (2008).

[62] A. G. MacPhee et al., Rev. Sci. Instrum. 79, 10F302 (2008).

[63] M. G. Haines et al., Phys. Rev. Lett. 102, 045008 (2009).

[64] A. L. Lei et al., Phys. Plasmas 16, 056307 (2009).

[65] J. Tonge et al., Phys. Plasmas 16, 056311 (2009).

[66] Tomoyuki Johzaki et al., Phys. Plasmas 16, 062706 (2009).

[67] Hong-bo Cai et al., Phys. Rev. Lett. 102, 245001 (2009).

[68] C. D. Chen et al., Phys. Plasmas 16, 082705 (2009).

[69] A. Bret, Phys. Plasmas 16, 094505 (2009).

[70] J. J. Honrubia et al., Phys. Plasmas 16, 102701 (2009).

[71] S. Yu. GusâĂŹkov et al., Plasma Physics Reports 36, 473 (2010).

[72] R. Sadighi-Bonabi et al., Laser and Particle Beams 28, 101 (2010).

[73] M Tabak et al., Journal of Physics Conference Series 244, 022066 (2010).

[74] W M Wang et al., Journal of Physics Conference Series 244, 022070 (2010).

[75] Atsushi Sunahara et al., Journal of Physics Conference Series 244, 022079 (2010).

[76] H Nagatomo et al., Journal of Physics Conference Series 244, 022050 (2010).

[77] Hong-bo Cai et al., Journal of Physics Conference Series 244, 022030 (2010).

[78] K U Akli et al., Journal of Instrumentation 5, P07008 (2010).

[79] Hong-bo Cai, Kunioki Mima, Atsushi Sunahara, Tomoyuki Johzaki, Hideo Nagatomo, Shao-ping Zhu, and X. T. He, Phys. Plasmas 17, 023106 (2010).

[80] A. J. Kemp, B. I. Cohen, and L. Divol,Phys. Plasmas 17, 056702 (2010).

[81] Shinsuke Fujioka, Takashi Fujiwara, Minoru Tanabe, Hiroaki Nishimura, Hideo Nagatomo, Shinji Ohira, Yuichi Inubushi, Hiroyuki Shiraga, and Hiroshi Azechi, Rev. Sci. Instrum. 81, 10E529 (2010).

[82] S. Micheau, A. Debayle, E. dâĂŹHumiÃĺres, J. J. Honrubia, B. Qiao, M. Zepf, M. Borghesi, and M. Geissler,Phys. Plasmas 17, 122703 (2010).

[83] Sizhong Wu, Cangtao Zhou, Shaoping Zhu, Hua Zhang, and Xiantu He,Phys. Plasmas 18, 022703 (2011).

[84] Enrique Henestroza, B. Grant Logan, and L. John Perkins, Phys. Plasmas 18, 032702 (2011).

[85] Xiaoling Yang, George H. Miley, Kirk A. Flippo, and Heinrich Hora, Phys. Plasmas 18, 032703 (2011).

[86] A. Pukhov and J. Meyer-ter-Vehn, Proceedings of the 12th International Conference on Laser Interaction and Related Plasma Phenomena, Osaka, April 24-28, 1995, edited by S. Nakai and G. H. Miley, AIP Conf. Proc. 369 (American Institute of Physics, Woodbury, NY, 1996).

[87] A. Pukhov and J. Meyer-ter-Vehn, Phys. Rev. Lett. 79, 2686 (1997).

[88] M. Honda, J. Meyer-ter-Vehn, and A. Pukhov, Phys. Rev. Lett. 85, 2128 (2000).

[89] P A Norreys, K L Lancaster, H Habara, J R Davies, J T MendonÃğa, R J Clarke, B Dromey, A Gopal, S Karsch, R Kodama, Plasma Physics and Controlled Fusion, 47, L49 (2005)

[90] M Murakami, H Nagatomo, H Azechi, F Ogando, M Perlado, S Eliezer, Nuclear Fusion 46, 99 (2006).

[91] A. L. Lei, A. Pukhov, R. Kodama, T. Yabuuchi, K. Adumi, K. Endo, R. R. Freeman, H. Habara, Y. Kitagawa, K. Kondo, G. R. Kumar, T. Matsuoka, K. Mima, H. Nagatomo, T. Norimatsu, O. Shorokhov, R. Snavely, X. Q. Yang, J. Zheng, and K. A. Tanaka, Phys. Rev. E 76, 066403 (2007).

[92] Roger G Evans, Plasma Physics and Controlled Fusion 49, B87 (2007).

[93] N. Naumova, T. Schlegel, V. T. Tikhonchuk, C. Labaune, I. V. Sokolov, and G. Mourou, Phys. Rev. Lett. 102, 025002 (2009).

[94] A. L. Lei, K. A. Tanaka, R. Kodama, K. Adumi, H. Habara, Y. Kitagawa, K. Kondo, T. Matsuoka, T. Tanimoto, T. Yabuuchi, Physics of Plasmas 16, 056307 (2009).

[95] J H Nuckolls, Journal of Physics Conference Series 244, 012007 (2010).

[96] Kunioki Mima, Nuclear Fusion 50, 014006 (2010).

[97] S. Yu. GusâĂŹkov et al., Plasma Physics Reports 36, 473 (2010).

[98] S Atzeni, Plasma Physics and Controlled Fusion 51, 124029 (2009).

[99] S. A. Slutz et al., Phys. Plasmas 10, 1875 (2003).

[100] A. A. Andreev et al., JETP 96, 695 (2003).

[101] S. A. Slutz et al., Phys. Plasmas 10, 429 (2003).

[102] J. M. Dawson, Phys. Rev. 113, 383 (1959).

[103] P. K. Kaw, A. T. Lin, J. M. Dawson, Phys. Fluids 16, 1967 (1973).

[104] E. Infeld, G. Rowlands, S. TorvÃľn, Phys. Rev. Lett. 62, 2269 (1989).

[105] C. Nappi, A. Forlani, and R. Fedele, Phys. Scr. 43, 301 (1991).

[106] S. Sengupta, P. K. Kaw, Phys. Rev. Lett. 82, 1867 (1999).

[107] E. Infeld and G. Rowlands, Phys. Rev. Lett. 62, 1122 (1989).

[108] S. Sengupta, V. Saxena, P. K. Kaw, A. Sen, and A. Das, Phys. Rev. E 79, 026404 (2009).

[109] S. Sengupta et al., Plasma Phys. Control. Fusion 53,074014 (2011).

[110] S. V. Bulanov, F. Pegoraro, A. M. Pukhov, and A. S. Sakharov, Phys. Rev. Lett. 78, 4205âĂŞ4208 (1997).

[111] L. Landau, J. Phys. 10, 25 (1946).

[112] T. O'Neil, Phys. Fluids 8, 2255 (1965).

[113] I. B. Bernstein, J. M. Green, and M. D. Kruskal, Phys. Rev. 108, 546 (1957).

[114] R. W. Gould, T. M. O'Neil and J. H. Malmberg, Phys. Rev. Lett. 19, 219âĂŞ222 (1967).

[115] J. H. Malmberg, C. B. Wharton, R. W. Gould, and T. M. O'Neil, Phys. Rev. Lett. 20, 95âĂŞ97 (1968).

[116] R. C. Davidson, P.P. Schram, Nucl. Fusion 8, 183 (1968).

[117] R.C. Davidson, Methods in Nonlinear Plasma Physics (Academic, New York, 1972).

[118] E. Infeld, G. Rowlands, A. A. Skorupski, Phys. Rev. Lett. 102, 145005 (2009).

[119] A. I. Akhiezer and R. V. Polovin, Sov. Phys. JETP 3, 696 (1956).

[120] J.Albritton, G. Rowlands, Nucl. Fusion, 15, 1199 (1975).

[121] T. P. Coffey, Phys. of Fluids 14, 1402 (1971).

[122] Jin-Gen Wang, G. L. Payne, D. R. Nicholson, Phys. Fluids B 4, 1432 (1992).

[123] A. A. Galeev et. al., *Sov. Phys. JETP* **54**, 306 (1981).

[124] Y. Takeda et. al., Phys. Rev. Lett, **74**, 1998 (1995).

[125] G. Lehmann, E. W. Laedke and K. H. Spatschek, Phys. Plasmas, 14, 103109 (2007).

[126] V. Saxena et al., Phys. Plasmas 14, 072307 (2007).

[127] E. Infeld and G. Rowlands, Nonlinear Waves, Solitons and Chaos (Cambridge University Press, Cambridge, England, 2000), 2nd ed., Chap. 6; J. Tech. Phys. 28, 607 (1997); 29, 3 (1998).

[128] C. K. Birdsall and A. B. Langdon, Plasma Physics Via Computer Simulation McGraw-Hill, Singapore, (1985), Chap. 3 and Chap. 12, p. 274.

[129] J. P. Boris , D. L. Book, Methods Comput. Phys. 16, 85 (1976).

[130] P. D. Lax, B. Wendroff, Comm. Pure Appl. Math. 17, 381 (1964).

[131] V. E. Zakharov, Sov. Phys. JETP 35, 908 (1972).

[132] C. D. Decker, W. B. Mori, and T. Katsouleas, Phys. Rev. E 50, R3338 (1994).

[133] L. M. Gorbunov and V. I. Kirsanov, Sov. Phys. JETP 66, 290 (1987).

[134] J. B. Rosenzweig, P. Schoessow, B. Cole, W. Gai, R. Konecny, J. Norem, and J. Simpson, Phys. Rev. A 39, 1586 (1989).

[135] A. Bergmann and P. Mulser, Phys. Rev. E 47, 3585 (1983).

[136] R. M. G. M. Trines and P. A. Norreys,Phys. Plasmas 13, 123102 (2006).

[137] L. Demeio, P. F. Zweifel, Phys. Fluids B 2, 1252 (1990)

[138] Mark Buchanan, J. J. Dorning, Phys. Rev. Lett. 70, 3732 (1993); Phys. Rev. E 50, 1465 (1994).

[139] G. Manfredi, Phys. Rev. Lett. 79, 2815 (1997)

[140] M. Brunetti, F. Califano, F. Pegoraro Phys. Rev. E 62, 4109 (2000).

[141] F. Valentini, T. M. O'Neil, and D. H. E. Dubin, Phys. Plasmas 13, 052303 (2006).

[142] E. Infeld and G. Rowlands, Phys. Rev. Lett. 58, 2063 (1987).

[143] R. M. G. M. Trines, Phys. Rev. E 79, 056406 (2009).

[144] A. A. Kabantsev, F. Valentini, and C. F. Driscoll, AIP Conf. Proc. 862, 13 (2006); F. Valentini, T. M. O'Neil, and D. H. E. Dubin, ibid. 862, 3 (2006).

[145] M. V. Konyukov, Sov. Phys. JETP 37, 570 (1960).

[146] C. H. Sack, H. Schamel, Plasma Phys. Control. Fusion 27, 717 (1985).

[147] F. F. Chen, Introduction to Plasma Physics and Controlled Fusion: Vol 1: Plasma Physics

[148] E. Infeld and G. Rowlands, Phys. Rev. Lett., **58**, 2063 (1987).